Distribution Agreement

In presenting this thesis or dissertation as a partial fulfillment of the requirements for an advanced degree from Emory University, I hereby grant to Emory University and its agents the non-exclusive license to archive, make accessible, and display my thesis or dissertation in whole or in part in all forms of media, now or hereafter known, including display on the world wide web. I understand that I may select some access restrictions as part of the online submission of this thesis or dissertation. I retain all ownership rights to the copyright of the thesis or dissertation. I also retain the right to use in future works (such as articles or books) all or part of this thesis or dissertation.

Signature:

_____ _____

Kyle J. Gerber **Date**

A Comprehensive Analysis of the RGS14 Interactome in the Context of Area CA2 of the Hippocampus

By

Kyle J. Gerber
Doctor of Philosophy

Graduate Division of Biological and Biomedical Sciences
Molecular and Systems Pharmacology

_____
John R. Hepler, Ph.D.
Advisor

_____
Randy A. Hall, Ph.D.
Committee Member

_____
Gary Bassell, Ph.D.
Committee Member

_____
Stephen Traynelis, Ph.D.
Committee Member

Accepted:

_____
Lisa A. Tedesco, Ph.D.
Dean of the James T. Laney School of Graduate Studies

_____
Date

A Comprehensive Analysis of the RGS14 Interactome in the Context of Area CA2 of the Hippocampus

By

Kyle J. Gerber
B.S., Case Western Reserve University, 2013

Advisor: John R. Hepler, Ph.D.

An abstract of a dissertation submitted to the Faculty of the James T. Laney School of Graduate Studies of Emory University in partial fulfillment of the requirements for the degree of Doctor of Philosophy

Graduate Division of Biological and Biomedical Sciences
Molecular and Systems Pharmacology
2019

Abstract

A Comprehensive Analysis of the RGS14 Interactome in the Context of Area CA2 of the Hippocampus

By Kyle J. Gerber

Regulator of G protein signaling (RGS) proteins are key modulators of heterotrimeric G protein signaling downstream of G protein coupled receptors throughout the body. Many of these RGS proteins, including RGS2, RGS4, RGS7, RGS9, and RGS14, modulate synaptic signaling throughout the brain. RGS14 in particular, modulates synaptic plasticity in the CA2 region of the hippocampus. The hippocampus as a whole is essential for learning and memory but area CA2 has been largely ignored until recently due to its small size and lack of plasticity compared to the neighboring CA1 region. Many recent studies have taken advantage of proteins expressed specifically in CA2, including RGS14 and amigo-2, to identify and examine this enigmatic region of the brain. Using targeted dissections with the aid of enhanced green fluorescent protein (eGFP) expressed under the amigo-2 promoter, we were able to perform a proteomic analysis of area CA2 and CA1 to reveal a proteomic profile for CA2 (vs. CA1), identifying a wealth of potential targets for future studies that will allow us to understand the physiological and functional differences between area CA2 and CA1.

One of the many proteins we found to be highly expressed in area CA2 was RGS14. RGS14 naturally suppresses long-term potentiation (LTP), a cellular correlate of learning and memory, in area CA2. The mechanism by which RGS14 suppresses this form of synaptic plasticity is unknown. By immunoprecipitating RGS14 out of mouse brain and analyzing all interacting proteins through mass spectrometry analysis, we revealed an RGS14 interactome containing functional interactors with RGS14 that will allow us to elucidate the mechanism by which RGS14 suppresses LTP. The top interactors with RGS14 were myosins and other actin-binding proteins that facilitate transport of cargo throughout the cell as well as control the structure and function of dendritic spines, which are essential for the proper expression of LTP. By combining our RGS14 interactome data with our CA2 proteome, we were able to identify myosin IIA and drebrin 1 as likely interactors with RGS14 that merit further study. Our interactome also showed that RGS14 interacts with 14-3-3 proteins, ubiquitously expressed proteins that typically bind phosphorylated serine or threonine residues at conserved motifs to affect substrate function, interactions, and localization. We find that RGS14 interacts with 14-3-3 at two unique sites. One site, downstream of RGS14's RGS domain is phosphorylation-dependent. Binding of 14-3-3 inhibits active Gαi-GTP binding at the RGS domain, likely preventing RGS14 from catalyzing cleavage of the GTP on Gαi and ending the signal transduction cascade initiated by GPCR activation. The other 14-3-3 binding site on RGS14 is phosphorylation-independent. Binding of 14-3-3 to this site prevents RGS14 translocation into the nucleus, where it may modulate transcription. Here, we reveal both a proteome for area CA2 and an interactome for a CA2-expressed protein, RGS14. This interactome has revealed a functional interaction between RGS14 and 14-3-3 as well as the presence of many other potential functional interactors. Future studies examining the RGS14 interactome in the context of the CA2 proteome will elucidate the functional binding partners responsible for RGS14's suppression of synaptic plasticity as well as other potential functions in other parts of the cell, including the nucleus.

A Comprehensive Analysis of the RGS14 Interactome in the Context of Area CA2 of the Hippocampus

By

Kyle J. Gerber
B.S., Case Western Reserve University, 2013

Advisor: John R. Hepler, Ph.D.

A dissertation submitted to the Faculty of the James T. Laney School of Graduate Studies of Emory University in partial fulfillment of the requirements for the degree of Doctor of Philosophy

Graduate Division of Biological and Biomedical Sciences
Molecular and Systems Pharmacology
2019

Table of Contents

Index of Figure and Tables

Chapter 1:

Introduction

This chapter contains figures and text that have been modified from the published manuscript: Gerber, K. J., K. E. Squires and J. R. Hepler (2016). "Roles for Regulator of G Protein Signaling Proteins in Synaptic Signaling and Plasticity." Mol Pharmacol **89**(2): 273-286.

1.1 Overview of GPCR regulation of synaptic plasticity

G protein coupled receptors (GPCRs) are the largest class of cell surface receptor with over 800 GPCRs having been identified in the human genome (Fredriksson et al. 2003). These receptors can recognize and be activated by a large variety of ligands including lipids, peptides, hormones, nucleotides, and neurotransmitters. Reflective of this huge diversity in activators, GPCRs are expressed throughout the body, often with distinct expression patterns in specific tissues and cell types. For these regions, GPCRs are widely recognized as excellent drug targets, with approximately 30 percent of all pharmaceuticals targeting these receptors to either exacerbate or block their effects on downstream signaling in the cells in which they are expressed (Jacoby et al. 2006).

While frequently targeted to modulate normal physiology and signaling, within the brain G protein coupled receptors (GPCRs) are necessary for normal, functional neurotransmission throughout the central nervous system (CNS), controlling neurophysiological processes ranging from movement to mood (Lagerstrom and Schioth 2008; Betke, Wells, and Hamm 2012; Rojas and Dingledine 2013). Receptor activation of heterotrimeric G proteins (Gαβγ) results in release of Gα-GTP and Gβγ that stimulate downstream effectors and second messenger pathways to mediate intracellular physiology (Bourne, Sanders, and McCormick 1990; Simon, Strathmann, and Gautam 1991; Hepler and Gilman 1992; Hamm 1998). GPCR and linked G protein signaling is tightly controlled by the family of *r*egulator of *G* protein *s*ignaling (RGS) proteins. RGS proteins act as GTPase activating proteins (GAPs) on the alpha subunits of the Gαi and Gαq subfamilies of heterotrimeric G proteins, greatly enhancing the intrinsic GTPase activity of the Gα subunit to facilitate the termination of downstream signaling by both the Gα and Gβγ subunits (Ross and Wilkie 2000; Hollinger and Hepler 2002; De Vries et al. 2000; Willars 2006). RGS proteins are a

structurally diverse family of signaling proteins with many identified signaling partners distinct from Gα and GPCRs. In this regard, considerable evidence shows that many RGS proteins have cell signaling roles in addition to their shared established roles as GAPs for G protein alpha subunits (Gα) (Burchett 2000; Sethakorn, Yau, and Dulin 2010; Abramow-Newerly et al. 2006).

GPCR signaling regulates key aspects of both pre- and postsynaptic neurotransmission, leading to changes in synaptic plasticity, including long-term potentiation (LTP), long-term depression (LTD), reversal of LTP (depotentiation), and presynaptic vesicle release potential. Various metabotropic GPCRs either positively or negatively regulate presynaptic neurotransmitter release (Tedford and Zamponi 2006; Betke, Wells, and Hamm 2012). On postsynaptic membranes, GPCRs and G protein signaling pathways regulate neuronal excitability, modulating fast acting neurotransmission mediated by ligand-gated ion channels including glutamate (Chalifoux and Carter 2010; Liu et al. 2006; Rojas and Dingledine 2013) and gamma-aminobutyric acid (GABA) receptors (Bormann 1988). Following GPCR activation of Gα, released Gβγ directly binds to and activates G protein-coupled inwardly rectifying potassium (GIRK) channels. GIRK channels hyperpolarize the neuron and dampen the overall capacity of the postsynaptic signaling to potentiate (Dascal 1997), a process known as depotentiation, or the reversal of LTP. As such, GIRK channels are required for depotentiation and many RGS proteins regulate the rate at which GPCR-coupled GIRK channels close following agonist removal (Doupnik et al. 1997; Saitoh et al. 1997; Saitoh et al. 2001; Ulens, Daenens, and Tytgat 2000). Presynaptically, active Gβγ subunits can inhibit voltage-gated calcium (Ca_V) channels necessary for calcium-dependent neurotransmitter release following an action potential (Bormann 1988; Zamponi and Currie 2013). In this case, RGS proteins can antagonize the effects of Gβγ on N- and P/Q-type Ca_V channels ($Ca_V2.2$ and $Ca_V2.1$), facilitating neurotransmitter release (Kammermeier and Ikeda 1999; Mark,

Wittemann, and Herlitze 2000; Jeong and Ikeda 2000). Additionally, canonical heterotrimeric G protein signaling through Gα subunits has been shown to affect plasticity via modulation of postsynaptic glutamate receptors (Liu et al. 2006; Chalifoux and Carter 2010) and multiple other signaling pathways necessary for synaptic plasticity.

1.2 Overview of RGS protein regulation of synaptic plasticity

Our current understanding of roles for RGS proteins in physiology and behavior has been greatly aided by the development and use of RGS-insensitive Gα subunits (DiBello et al. 1998; Fu et al. 2004; Kaur et al. 2011), allowing examination of neurophysiology under conditions that mimic functional uncoupling of Gα-RGS. Studies with these mutants have revealed key roles for RGS proteins in multiple signaling pathways in neurons, as well as pre- and postsynaptic signaling and plasticity specifically (Goldenstein et al. 2009; Talbot et al. 2010; Chen and Lambert 2000). By examining the role of RGS proteins in synaptic signaling, we can better understand the function of GPCR and G protein signaling in synaptic plasticity as well as diseases associated with RGS protein dysfunction.

While many RGS proteins are expressed throughout the brain, I chose to focus on a select few that have a clearly defined role in modulating synaptic signaling and plasticity as opposed to cellular signaling in the brain as a whole. These RGS proteins are RGS2, RGS4, RGS7, RGS9-2, and RGS14. Here, I highlight and review current knowledge of the function of these RGS proteins demonstrated to have a clear role in modulating synaptic signaling and plasticity throughout the brain.

1.2.1 RGS2 regulation of synaptic plasticity

RGS2 is a ~24 kDa protein consisting of a single RGS domain with minimal flanking amino and carboxy terminal regions. RGS2 was first discovered and characterized as a member of

the R4 family of RGS proteins (Siderovski et al. 1996), exhibiting selective GAP activity toward Gαq subunits (Heximer et al. 1997), though further studies have reported situational and receptor-dependent modulation of Gαi/o signaling as well (Han et al. 2006; Herlitze, Ruppersberg, and Mark 1999; Ingi et al. 1998; Heximer et al. 1999) (Table 1). While many RGS proteins can act as a GAP on Gαq and/or Gαi/o, a key feature of RGS2 is the induction of its expression in response to stimuli capable of evoking plasticity in multiple brain regions, leading to the characterization of RGS2 as an immediate early gene. This phenomenon was first seen when RGS2 mRNA expression was induced in the cortex, striatum, and hippocampus following maximum electroconvulsive shock (MECS), a reliable means with which to induce immediate early gene expression throughout the brain. More targeted induction of expression has been shown to occur in the striatum (caudate putamen and nucleus accumbens) of rats following amphetamine administration (Taymans et al. 2002). In a model more closely related to synaptic plasticity, high frequency stimulation (HFS), which is commonly used to induce hippocampal LTP, has been shown to strongly induce the expression of RGS2 mRNA within the dentate gyrus of the hippocampus (Ingi et al. 1998). Furthermore, stable expression of RGS2 with no induction protocol has been found throughout the brain in the same regions in which its expression is induced: the hippocampus, cortex, striatum, ventral tegmental area (VTA), and amygdala (Grafstein-Dunn et al. 2001; Ingi and Aoki 2002; Taymans et al. 2002).

Due to its high expression throughout the brain and its unique role as an immediate early gene, functions for RGS2 in neurological diseases and disorders have been extensively studied. Multiple reports have shown a role for this RGS protein in modulating anxiety, with polymorphisms in RGS2 associated with generalized anxiety disorder (Hohoff et al. 2015; Koenen et al. 2009; Smoller et al. 2008), panic disorder (Hohoff et al. 2015; Koenen et al. 2009; Otowa et

al. 2011), post-traumatic stress disorder (Amstadter et al. 2009), as well as suicide (Cui et al. 2008) in humans. Studies in mice have also shown an association between RGS2 and anxiety (Lifschytz et al. 2012; Oliveira-Dos-Santos et al. 2000; Yalcin et al. 2004; Okimoto et al. 2012) with decreased RGS2 expression causing anxiety (Lifschytz et al. 2012; Oliveira-Dos-Santos et al. 2000) and depression-like (Lifschytz et al. 2012) phenotypes. In order to better treat these diseases associated with RGS2, it is necessary to understand how RGS2 modulates synaptic plasticity and signaling.

Functions for RGS2 in synaptic signaling and plasticity have been examined largely within the hippocampus and VTA. Within the hippocampus, RGS2 regulates short-term synaptic plasticity. High concentrations of RGS2 within the neuron appear to facilitate paired pulse depression, while low expression of RGS2 leads to paired pulse facilitation (PPF). In other words, probability of neurotransmitter release is high in the presence of RGS2 and low in its absence. Notably, pertussis toxin (PTX) blocks the PPF in RGS2-knockout (KO) mice, indicating that RGS2's effects at the presynaptic terminal in this case are due to its modulation of Gαi/o-coupled GPCR signaling as opposed to Gαq (Han et al. 2006). Activation of Gαi/o leads to the dissociation of Gβγ subunits which can inhibit presynaptic voltage-gated $Ca_V2.2$ channels, preventing calcium influx necessary for neurotransmitter release (Ikeda 1996; Kajikawa, Saitoh, and Takahashi 2001) (Figure 1A). Decreased expression of RGS2 leads to increased Gβγ-mediated inhibition of calcium influx and decreased probability of neurotransmitter release from the synapse, hence the observed PPF (Han et al. 2006). This interpretation is strengthened by *in vitro* evidence showing RGS2-mediated facilitation of $Ca_V2.1$ calcium channels, which are also inhibited by Gβγ subunits (Mark, Wittemann, and Herlitze 2000).

RGS2 also has reported roles in postsynaptic spines within the hippocampus in the context of long-term synaptic plasticity (Figure 1C). However, studies with RGS2-KO mice examining this topic are conflicting. There is no change in canonical hippocampal LTP as compared to RGS2 heterozygous mice (Oliveira-Dos-Santos et al. 2000), but increased LTP as compared to wild type (Hutchison, Chidiac, and Leung 2009). However hippocampal-dependent learning and memory does not appear to be affected in RGS2-KO mice (Oliveira-Dos-Santos et al. 2000), leaving RGS2's role in modulating canonical hippocampal LTP unclear. RGS2 has been shown to modulate signaling through mGluR1a, with increases in RGS2 expression blocking Gαq mediated signaling while leaving Gαi-mediated signaling unaffected (Kammermeier and Ikeda 1999). Furthermore, mGluR1a has been shown to be responsible for a unique form of postsynaptic NMDA receptor-independent LTP within hippocampal interneurons, which possibly could be regulated by changes in expression of RGS2 (Perez, Morin, and Lacaille 2001). The numbers of apical and basilar spines of dendrites in CA1 hippocampal neurons are also significantly decreased in RGS2-KO mice (Oliveira-Dos-Santos et al. 2000), with the amount of spines being indicative of overall synapse numbers and synaptic plasticity (Moser 1999). These changes in spine number could be explained by the discovery that RGS2 binds tubulin directly, stimulating microtubule polymerization (Heo et al. 2006) and potentially aiding in the development of dendritic spines (Gu, Firestein, and Zheng 2008). Additionally, CA1 hippocampal neurons of RGS2-KO mice show decreased overall basal electrical activity as measured by decreased field excitatory postsynaptic potential (fEPSP) amplitude following stimulation via Schaeffer collaterals (Oliveira-Dos-Santos et al. 2000).

Roles for RGS2 also have been examined in the VTA (Labouebe et al. 2007). RGS2 is selectively expressed postsynaptically in tyrosine hydroxylase-positive dopamine neurons within

the VTA. Here, RGS2 associates specifically with GIRK3, one of four GIRK channel subunits, to decrease the coupling efficiency between the $GABA_B$ receptor and GIRK channels (Labouebe et al. 2007) (Figure 1C). These GIRK channels mediate the inhibitory postsynaptic effects of Gαi/o-coupled receptors, including the $GABA_B$ receptor. Because RGS2 is not highly expressed in GABA neurons, $GABA_B$ receptor-GIRK channel coupling efficiency is much higher in GABA neurons of the VTA than those that release dopamine. This allows application of γ-hydroxybutyrate (GHB), a $GABA_B$ receptor agonist, to cause disinhibition of dopamine neurons in the VTA, which are typically inhibited by GABA neurons, leading to induction of addictive behavior. However, chronic exposure of mice to GHB reduces the mRNA expression of RGS2 in dopamine neurons, increasing $GABA_B$–GIRK channel coupling and providing a possible mechanism through which tolerance to GHB occurs and demonstrating a novel mechanism through which changes in RGS2 expression mediate signaling at the synapses of dopamine neurons in the VTA (Labouebe et al. 2007).

Roles for RGS2 in the brain also have been examined outside the hippocampus and VTA, but are less well defined. In the amygdala, RGS2 expression is induced upon administration of oxytocin (Okimoto et al. 2012), potentially mediating the anxiolytic effects of the neuropeptide. This may explain the relationship between anxiety and RGS2 although additional studies where RGS2 expression cannot be induced by oxytocin (RGS2-KO mice) must be performed to ensure that RGS2 is necessary to mediate oxytocin's anxiolytic effect. RGS2 also is expressed in olfactory neurons where it inhibits the activity of adenylyl cyclase III downstream of active olfactory receptors, regulating signal transduction and possibly contributing to long-term adaptation to odorants (Sinnarajah et al. 2001). Overall, the status of RGS2 as an immediate early gene highly

expressed in multiple types of neurons throughout the brain allows it to play a unique role in modulating G protein signaling at the synapse.

1.2.2 RGS4 regulation of synaptic plasticity

Another member of the R4 family of RGS proteins, RGS4, also acts as a GAP on both Gαi/o (Berman, Wilkie, and Gilman 1996; Huang et al. 1997) and Gαq subunits (Hepler et al. 1997; Huang et al. 1997) (Table 1). Similar to RGS2, RGS4 is a ~24 kDa protein consisting of a single RGS domain with modest flanking amino and carboxy terminal regions. Like RGS2, RGS4 is expressed throughout the brain (Ingi and Aoki 2002; Gold et al. 1997), with expression reported in the prefrontal cortex (Ding and Hegde 2009; Mirnics et al. 2001; Paspalas, Selemon, and Arnsten 2009), hippocampus (Gold et al. 1997; Heraud-Farlow et al. 2013; Saugstad et al. 1998), thalamus (Gold et al. 1997; Ingi and Aoki 2002; Kim et al. 2014; Ni et al. 1999), and striatum (Larminie et al. 2004). Furthermore, in studies comparing abundance of mRNA coding for RGS proteins, RGS4 has the highest measured levels within the brain (Larminie et al. 2004), though a peculiar property of RGS4 is that its basal protein levels are typically low due to a robustly regulated degradation of the protein (Davydov and Varshavsky 2000; Lee et al. 2005; Bodenstein, Sunahara, and Neubig 2007). With such a broad expression pattern across brain regions, RGS4 has been widely studied for its role in physiology relating to neuronal signaling and plasticity, as well as in neurological diseases. Here, we will examine the function of RGS4 in the brain regions where its effect on synaptic plasticity and signaling is best characterized: the hippocampus, striatum, hypothalamus, and prefrontal cortex.

Potential roles for RGS4 in the modulation of GPCR signaling in brain were first described in the hippocampus. In the CA1 region, the group I metabotropic glutamate receptor, mGluR5, is localized perisynaptically in dendrites (Ottersen and Landsend 1997). Here, activation of mGluR5

mediates suppression of the afterhyperpolarization current that follows action potential firing as well as potentiation of NMDA receptor currents (Mannaioni et al. 2001), thereby increasing neuronal excitability by intensifying both firing and depolarization, respectively. RGS4 has been shown to inhibit signaling through group I mGluRs (mGluR1 and 5), blocking mGluR5-mediated inhibition of the afterhyperpolarization current in CA1 neurons (Saugstad et al. 1998) (Figure 1C). However, the effect of RGS4 on mGluR5's potentiation of NMDA receptor currents as well as its effect on signaling through mGluR1 within the hippocampus have not been examined. While the role of endogenous RGS4 within the hippocampus is not fully understood, changes in RGS4 expression potentially could regulate group I mGluR-mediated changes in neuronal excitability within the CA1 region as well as other regions of the hippocampus.

While the precise role of RGS4 in modulating synaptic signaling and plasticity in the hippocampus remains poorly defined, roles for RGS4 in the striatum are better understood. In Parkinson's disease (PD), decreased striatal dopamine leads to increased striatal acetylcholine release, which exacerbates the motor symptoms of the disease. Notably, dopamine depletion in the striatum also upregulates RGS4 expression specifically in cholinergic interneurons (Ding et al. 2006). Here, RGS4 diminishes signaling through presynaptic M4 muscarinic acetylcholine autoreceptors (Figure 1B). Activation of Gαo-coupled M4 receptors in striatal cholinergic interneurons causes Gβγ-mediated inhibition of voltage-gated $Ca_V2.2$ (N-type) channels, leading to decreased acetylcholine release into the synapse. Increased RGS4 expression blocks this inhibition and allows more acetylcholine release, exacerbating Parkinsonian motor symptoms (Ding et al. 2006).

Within the striatum, RGS4 also regulates dopaminergic control of striatal LTD. Here, RGS4 modulates G protein signaling postsynaptically in indirect pathway medium spiny neurons

(MSNs), the primary projection neurons of the striatum. Striatal endocannabinoid-dependent LTD (eCB-LTD) is induced by postsynaptic production of endocannabinoids (eCBs), which act on presynaptic CB1 receptors to lower the probability of neurotransmitter release (Figure 1D). Activation of group I mGluRs (Gq-coupled) is necessary for eCB-LTD, while activation of Gαi-coupled D2 dopamine receptors (D2DRs) positively modulates this form of synaptic plasticity (Kreitzer and Malenka 2005). Activation of Gαs-coupled adenosine A2A receptors antagonizes LTD induction (Lerner et al. 2010). Interestingly, in RGS4-KO mice, eCB-LTD can be induced even in the presence of D2DR antagonist and adenosine A2A receptor agonist (Lerner and Kreitzer 2012). Activation of the A2A receptor increases PKA activity, which has been shown to induce RGS4 activity via phosphorylation (Huang et al. 2007). This allows RGS4 to inhibit mGluR1/5 and D2DR-mediated release of eCBs, blocking LTD. Furthermore, when RGS4's block on eCB-LTD is removed, mice in a model of Parkinson's exhibit fewer behavioral deficits (Lerner and Kreitzer 2012). In this case as well as in the case of M4 receptor signaling in striatal cholinergic interneurons, inhibition of RGS4 could be a valuable non-dopaminergic therapeutic option that targets multiple signaling pathways within the striatum in the treatment of PD.

Outside of its links to PD in striatum, RGS4 has been studied most extensively in the context of neurological disease in the prefrontal cortex. Polymorphisms in RGS4 and decreased protein expression in the dorsolateral prefrontal cortex are strongly implicated in schizophrenia (Ding and Hegde 2009; Gu, Jiang, and Yan 2007; Mirnics et al. 2001; Paspalas, Selemon, and Arnsten 2009; Prasad et al. 2010; Prasad et al. 2005; Vrajova et al. 2011). One approach to understanding RGS4 roles in signaling in the prefrontal cortex has been to examine its subcellular localization in pyramidal neurons there. In macaques, postsynaptic RGS4 immunoreactivity appears high in extrasynaptic and perisynaptic regions of asymmetric synapses, which are typically

excitatory. Furthermore, at inhibitory symmetric synapses, RGS4 expression is high within presynaptic regions of axons (Paspalas, Selemon, and Arnsten 2009), indicating a role for RGS4 modulation of G protein signaling both pre- and postsynaptically in the prefrontal cortex. In the context of signaling at the synapse, RGS4 has been shown to specifically modulate 5-HT_{1A} serotonin receptor signaling, blocking postsynaptic serotonin-mediated inhibition of NMDA receptor current (Figure 1D), thereby providing a possible functional role for RGS4 in the pathogenesis of schizophrenia (Gu, Jiang, and Yan 2007). Activation of other GPCRs in the prefrontal cortex can also modulate postsynaptic glutamate receptor currents. Activation of α2 adrenergic receptors (α2ARs) reduces AMPA receptor currents while activation of $GABA_B$ receptors ($GABA_B$Rs) reduces NMDA receptor calcium influx. Both α2ARs and $GABA_B$Rs are Gαi-coupled, decreasing PKA activity and modulating glutamate receptor activity. Even when all of these receptors are expressed in the same spine, RGS4 appears capable of limiting crosstalk between the two Gαi-coupled receptors, aiding the inactivation of the G proteins and preventing interference between the two receptors' neuromodulatory functions despite their close proximity (Lur and Higley 2015). Decreases in RGS4 expression in schizophrenia could lead to increased crosstalk between different signaling pathways, leading to aberrant function.

Finally, RGS4 also has been shown to play a role in synaptic signaling and plasticity in the hypothalamus. Parvocellular neuroendocrine cells (PNCs) in the paraventricular nucleus (PVN) of the hypothalamus are at the head of the hypothalamic-pituitary-adrenal (HPA) axis, both mediating glucocorticoid release and responding to negative feedback (Wamsteeker and Bains 2010). Sustained stress unmasks presynaptic LTD_{GABA} in which the probability of GABA release onto these neurons is decreased by retrograde opioid release (Wamsteeker Cusulin et al. 2013). Notably, due to the decreased capacity for chloride extrusion of PNCs during stress, GABA is actually

excitatory (Hewitt et al. 2009), meaning that in this case LTD_{GABA} is decreasing excitation and potentially imposing a ceiling on HPA activation during prolonged glucocorticoid release. This LTD_{GABA} requires activation of postsynaptic mGluR5 in the PNC, which mediates the retrograde release of opioids from the somatodendritic compartment. RGS4 typically inhibits mGluR5 signaling here (Wamsteeker Cusulin et al. 2013). However, glucocorticoid receptor activation suppresses RGS4 expression (Ni et al. 1999), which increases mGluR5 signaling, thereby unmasking LTD_{GABA} (Wamsteeker Cusulin et al. 2013) and presenting a role for RGS4 as an inhibitor of synaptic plasticity in this system (Figure 1C). Overall, RGS4's expression in multiple brain regions as well as multiple subcellular compartments provides insight into the many ways in which the duration, location, and intensity of G protein activation can affect synaptic signaling and plasticity throughout the brain.

1.2.3 RGS7 and RGS9-2 regulation of synaptic plasticity

Shared Signaling properties: RGS7 and RGS9-2 are closely related proteins within the R7 subfamily of RGS proteins that share structural similarities and binding partners (Table 1). Unlike RGS2 and RGS4, which are small, simple RGS proteins containing a single RGS domain, RGS7 and RGS9 are larger, more complex proteins containing multi-domains that bind various common binding partners. Both proteins serve as a GAP for Gαi/o family members with varying degrees of selectivity for the different Gαi and Gαo subunits (Hooks et al. 2003). In addition to the canonical RGS domain, both proteins also contain a DEP (disheveled, Egl-10, pleckstrin) domain, an R7H (R7 homology) domain, and a GGL (G protein gamma subunit-like) domain. The GGL domain shares close homology with G protein gamma subunits and specifically binds G protein β5 (Gβ5) with high affinity (Snow et al. 1999). Therefore, RGS7 and RGS9-2 each exist as obligate heterodimers in complex with Gβ5 (Hollinger and Hepler 2002; Witherow et al. 2000; Snow et al.

1999). Binding partners and functions for the R7H domain remain elusive. The DEP domain binds R7BP, which can form a reversible complex with either RGS7:Gβ5 or RGS9-2:Gβ5 (Drenan et al. 2005; Martemyanov et al. 2005; Grabowska et al. 2008). R7BP is a regulatory protein that, when palmitoylated, anchors the RGS7:Gβ5 and the RGS9:Gβ5 complexes at the plasma membrane (Drenan et al. 2006; Jia, Linder, and Blumer 2011; Drenan et al. 2005), and protects these RGS proteins from degradation. R7BP palmitoylation is regulated by Gαi/o signaling, and R7BP facilitates R7:Gβ5 complex association with GIRK channels, which speeds up deactivation kinetics (Jia et al. 2014). Roles of R7BP in R7 family RGS signaling have been thoroughly reviewed (Jayaraman et al. 2009).

R7BP can serve to regulate the balance between RGS7 and RGS9-2 signaling by preferentially anchoring either protein at the membrane, leaving the other unprotected in the cytosol and subject to degradation. For example, RGS7 and RGS9-2 are both expressed within the same postsynaptic dendritic compartments of striatal neurons. R7BP binding (or lack thereof) dictates RGS protein plasma membrane localization versus degradation, and therefore the cellular ratio of RGS9-2 versus RGS7. Under basal conditions, R7BP preferentially couples to RGS9-2 at the plasma membrane. This system is tightly regulated by increased neuronal activity, increased cellular oxygen and calcium levels, and activation of protein kinase C, all of which can shift the ratio toward degradation of RGS9-2 (Anderson, Lujan, and Martemyanov 2009). In this case, R7BP uncouples from RGS9-2, is released into the cytosol, and binds RGS7 to recruit it to the membrane, where it is protected from degradation. Of note, recent reports suggest that RGS7 is membrane-recruited and stabilized by the orphan GPCR, GPR158 (Orlandi et al. 2012). Interestingly, GPR158 contains a C terminal region that is homologous with R7BP, which competitively binds the DEP domain of RGS7, and binding of RGS7 to GPR158 potentiates GAP

activity of RGS7 (Orlandi et al. 2015; Orlandi et al. 2012). Though GPR158 and R7BP form a mutually exclusive complex with RGS7 (Orlandi et al. 2012), future studies are needed to establish whether these binding partners are functionally redundant, divergent, or synergistic. In summary, RGS7 and RGS9-2 have very similar signaling properties despite being divergent in their brain expression pattern and regulation.

***RGS7*:** RGS7 is found throughout the brain (Khawaja et al. 1999), with reports indicating dense mRNA expression in the cerebellum, hypothalamus, thalamus (Lopez-Fando et al. 2005), and mRNA and protein expression in hippocampus (Shelat et al. 2006; Fajardo-Serrano et al. 2013) and striatum (Anderson, Lujan, and Martemyanov 2009; Larminie et al. 2004) (Table 1). Within the hippocampus, RGS7 is found mostly extrasynaptically in dendrites at asymmetric (primarily excitatory) synapses (Fajardo-Serrano et al. 2013), with Gβ5 regulating the cellular distribution of RGS7 (Rose et al. 2000). RGS7 acts as a GAP for Gαo and Gαi subunits (Rose et al. 2000; Posner, Gilman, and Harris 1999; Lan et al. 1998; Shuey et al. 1998) and negatively modulates $GABA_BR$ signaling (Fajardo-Serrano et al. 2013; Ostrovskaya et al. 2014). Of note, RGS7 interacts in a phosphorylation-dependent manner with the regulatory protein 14-3-3, which binds the RGS domain of RGS7 to inhibit its GAP activity (Benzing et al. 2000). TNF-α negatively regulates this interaction (Benzing et al. 2002), and simultaneously prevents proteasomal degradation of RGS7, consequentially leading to stabilization and upregulation of RGS7 protein (Benzing et al. 1999).

Within postsynaptic membranes of neurons, the RGS7:Gβ5 complex regulates GIRK channels (Saitoh et al. 1999; Kovoor et al. 2000; Fajardo-Serrano et al. 2013; Xie et al. 2010; Ostrovskaya et al. 2014), which serve important roles in mediating hyperpolarization of the neuron (Figure 1C). This process can be regulated by 14-3-3. RGS7 greatly accelerates the deactivation GIRK in oocytes, and the introduction of 14-3-3 reduces the RGS7-mediated deactivation of GIRK

currents, consistent with its negative regulatory effects on RGS7 GAP activity (Benzing et al. 2002). Co-expression with R7BP enhances the capacity of RGS7 to regulate GIRK channel activity, presumably by stabilizing RGS7:Gβ5 at the plasma membrane (Drenan et al. 2005). Compelling evidence suggests that RGS7's effect on GIRK channels is due to its action at the $GABA_BR$. RGS7, Gβ5, $GABA_BR$ and GIRK all coexist in a macromolecular complex (Fajardo-Serrano et al. 2013), and genetic knockout of either RGS7 (Ostrovskaya et al. 2014), Gβ5 (Xie et al. 2010), or R7BP (Ostrovskaya et al. 2014) delays deactivation of $GABA_BR$-coupled GIRK currents. Furthermore, ablation of RGS7 or R7BP increases coupling efficiency between $GABA_BR$ and GIRK (Ostrovskaya et al. 2014), in that lower doses of the $GABA_BR$ agonist baclofen produce a stronger GIRK current. Additionally, ablation of RGS7 decreases the intrinsic excitability of hippocampal pyramidal neurons, and impairs LTD and depotentiation (which is reliant on GIRK channels). This was shown to be a postsynaptic mechanism, as paired pulse facilitation was unaltered in the RGS7 knockout mice, which is consistent with RGS7's subcellular expression pattern. In summary, RGS7 is tightly coupled with $GABA_BR$-GIRK signaling on postsynaptic dendrites and spines, which serves as a major player in the modulation of depotentiation of LTP.

Though defined roles for RGS7 in human diseases are unclear, mouse models have begun to elucidate roles for RGS7 in plasticity and behavioral output. Consistent with RGS7 regulation of hippocampal excitability, RGS7 knockout mice show deficits in several tasks of learning and memory, including contextual fear learning, and spatial/contextual learning and memory (Morris water maze, and novel object recognition) (Ostrovskaya et al. 2014). Evidence for RGS7 mediating the effects of the $GABA_BR$ on neuronal excitability extends to behavior. As discussed, Gβ5 is an obligate dimer with RGS7, and loss of Gβ5 results in loss of R7 family of RGS proteins, including RGS7 (Chen et al. 2003). Gβ5 knockout mice show a dose-dependent decrease in locomotion in

response to the $GABA_B$ agonist baclofen (Xie et al. 2010). Within the striatum, RGS7 knockdown enhances locomotor sensitization to cocaine (Anderson et al. 2010), but not in R7BP knockout mice, suggesting a unique role, separate from RGS9-2, in psychostimulant-induced behavior. RGS7 also has been associated with panic disorder (Hohoff et al. 2009) as well as ischemia (Shelat et al. 2006), though RGS7's roles in these neurological disorders, if any, need further elucidation.

***RGS9-2*:** RGS9 was originally cloned from retina (now identified as RGS9-1), and characterized as a retina specific GAP for the resident G protein, transducin (Gαt) (Cowan et al. 1998; He, Cowan, and Wensel 1998). However, this sequence was recognized as a shorter splice variant of a longer, striatum-specific isoform of RGS9, which was named RGS9-2 (Rahman et al. 1999). Subsequent work demonstrated that RGS9-2 also is found in other brain regions, specifically periaqueductal grey (PAG) (Zachariou et al. 2003) and thalamus (Lopez-Fando et al. 2005) (Table 1). RGS9-2 was initially characterized as a GAP for Gαi/o coupled to the μ-opioid receptor (MOR) (Rahman et al. 1999), and was later found to modulate D2 dopamine receptor (D2DR) signaling and trafficking. Consistent with these findings, RGS9-2 colocalizes with D2DR and enkephalin in medium spiny neurons (Rahman et al. 2003; Kovoor et al. 2005). The DEP binding protein, R7BP, which protects RGS9-2 from proteasomal degradation (Anderson et al. 2007), is reported to mediate RGS9-2 interaction with the D2DR at the plasma membrane. In one study, an expressed DEP motif alone was recruited to the membrane by D2DR, whereas DEP-less RGS9-2 remained in the cytosol, indicating that the DEP domain is both necessary and sufficient for targeting RGS9-2 to the D2DR and the plasma membrane (Kovoor et al. 2005).

Similar to RGS7, RGS9-2 accelerates the off-kinetics for D2-coupled GIRK channels when co-expressed in oocytes (Rahman et al. 2003) (Figure 1D), an effect that is dependent on the DEP domain (Kovoor et al. 2005), and a functional RGS domain (Celver, Sharma, and Kovoor 2010).

In medium spiny neuron (MSN) slice preparations of RGS9-2 knockout (RGS9-2-KO) mice, glutamate-evoked inward currents are inhibited by a D2DR agonist, suggesting a functional role of RGS9-2 in postsynaptic excitability. Indeed, RGS9-2-KO mice show severe abnormal movements following administration of a D2DR agonist (Kovoor et al. 2005). RGS9-2 also regulates receptor internalization, a method of modulating neuronal excitability. Overexpression of the RGS9-2:Gβ5 complex (but not full length RGS9-2 alone or DEP-less RGS9-2) inhibits agonist-dependent D2DR internalization (Celver, Sharma, and Kovoor 2010). MOR signaling and sensitization is also heavily dependent on RGS9-2 activity (Figure 1D). RGS9-2 depletion (and Gβ5 depletion, consistent with the requisite dimer) enhances the analgesic potency and duration of morphine (Sanchez-Blazquez et al. 2003) as well as MOR endocytosis (Psifogeorgou et al. 2007), likely due to unabated stimulation of MOR-activated signals. Further supporting evidence for RGS9-2 functional interactions with MOR signaling includes the finding that RGS9-2 inhibits morphine-induced ERK activation (while a DEP-less RSG9-2 enhances pERK), along with the observation that RGS9-2 translocates to the plasma membrane following MOR activation (Psifogeorgou et al. 2007). In summary, RGS9-2 modulates receptor-membrane localization as well as postsynaptic neuronal excitability by regulating Gαi/o-linked GPCRs coupled to GIRK channels.

Beyond the synapse, RGS9-2 protein expression is both influenced by (Burchett et al. 1998; Rahman et al. 2003), and regulates (Rahman et al. 2003) psychostimulant-induced behavior. These observations are not unexpected given the striatal expression of RGS9-2. In these studies, RGS9-2 overexpression inhibits cocaine-induced hyperactivity, whereas RGS9-2 knockout mice show enhanced sensitivity to cocaine-induced hyperactivity and place preference (Rahman et al. 2003). Perhaps due to its role in dopaminergic signaling in the striatum, RGS9-2 also has been implicated

in both schizophrenia (Seeman et al. 2007) and dyskinesias (Kovoor et al. 2005). Activation of opiate receptors alters and is affected by RGS9-2 expression. For example, acute morphine treatment increases RGS9-2 protein expression, whereas chronic morphine treatment decreases RGS9-2 in the nucleus accumbens (Psifogeorgou et al. 2007; Zachariou et al. 2003). This finding correlates with behavioral output driven by opiates. RGS9-2 knockout mice have a 10-fold greater sensitivity to the rewarding effects of morphine, as measured by place preference (Zachariou et al. 2003), a phenotype that is rescued by local, virally-driven overexpression of RGS9-2. RGS9-2-KO animals also are more sensitive to morphine analgesia (Garzon, Lopez-Fando, and Sanchez-Blazquez 2003), and have delayed tolerance to, and enhanced physical dependence on, morphine (Zachariou et al. 2003). In summary, RGS9-2 plays a prominent role in both psychostimulant- and opiate-induced plasticity, likely by regulating slow acting GPCR modulatory signals at synapses.

1.3 RGS14 protein architecture

RGS14, a member of the R12 subfamily of RGS proteins, is a selective GAP for Gαi/o (Traver et al. 2000; Cho et al. 2000; Hollinger et al. 2001), having no effect on the GTPase activities of other Gα. Like RGS7 and RG9-2, RGS14 has a complex domain structure (Snow et al. 1997) that contains additional domains/motifs that interact with both heterotrimeric and monomeric G proteins, modulating their function. The GPR motif (also known as a GoLoco motif) of RGS14 specifically binds inactive Gαi1-GDP and Gαi3-GDP subunits (Hollinger et al. 2001; Mittal and Linder 2004; Kimple et al. 2001), thereby serving to recruit cytosolic RGS14 to the plasma membrane and anchoring it there (Shu et al. 2007). In so doing, the GPR motif promotes formation of a RGS14:Gαi complex that is capable of interacting with GPCRs in the absence of Gβγ (Vellano, Maher, et al. 2011). Furthermore, RGS14 interacts with the monomeric G proteins Rap1 (Traver et al. 2000), Rap2 (Traver et al. 2000), and H-Ras (Willard et al. 2009; Shu,

Ramineni, and Hepler 2010; Vellano et al. 2013) at its tandem Rap/Ras binding domains, although H-Ras is likely the functional binding partner in cells (Willard et al. 2009; Vellano et al. 2013).

RGS	Binding Partners at Defined Domains*	Brain Distribution	Subcellular Localization	Role in Synaptic Plasticity/Signaling	Links to Neurological Disease
RGS2	**$G\alpha_q$ at the RGS domain**(Heximer et al. 1997; Ingi et al. 1998) **$G\alpha_{i/o}$ at the RGS domain** (Han et al. 2006; Ingi et al. 1998)	**Hippocampus** (Han et al. 2006)	**Presynaptic in hippocampal pyramidal neurons** (Han et al. 2006)	**Regulates short term synaptic plasticity in the hippocampus** (Han et al. 2006) **Disinhibits GABA mediated inhibition of dopamine neurons in the VTA** (Labouebe et al. 2007)	**Anxiety** (Doupnik et al. 1997; Hohoff et al. 2015; Lifschytz et al. 2012; Okimoto et al. 2012) **Depression** (Lifschytz et al. 2012; Mandelli and Serretti 2013) **Post-traumatic stress disorder** (Amstadter et al. 2009) **Suicide** (Cui et al. 2008) **Panic disorder** (Koenen et al. 2009; Otowa et al. 2011; Hohoff et al. 2015)
		Striatum (Labouebe et al. 2007)	**Postsynaptic in dopamine neurons in the VTA** (Labouebe et al. 2007)		
		Amygdala (Okimoto et al. 2012)	NA		
		Thalamus (Ingi and Aoki 2002), **Neocortex** (Ingi and Aoki 2002), **Cerebellum** (Ingi and Aoki 2002)	NA		
RGS4	**$G\alpha_q$ at the RGS domain** (Hepler et al. 1997) **$G\alpha_{i/o}$ at the RGS domain** (Berman, Wilkie, and Gilman 1996)	**Layer V Prefrontal Cortex** (Paspalas, Selemon, and Arnsten 2009)	**Distal Dendrites, Spines, and Axons** (Paspalas, Selemon, and Arnsten 2009)	**Block postsynaptic serotonin-mediated signaling** (Gu, Jiang, and Yan 2007) **and prevent signaling crosstalk between multiple GPCRS at the synapse** (Paspalas, Selemon, and Arnsten 2009) **LTD_{GABA}** (Wamsteeker Cusulin et al. 2013) **Increase neuronal excitability** (Saugstad et al. 1998) **Inhibition of M4 autoreceptor signaling** (Ding et al. 2006) **Striatal LTD** (Lerner and Kreitzer 2012)	**Fragile X Syndrome** (Pacey et al. 2011) **Schizophrenia** (Prasad et al. 2010; Prasad et al. 2005) **Parkinson's Disease** (Ding et al. 2006; Lerner and Kreitzer 2012)
		Hypothalamus (Gold et al. 1997; Ni et al. 1999; Wamsteeker Cusulin et al. 2013; Kim et al. 2014)	**Parvocellular neuroendocrine cells in the paraventricular nucleus** (Wamsteeker Cusulin et al. 2013)		
		Hippocampus (Gold et al. 1997; Heraud-Farlow et al. 2013; Saugstad et al. 1998)	**Postsynaptic in CA1 pyramidal neurons** (Gold et al. 1997; Heraud-Farlow et al. 2013; Saugstad et al. 1998)		
		Striatum (Geurts, Maloteaux, and Hermans 2003; Ding et al. 2006; Schwendt and McGinty 2007; Lerner and Kreitzer 2012)	**Presynaptic in cholinergic interneurons** (Ding et al. 2006) **Postsynaptic in indirect pathway medium spiny neurons** (Lerner and Kreitzer 2012)		
RGS7	**$G\alpha_{i/o}$ at the RGS domain** (Posner, Gilman, and Harris 1999; Rose et al. 2000; Hooks et al. 2003) **Gβ5 at the GGL domain** (Snow et al. 1999) **R7BP at the DEP domain** (Drenan et al. 2005; Martemyanov et al. 2005)	**Hippocampus** (Ingi and Aoki 2002; Khawaja et al. 1999; Fajardo-Serrano et al. 2013; Ostrovskaya et al. 2014; Shelat et al. 2006; Xie et al. 2010)	**Extrasynaptic in dendrites** (Fajardo-Serrano et al. 2013)	**Accelerates GIRK deactivation via $GABA_B$ Receptors** (Fajardo-Serrano et al. 2013) **LTD and depotentiation in hippocampus** (Ostrovskaya et al. 2014)	**Hippocampal Ischemia** (Shelat et al. 2006) **Panic disorder** (Hohoff et al. 2009)
		Striatum (Khawaja et al. 1999; Anderson et al. 2010; Anderson, Lujan, and	**Postsynaptic** (Anderson, Lujan, and Martemyanov 2009; Anderson et al. 2010)		

		Martemyanov 2009; Lopez-Fando et al. 2005)			
		Cerebellum (Ingi and Aoki 2002; Khawaja et al. 1999) **Thalamus** (Ingi and Aoki 2002; Khawaja et al. 1999) **Hypothalamus** (Khawaja et al. 1999) **Amygdala** (Khawaja et al. 1999)	NA		
RGS9-2	**$G\alpha_{i/o}$ at the RGS domain** (Hooks et al. 2003) **Gβ5 at the GGL domain** (Makino et al. 1999) **R7BP at the DEP domain** (Martemyanov et al. 2005)	**Striatum** (Rahman et al. 1999; Gold et al. 1997)	**Extrasynaptic in dendrites** (Mancuso et al. 2010)	**Accelerates GIRK deactivation rate via D2 dopamine receptors** (Rahman et al. 2003; Kovoor et al. 2005; Celver, Sharma, and Kovoor 2010)	**Dyskinesias** (Kovoor et al. 2005) **Schizophrenia** (Seeman et al. 2007)
		Periaqueductal grey (Zachariou et al. 2003)	NA		
		Thalamus (Lopez-Fando et al. 2005)	NA		
RGS14	**$G\alpha_{i/o}$ at the RGS domain** (Hollinger et al. 2001; Cho et al. 2000; Traver et al. 2000) **H-Ras at the R1 Ras binding domain** (Vellano et al. 2013; Willard et al. 2009) **Gαi1/3 at the GPR (GoLoco) motif** (Hollinger et al. 2001; Kimple et al. 2001; Mittal and Linder 2004)	**Hippocampus** (Evans et al. 2014; Lee et al. 2010; Traver et al. 2000)	**Somatodendritic compartment of CA2 pyramidal neurons including the PSD** (Lee et al. 2010)	**Suppresses LTP in CA2 hippocampal neurons** (Lee et al. 2010; Vellano, Lee, et al. 2011)	**Anxiety** (Parker, Sokoloff, et al. 2012)
		Piriform cortex (Evans et al. 2014; Grafstein-Dunn et al. 2001) **Orbital cortex** (Evans et al. 2014) **Striatum** (Lopez-Aranda et al. 2006)	NA		

Table 1.1. Summary of RGS protein functions at the synapse and possible role in disease. Here, we list the binding partners, brain distribution, subcellular localization, functional signaling roles, and possible roles in disease of specific RGS proteins (RGS2, RGS4, RGS7, RGS9-2, RGS14) that have been clearly demonstrated to serve critical roles in modulating synaptic signaling and plasticity throughout the brain.

*Additional binding partners for many of these RGS proteins have been identified and shown to have functional roles modulating or mediating RGS protein signaling (Abramow-Newerly et al. 2006; Sethakorn, Yau, and Dulin 2010).

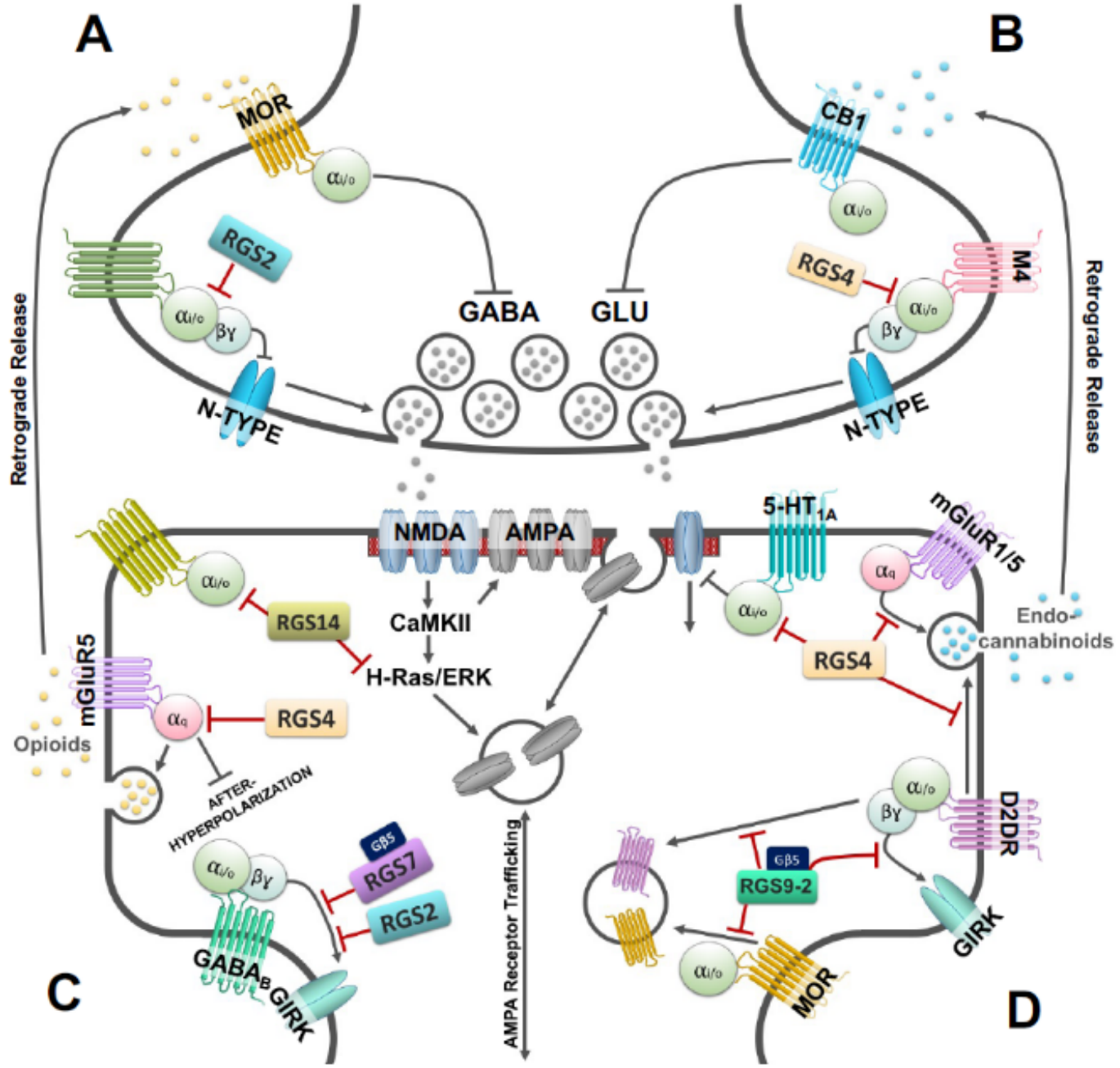

Figure 1.1. RGS Protein Regulation of Synaptic Signaling. RGS proteins regulate many aspects of pre- and post- synaptic signaling. **A)** Activation of presynaptic GPCRs releases Gβγ to inhibit

$Ca_V2.2$ (N-Type) Ca^{2+} channels and suppress neurotransmitter (glutamate, Glu and gamma-aminobutyric acid, GABA) release. Stimulated upregulation of RGS2 expression blocks Gβγ inhibition of $Ca_V2.2$ channels. **B)** Presynaptic release of acetylcholine activates M4 muscarinic acetylcholine autoreceptors that release Gβγ, and inhibit $Ca_V2.2$ channels to suppress neurotransmitter release. RGS4 blocks Gβγ inhibition of $Ca_V2.2$ channels. **C)** RGS14 associates with Gαi/o and forms a stable complex with Gαi at the plasma membrane, where it regulates H-Ras/ERK- and possibly calmodulin and CaMKII-dependent signaling events that underlie induction of LTP. Independent of this, RGS4 inhibits mGluR5 and Gαq-mediated suppression of the afterhyperpolarization current following action potential firing. Postsynaptic mGluR5 signaling also stimulates retrograde opioid release, which activates presynaptic mu-opioid receptors (MORs), suppressing presynaptic GABA release. RGS4 blocks mGluR5-mediated retrograde opioid release from parvocellular neuroendocrine cells (PNCs) in the hypothalamus, increasing GABA release onto these neurons. RGS2 and the RGS7-Gβ5 complex both block postsynaptic $GABA_B$ receptor-stimulated GIRK currents by promoting Gβγ deactivation. **D)** RGS4 blocks postsynaptic serotonin 5-HT1A receptor and Gαi/o-mediated inhibition of NMDA receptor currents. Postsynaptic mGluR5 and dopamine D2 receptor signaling stimulates retrograde release of endocannabinoids that stimulate presynaptic cannabinoid CB1 receptors to suppress Glu release and induce long-term depression (LTD) at the synapse. RGS4 suppresses both mGluR5/Gαq and D2DR/Gαi/o-mediated retrograde opioid release to inhibit induction of LTD. The RGS9-2:Gβ5 complex blocks postsynaptic $GABA_B$ receptor-stimulated GIRK currents by enhancing Gβγ deactivation. Finally, the RGS9-2:Gβ5 complex inhibits agonist-induced internalization of MORs and D2DRs. See the text for further details.

1.4 RGS14 interactions outside defined domains

Outside of the G proteins that have been found to interact directly with RGS14's recognized domains and binding motifs, proteomic analysis of proteins coimmunoprecipitated out of mouse brain with RGS14 has allowed us to identify a much wider range of potential functional binding partners. Two that have been further validated are Ca2+/calmodulin (CaM) and Ca2+/calmodulin-dependent protein kinase II (CaMKII) (Evans and Hepler 2012; Evans, Gerber, et al. 2018). CaM directly interacts with RGS14 in a calcium-dependent manner somewhere within tandem RBD region of RGS14, inducing conformational changes in RGS14 that may place it in a favorable state for interaction with a downstream CaM effector (Evans, Gerber, et al. 2018). Not only does RGS14 interact with CaMKII, but CaMKII is also capable of phosphorylating RGS14 at multiple sites (Evans, Gerber, et al. 2018). Furthermore, both CaM and CaMKII interact with RGS14 in hippocampal neurons (Evans, Gerber, et al. 2018), providing substantial evidence for calcium-dependent regulation of RGS14 function in its native environment, pyramidal cells in the CA2 region of the hippocampus.

RGS14 also interacts with the ubiquitously expressed phospho-serine and -threonine-binding protein, 14-3-3 (Gerber, Squires, and Hepler 2018). This interaction is potentiated by downstream signaling stemming from H-Ras activation though the specific kinase responsible for phosphorylating the residue on RGS14 to facilitate this phosphorylation-dependent interaction is unknown. Identification of this kinase has been especially difficult as H-Ras signaling needs to be active for an extended time to cause RGS14:14-3-3 interaction indicating that this interaction is facilitated by changes in the cellular environment at a transcriptional level instead of a more straightforward phosphorylation cascade. Regardless of the kinase directly responsible for mediating this interaction, binding of 14-3-3 at phosphorylated serine 218 of RGS14 inhibits Gαi1

binding to RGS14's RGS domain, presumably preventing RGS14 from acting as a GAP for Gαi when 14-3-3 is bound. This is the first known mechanism of phosphorylation-dependent regulation of RGS14 GAP activity. In addition to RGS14's phosphorylation-dependent interaction with 14-3-3 at serine 218, evidence has also been shown for a phosphorylation-independent interaction between RGS14 and 14-3-3 at a unique site separate from the interaction occurring at serine 218. Interestingly, this site appears to have control RGS14 translocation in and out of the nucleus, with 14-3-3 binding sequestering RGS14 in the cytosol, preventing its import into the nucleus (Gerber, Squires, and Hepler 2018).

RGS14 has long been known to translocate in and out of the nucleus (Cho, Kim, and Kehrl 2005). While RGS14 appears to be predominantly cytosolic, when cells expressing RGS14 are treated with leptomycin B, an inhibitor of nuclear export by CRM-1, RGS14 accumulates in the nucleus(Cho, Kim, and Kehrl 2005; Shu et al. 2007; Branch and Hepler 2017; Gerber, Squires, and Hepler 2018). This indicates that RGS14 is constantly shuttling in and out of the nucleus. More recently, endogenously expressed RGS14 has also been shown to shuttle in and out of the nucleus in B35 neuroblastoma cells(Branch and Hepler 2017), showing that this localization is not unique to exogenously expressed protein outside of its typical environment. Furthermore, we have shown that endogenously expressed RGS14 can be seen in the nucleus in primate brain(Squires et al. 2018) and that RGS14 maintains its ability to shuttle in and out of the nucleus in hippocampal neurons(Gerber, Squires, and Hepler 2018). All of these data point to a clear role for RGS14 in the nucleus, possible controlling transcription and subsequent translation, though further study is required to elucidate RGS14's function in this part of the cell. It is also unclear if RGS14's presence in the nucleus is tied to its role as a suppressor of synaptic plasticity.

While RGS14 shuttles in and out of the nucleus, it can also be anchored to cell membranes isolated from brain (Hollinger et al. 2001) . Examining contributions of specific binding partners to RGS14 membrane localization, inactive Gαi1 and 3 have been shown to anchor RGS14 to the plasma membrane through interaction at RGS14's GPR motif(Shu et al. 2007; Brown et al. 2015). Active Gαo also recruits RGS14 to the plasma membrane presumably through binding at the RGS domain of RGS14(Brown et al. 2015). Additionally, active H-Ras is also capable recruiting RGS14 to the plasma membrane through interaction at the R1 domain (Shu, Ramineni, and Hepler 2010). Notably, RGS14 interactions with inactive Gαi anchors RGS14 to the membrane and prevents its translocation to the nucleus providing a potential mechanism by which RGS14 nuclear localization is regulated(Shu et al. 2007). It is likely that this effect extends to the other binding partners capable of recruiting RGS14 to the plasma membrane as well. This interplay between RGS14 nuclear and plasma membrane localization almost certainly has a role in RGS14's function as a suppressor of synaptic plasticity but specific contributions of RGS14 subcellular localization to its regulation of neuronal signaling have yet to be identified.

1.5 RGS14 is a native suppressor of LTP in area CA2

The first hints of RGS14 function in neuronal signaling came from studies of its protein expression patterns in brain (Table 1), with protein and mRNA expression in adult rodents limited largely to the hippocampus and olfactory cortex(Evans et al. 2014; Lee et al. 2010; Lein et al. 2007). Within the hippocampus of rodents, RGS14 expression is limited to area CA2, specifically within postsynaptic dendrites and spines of pyramidal neurons (Lee et al. 2010; Evans et al. 2014; Traver et al. 2000). While RGS14 is still enriched in the CA2 region of the hippocampus of primates, it has a broader expression pattern, with significant expression in the basal ganglia and amygdala(Squires et al. 2018). Outside of the hippocampus, the function of RGS14 is unknown.

Notably, within the hippocampus proximal dendrites of CA2 neurons that receive Schaffer collateral projections from area CA3 are incapable of eliciting LTP under the same conditions that reliably provoke LTP in hippocampal CA1 neurons (Zhao et al. 2007). However, mice lacking RGS14 (RGS14-KO) exhibit robust LTP in CA2 neurons, demonstrating that RGS14 is a natural suppressor of synaptic plasticity within these neurons (Lee et al. 2010). Consistent with this idea, RGS14-KO mice perform markedly better than wild type mice in hippocampal-dependent tasks of spatial/contextual learning (Morris water maze) and memory (novel object recognition) that are associated with LTP (Lee et al. 2010).

The exact mechanism by which RGS14 suppresses LTP is currently unclear, though RGS14 engages signaling proteins and pathways that are critical for LTP. RGS14 binds active H-Ras to inhibit ERK activation (Shu, Ramineni, and Hepler 2010), which is necessary for AMPA receptor trafficking and LTP in CA1 neurons (Atkins et al. 1998; English and Sweatt 1997). RGS14 also can bind calcium-activated calmodulin (Ca^{2+}/CaM) in a calcium-dependent manner (Evans and Hepler 2012; Evans, Gerber, et al. 2018), which is essential for regulating both CaMKII- and ERK-dependent signaling events that underlie induction of LTP as well as CaMKII itself (Evans, Gerber, et al. 2018). Furthermore, RGS14 has recently been shown to regulate postsynaptic calcium levels with calcium transients in area CA2 of wild type mice during induction of plasticity being significantly attenuated compared to CA2 pyramidal cells in RGS14-KO mice(Evans, Parra-Bueno, et al. 2018). The mechanism by which RGS14 regulates postsynaptic calcium handling though is unclear. In relation to RGS14 control of G protein signaling, recent evidence suggests that the RGS domain of RGS14 maintains GAP activity when its GPR motif is bound to inactive Gαi subunits at the plasma membrane (Brown et al. 2015). This supports a model (Brown et al. 2015) in which cytosolic RGS14 could be recruited initially to the postsynaptic

density (PSD) through its RGS domain following GPCR and Gαi activation, where its GPR motif captures the resulting inactive Gαi-GDP (Figure 1C). In this way, the newly formed RGS14:Gαi complex is properly placed to GAP other nearby Gαi/o-GTP enabling those resulting Gαi-GDP to recruit and cluster additional RGS14:Gαi complexes to form a signaling node at or near the plasma membrane and possibly the PSD(Brown et al. 2015). In this speculative scenario, RGS14 would be well positioned to intercept local signals necessary for the induction of LTP, such as H-Ras activation of ERK and/or Ca^{2+}/CaM activation of CaMKII. Further studies are necessary to confirm this model. In summary, RGS14's modulation of synaptic plasticity in hippocampal area CA2 provides a unique example of RGS protein action at the synapse, with the RGS domain acting in concert with multiple other domains and signaling partners/pathways to tightly modulate downstream synaptic signaling.

1.6 Overall Hypothesis and Objective of this Research

The CA2 region of the hippocampus can be identified through anatomical details that distinguish it from the surrounding CA regions as well as through unique protein expression and physiology. One of the key differences between CA2 and CA1 is CA2's resistance to multiple forms of plasticity including long-term potentiation (Simons et al. 2009; Lee et al. 2010; Caruana, Alexander, and Dudek 2012; Evans, Parra-Bueno, et al. 2018; Zhao et al. 2007), which has been shown to be necessary for normal learning and memory in CA1. Multiple factors have been shown to contribute to this lack of plasticity, including the expression of RGS14 (Lee et al. 2010). RGS14 expression has been shown to be sufficient to suppress LTP in hippocampal neurons but the exact mechanism of this suppression is still unclear. The primary goal of my dissertation project was to identify key protein-protein interactions that mediate RGS14 function in the CA2 region of the hippocampus.

The first aim of this project was to use unbiased proteomic analysis to determine the RGS14 interactome in mouse brain. While many RGS14 binding partners have been identified and studied *in vitro* (Traver et al. 2000; Cho et al. 2000; Hollinger, Ramineni, and Hepler 2003; Shu et al. 2007; Willard et al. 2009; Shu, Ramineni, and Hepler 2010; Vellano, Maher, et al. 2011; Vellano et al. 2013; Zhao et al. 2013; Brown et al. 2015; Brown, Lambert, and Hepler 2016; Branch and Hepler 2017), little is known about potential RGS14 binding partners that do not have a defined interaction domain or motif within RGS14 that may heavily contribute to RGS14's function as a suppressor of synaptic plasticity. In order to understand the mechanism through which RGS14 suppresses LTP in the CA2 region of the hippocampus, I wanted to generate a comprehensive understanding of the RGS14 interactome in mouse brain. To this end, I performed immunoprecipitations of RGS14 from mouse brain, which were then submitted to proteomic analysis to identify potential functional binding partners for RGS14. These results are discussed in Chapter 2.

The second aim of this project was to better understand the proteomic profile of area CA2 as compared to area CA1 to understand cellular environment in which RGS14 is acting to suppress plasticity. While many studies have focused on the differences between areas CA1 and CA3 (Gozal et al. 2002; von Ziegler et al. 2018), the CA2 region has been largely ignored and the specific proteins and signaling events responsible for its physiological differences from CA1 are poorly understood. To gain insight into the proteins mediating the physiology that makes CA2 unique from area CA1, I needed to know which proteins were preferentially expressed in CA2 (vs. CA1). Using dissection directed by GFP expressed specifically in area CA2, I performed a proteomic analysis identifying a CA2 specific proteome, identifying proteins that may mediate physiological

differences between CA2 and CA1 as well as providing context for our RGS14 interactome in the region in which RGS14 is natively expressed. These findings are discussed in Chapter 3.

The third aim of this project was to use information from the first two aims to identify and further study a functional interaction between RGS14 and another protein. The protein I chose was 14-3-3, which is highly expressed throughout the hippocampus, including in area CA2 (Baxter et al. 2002; Qiao et al. 2014). 14-3-3 was also found to interact with RGS14 in our proteomic analysis in mouse brain. Using a combined approach of biochemical techniques, bioluminescence resonance energy transfer, primary hippocampal neuron culture, and immunocytochemistry and subsequent confocal microscopy, I elucidated the multifunctional interaction between RGS14 and 14-3-3 in hippocampal neurons. These findings are discussed in Chapter 4.

Overall, the goal of these studies was to investigate functional interactions between RGS14 and other proteins in the brain to better understand how RGS14 works in the context of the CA2 region of the hippocampus. This work broadens our understanding not only of the many proteins that RGS14 interacts with to suppress LTP but also our understanding of the CA2 region of the hippocampus in general. Knowing what makes CA2 different from CA1 and determining how RGS14 is functioning in this enigmatic brain region advances our understanding of the cellular mechanisms behind synaptic plasticity and learning and memory. This work furthers our understanding of the mechanism by which RGS14 suppresses LTP in area CA2 and leads to a point at which we may understand why a protein that suppresses learning and memory is expressed in the hippocampus.

Chapter 2:

Interactome Analysis Reveals Regulator of G Protein Signaling 14 (RGS14) as a Complex Scaffold Protein at the Synapse

This chapter contains figures and text that have been modified from the published manuscript: Evans, P. R., **Gerber, K. J.**, Dammer, E. B., Duong, D. M., Goswami, D., Lustberg, D. J., Zou, J., Yang, J. J., Dudek, S. M., Griffin, P. R., Seyfried, N. T., and Hepler, J. R. (2018) Interactome Analysis Reveals Regulator of G Protein Signaling 14 (RGS14) is a Novel Calcium/Calmodulin (Ca(2+)/CaM) and CaM Kinase II (CaMKII) Binding Partner, *J Proteome Res*. **17**(4): 1700-1711.

2.1 Introduction

Synaptic plasticity is a vital process through which neurons modulate the strength of specific synaptic connections and is thought to encode key aspects of memory. Simultaneous neuronal activity and glutamate release at synapses activate intracellular and extracellular signaling cascades that induce plasticity. Regulator of G Protein Signaling 14 (RGS14) is a complex RGS protein that naturally suppresses synaptic plasticity in hippocampal CA2 neurons and hippocampus-dependent learning and memory (Lee et al. 2010). RGS14 mRNA and protein are highly expressed in the brains of adult rodents and primates (Evans et al. 2014; Squires et al. 2018). In the adult mouse brain, RGS14 predominantly localizes to CA2 pyramidal neurons in the hippocampus (Evans et al. 2014) where it is enriched postsynaptically in dendrites and spines (Lee et al. 2010; Squires et al. 2018) Unlike pyramidal neurons in the neighboring CA1 subregion, CA2 pyramidal neurons resist long-term potentiation (LTP) of synaptic transmission (Zhao et al. 2007), a form of plasticity that is widely believed to serve as the cellular correlate of memory formation. Mice lacking RGS14 (RGS14 KO) display a robust and nascent capacity for LTP induction in CA2 neurons that is absent in wild-type (WT) littermates (Lee et al. 2010), and RGS14 KO mice also exhibit markedly enhanced spatial learning compared with WT littermates (Lee et al. 2010). Thus, RGS14 plays a critical role in naturally restricting CA2 synaptic plasticity and hippocampus-based learning.

RGS14 possesses multiple protein binding domains through which it engages various binding partners to integrate signaling pathways related to plasticity (Evans, Dudek, and Hepler 2015; Vellano, Lee, et al. 2011). Similar to other RGS proteins(Hollinger and Hepler 2002), RGS14 contains an RGS domain through which it directly binds activated Gαi/o-GTP subunits and stimulates their intrinsic GTPase activity to limit heterotrimeric G protein signaling (Traver et

al. 2000; Hollinger et al. 2001; Brown et al. 2015). Unlike most other proteins, RGS14 contains a G protein regulatory (GPR) motif, an additional G protein interacting domain (Traver et al. 2000; Hollinger et al. 2001; Cho et al. 2000), through which it selectively binds inactive $G\alpha i_{1/3}$-GDP to localize RGS14 to cellular membranes (Brown et al. 2015; Kimple et al. 2001; Mittal and Linder 2004; Shu et al. 2007). RGS14 also contains two tandem Ras/Rap-binding domains (RBDs, R1 and R2) through which it preferentially interacts with activated H-Ras-GTP and Rap2-GTP as well as Raf kinases (Traver et al. 2000; Shu, Ramineni, and Hepler 2010; Vellano et al. 2013; Kiel et al. 2005). RGS14 can functionally integrate G protein and MAPK signaling by inhibiting growth factor driven ERK1/2 activity through cooperative interactions between the GPR and first RBD (Shu, Ramineni, and Hepler 2010). Consistent with this idea, the plasticity unmasked in CA2 neurons of RGS14 KO mice due to loss of RGS14 requires intact ERK activity (Lee et al. 2010). However, additional cellular mechanisms by which RGS14 governs plasticity in its host CA2 hippocampal neurons remain elusive.

While some studies have investigated RGS14 binding partners and signaling functions as recombinant proteins in ectopic systems (Evans, Dudek, and Hepler 2015; Vellano, Lee, et al. 2011), none so far have examined these interactions in brain where RGS14 is enriched. Thus, to gain a better understanding of the signaling network RGS14 engages in CA2 neurons to limit synaptic plasticity therein, we initiated studies to identify endogenous binding partners of RGS14 in neurons. To accomplish this, we performed mass spectrometry analysis on native RGS14 protein complexes immunoprecipitated from mouse brain. We show that RGS14 interacts with a large number of proteins associated with the synapse, specifically the neuron spine, placing RGS14 in the perfect position to modulate synaptic signaling to suppress plasticity. Of the many groups of proteins with which we see RGS14 interacting, proteins associated with the myosin complex and

calmodulin-dependent kinase activity are the top interactors. Both of these groups are heavily implicated in the control of structural and synaptic plasticity and provide many interesting targets for future study that will help us understand the precise molecular mechanism by which RGS14 suppresses LTP in CA2 hippocampal neurons.

2.2 Experimental Procedures

Animals - Adult male and female wild-type C57BL/6J mice were used in this study. Animals in all experiments were housed under a 12 h/12 h light/dark cycle with access to food and water *ad libitum*. All experimental procedures conformed to US NIH guidelines and were approved by the animal care and use committees of Emory University and NIEHS/NIH.

Mouse Brain Coimmunoprecipitation and Proteolytic Digestion - Adult wild-type C57BL/6J mice were deeply anesthetized by isoflurane inhalation and euthanized by decapitation. Brains were rapidly removed from the skull and homogenized on ice using a glass dounce homogenizer with 10 strokes in an ice-cold buffer containing 50 mM Tris, 150 mM NaCl, 5 mM EDTA, 5 mM MgCl2, 2 mM DTT, Halt phosphatase inhibitor cocktail (1:100, Thermo Fisher), and one mini protease inhibitor cocktail tablet (Roche Applied Science), pH 7.4. Membranes were solubilized by the addition of 1% NP-40 for 1h at 4 °C and subsequently centrifuged to pellet debris. Cleared brain homogenates were incubated with an anti-RGS14 mouse monoclonal antibody (5 μg, NeuroMab) for 2 h at 4 °C. Next, 75 μL of Protein G Dynabeads (Thermo Fisher) was added to homogenates for 2 h to precipitate antibody-bound protein complexes. Protein G Dynabeads were washed thoroughly with ice-cold TBS and immediately digested for MS. IPs were simultaneously performed with generic mouse IgG (Millipore) as a control for comparative MS analysis. Three independent biological replicates were performed for each condition. Following four washes with ice cold TBS, the control beads or RGS14 immunoprecipitated samples were

resuspended in 50 mM NH4HCO3 buffer and protein reduced with 1 mM dithiothreitol (DTT) at 25 °C for 30 min, followed by 5 mM iodoacetimide (IAA) at 25 °C for 30 min in the dark. Protein was then digested overnight with 12.5 ng/μL trypsin (Promega) at 25 °C. Resulting peptides were desalted with a stage tip and dried under vacuum.

Mass Spectrometry Analysis of RGS14 Interacting Proteins - For LC-MS/MS analysis, peptides were resuspended in 10 μL of loading buffer (0.1% formic acid, 0.03% trifluoroacetic acid, 1% acetonitrile) essentially as previously described with slight modification (Umoh et al. 2018a). Peptide mixtures (2 μL) were separated on a selfpacked C18 (1.9 μm Dr. Maisch, Germany) fused silica column (25 cm × 75 μM internal diameter (ID); New Objective, Woburn, MA) by a Dionex Ultimate 3000 RSLCNano and monitored on a Fusion mass spectrometer (ThermoFisher Scientific, San Jose, CA). Elution was performed over a 120 min gradient at a rate of 250 nL/min with buffer B ranging from 3% to 80% (buffer A: 0.1% formic acid in water, buffer B: 0.1% formic in acetonitrile). The mass spectrometer cycle was programmed to collect at the top speed for 3 s cycles. The MS scans Journal of Proteome Research Article DOI: 10.1021/acs.jproteome.8b00027 J. Proteome Res. 2018, 17, 1700−1711 1701 (300−1500 *m/z* range, 200 000 AGC, 50 ms maximum ion time) were collected at a resolution of 120 000 at *m/z* 200 in profile mode and the HCD MS/MS spectra (1.5 *m/z* isolation width, 30% collision energy, 10 000 AGC target, 35 ms maximum ion time) were detected in the ion trap. Dynamic exclusion was set to exclude previous sequenced precursor ions for 20 s within a 10 ppm window. Precursor ions with +1, and +8 or higher charge states were excluded from sequencing.

MaxQuant for Label-Free Protein Quantification - Raw data files were analyzed using MaxQuant v1.5.3.30 with Thermo Foundation 2.0 for RAW file reading capability. The search engine Andromeda was used to build and search a Uniprot mouse reference (downloaded on Aug

14, 2015). Protein Methionine oxidation (+15.9949 Da) and protein N-terminal acetylation (+42.0106 Da) were variable modifications (up to 5 allowed per peptide); cysteine was assigned a fixed carbamidomethyl modification (+57.0215 Da). Only fully tryptic peptides were considered with up to 2 miscleavages in the database search. A precursor mass tolerance of ±20 ppm was applied prior to mass accuracy calibration and ±4.5 ppm after internal MaxQuant calibration. Other search settings included a maximum peptide mass of 6000 Da, a minimum peptide length of 7 residues, 0.5 Da Tolerance for ion trap HCD MS/MS scans. The false discovery rate (FDR) for peptide spectral matches and proteins were set to 1%. The label free quantitation (LFQ) algorithm in MaxQuant (Luber et al. 2010; Cox et al. 2014a) was used for protein quantitation. LFQ intensity of each protein for each mouse was averaged from three bead control IP samples and three RGS14 IP samples. No more than two missing values were considered in the RGS14 IP samples, which were imputed as previously described (Tyanova et al. 2016). Differentially expressed proteins were found by calculating Student's t test p values and fold difference | log2(*RGS14/nonspecific IgG*)| ≥ 0.58 (≥ ± 1.50 fold change). Volcano plots were plotted with ggplot2 package in R. The mass spectrometry proteomics data have been deposited to the ProteomeXchange Consortium via the PRIDE(Vizcaino et al. 2016) partner repository with the data set identifier PXD008461.

Gene Ontology Enrichment Analysis and Visualization - Functional enrichment of the differentially aggregated proteins was determined using the GO-Elite (v1.2.5) package (Zambon et al. 2012) as previously described (Hales et al. 2016). The set of total proteins identified and quantified (n = 1362) was used as the background. The input list included proteins significantly interacting ($p < 0.05$) with RGS14 (n = 233). Positive Z-score determines degree of over-representation of ontologies and Fisher exact P-value was used to assess the significance of the Z-score. For both increased and decreased proteins in the insoluble proteome, a Z-score cut off of

1.96, (P-value cut off of 0.05) with a minimum of 3 proteins per category was employed. Horizontal bar graph was plotted in R. A visualization of the GO terms for the RGS14 interactors was performed using the EnrichmentMAP plugin for Cytoscape v.3.2.1, after converting GO-Elite pruned output to DAVID format (Huang da, Sherman, and Lempicki 2009a, 2009b). A subset of proteins falling within six of those ontologies was further visualized as a circular chord plot using the R GOplot package.

2.3 Results

RGS14 is a complex, multidomain scaffold protein with many known interactors but the proteins that RGS14 interacts with to suppress plasticity in CA2 hippocampal neurons are unknown. To determine the proteins interacting with RGS14, endogenous RGS14 was immunoprecipitated (IP) from mouse brain and subjected to mass spectrometry to identify interacting proteins as described in Experimental Procedures. Of the 1362 total proteins identified and quantified, 233 specific RGS14 interactors were significantly enriched over IgG IP controls. All 233 hits met the following explicit selection criteria: the IP and control IgG pulldown were performed in triplicate, LFQ intensity missing values for the RGS14 were controlled so that imputation could not drive the differences, and a *t* test *p*value of <0.05 was enforced to arrive at the list of 233 candidate interactors. These data are shown in the half volcano plot (Figure 1A) with significantly enriched RGS14 interactors highlighted on the right boxed in yellow. A gene ontology (GO) analysis of RGS14 interacting proteins is shown in Figure 1B with hits grouped according to biological process, molecular function, and cellular component plotted as a function of Z-score. Of note, the most significant molecular function clusters represent actin binding, calmodulin(CaM)-dependent protein kinase (CaMK) activity, and CaM binding—all of which are critical for long-term potentiation (LTP) in the hippocampus. An enrichment map is provided for

all GO hits (Figure 1C) that depicts the discrete GO terms and the number of genes that overlap between these groups. The top enriched RGS14 interacting proteins are displayed in the circle plot ordered by enrichment with corresponding GO terms on the right (Figure 2). Consistent with the postsynaptic localization of RGS14 in CA2 pyramidal neurons (Lee et al. 2010; Squires et al. 2018), functional annotation groups a substantial portion of the interacting proteins to dendritic spines and synapses.

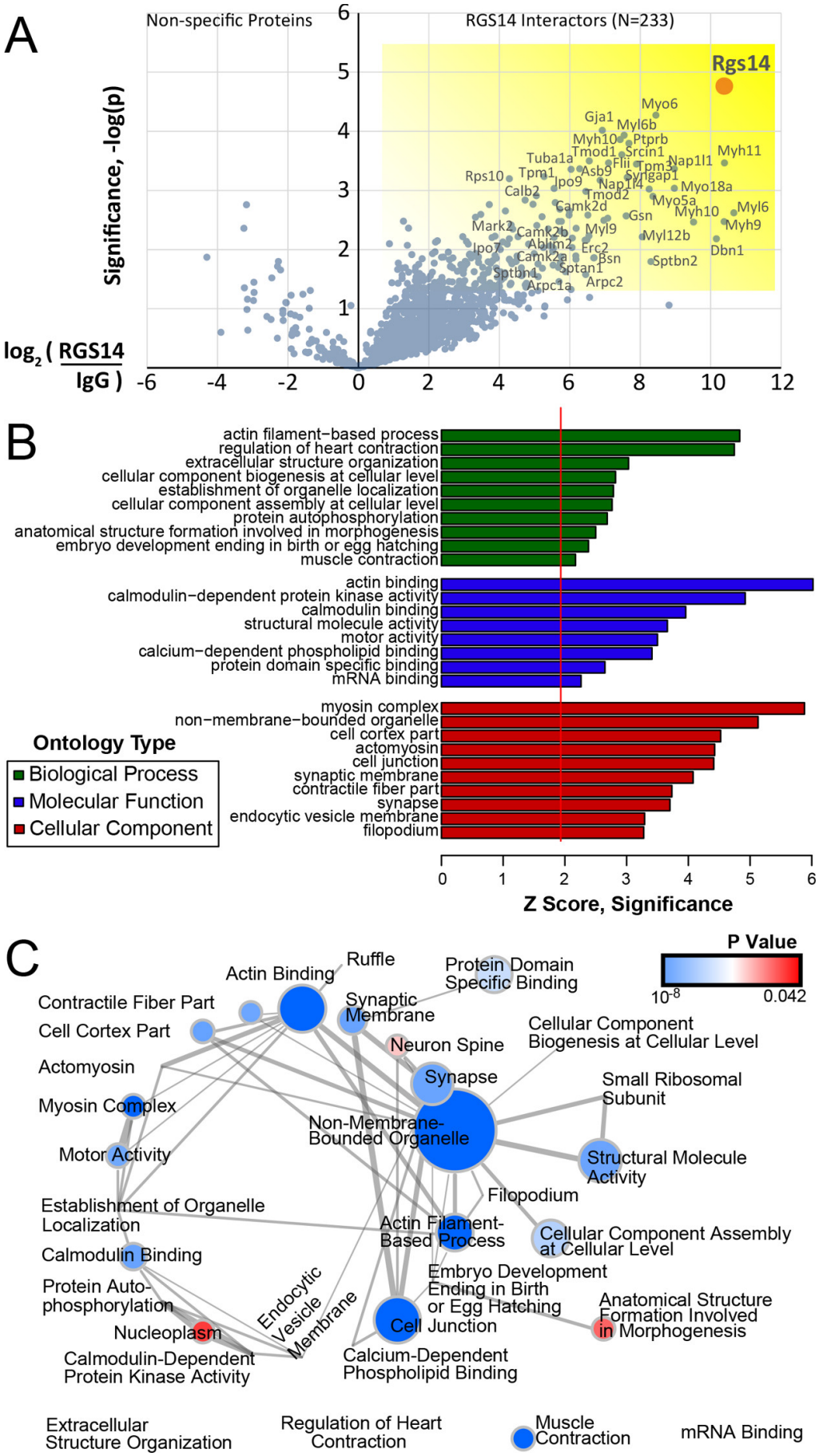
A
Non-specific Proteins
RGS14 Interactors (N=233)
Rgs14
Significance, -log(p)
log2 (RGS14 / IgG)
Myo6
Gja1
Myl6b
Myh10
Ptprb
Tmod1
Srcin1
Myh11
Tuba1a
Flii
Tpm3
Nap1l1
Rps10
Tpm1
Asb9
Synga p1
Ipo9
Nap1l4
Myo18a
Calb2
Tmod2
Myo5a
Camk2d
Gsn
Myh10
Myl6
Myh9
Mark2
Camk2b
Myl9
Myl12b
Ablim2
Ipo7
Erc2
Dbn1
Camk2a
Bsn
Sptbn2
Sptbn1
Sptan1
Arpc1a
Arpc2
B
actin filament−based process
regulation of heart contraction
extracellular structure organization
cellular component biogenesis at cellular level
establishment of organelle localization
cellular component assembly at cellular level
protein autophosphorylation
anatomical structure formation involved in morphogenesis
embryo development ending in birth or egg hatching
muscle contraction
actin binding
calmodulin−dependent protein kinase activity
calmodulin binding
structural molecule activity
motor activity
calcium−dependent phospholipid binding
protein domain specific binding
mRNA binding
myosin complex
non−membrane−bounded organelle
cell cortex part
actomyosin
cell junction
synaptic membrane
contractile fiber part
synapse
endocytic vesicle membrane
filopodium
Ontology Type
Biological Process
Molecular Function
Cellular Component
Z Score, Significance
C
P Value
Actin Binding
Ruffle
Protein Domain Specific Binding
Contractile Fiber Part
Synaptic Membrane
Cell Cortex Part
Cellular Component Biogenesis at Cellular Level
Neuron Spine
Actomyosin
Synapse
Small Ribosomal Subunit
Myosin Complex
Non-Membrane-Bounded Organelle
Motor Activity
Structural Molecule Activity
Filopodium
Establishment of Organelle Localization
Actin Filament-Based Process
Cellular Component Assembly at Cellular Level
Calmodulin Binding
Embryo Development Ending in Birth or Egg Hatching
Protein Auto-phosphorylation
Endocytic Vesicle Membrane
Anatomical Structure Formation Involved in Morphogenesis
Nucleoplasm
Cell Junction
Calmodulin-Dependent Protein Kinase Activity
Calcium-Dependent Phospholipid Binding
Extracellular Structure Organization
Regulation of Heart Contraction
Muscle Contraction
mRNA Binding

Figure 2.1. Global analysis of RGS14 interactors from whole mouse brain. (A) Volcano plot of RGS14 interactors (n = 3) enriched in pairwise experiments versus nonspecific IgG bead control pulldowns (n = 3). A total of 233 specific interactors of RGS14 were determined to be significantly enriched $p < 0.05$ and at least 1.5 fold over the average of the bead controls. (B) Overrepresented gene ontologies among the 233 RGS14 interactors were examined with GO-Elite, and up to the top 10 terms for each of 3 ontology types are shown. A Z score of 1.96 represents a significant overrepresentation ($p < 0.05$) relative to the background list of proteins identified in the experiment. (C) Enrichment map of all GO hits is visualized, with nodes representing discrete terms. Node size ranges from invisible (n = 5 genes) to large (n= 75 genes), and edges correspond to the number of genes overlapping between different terms. Four terms with no overlap to any of the identified terms are shown at the bottom. A P value of GO-Elite overrepresentation significance ranged from 6 × 10–8 (blue) to 0.042 (red).

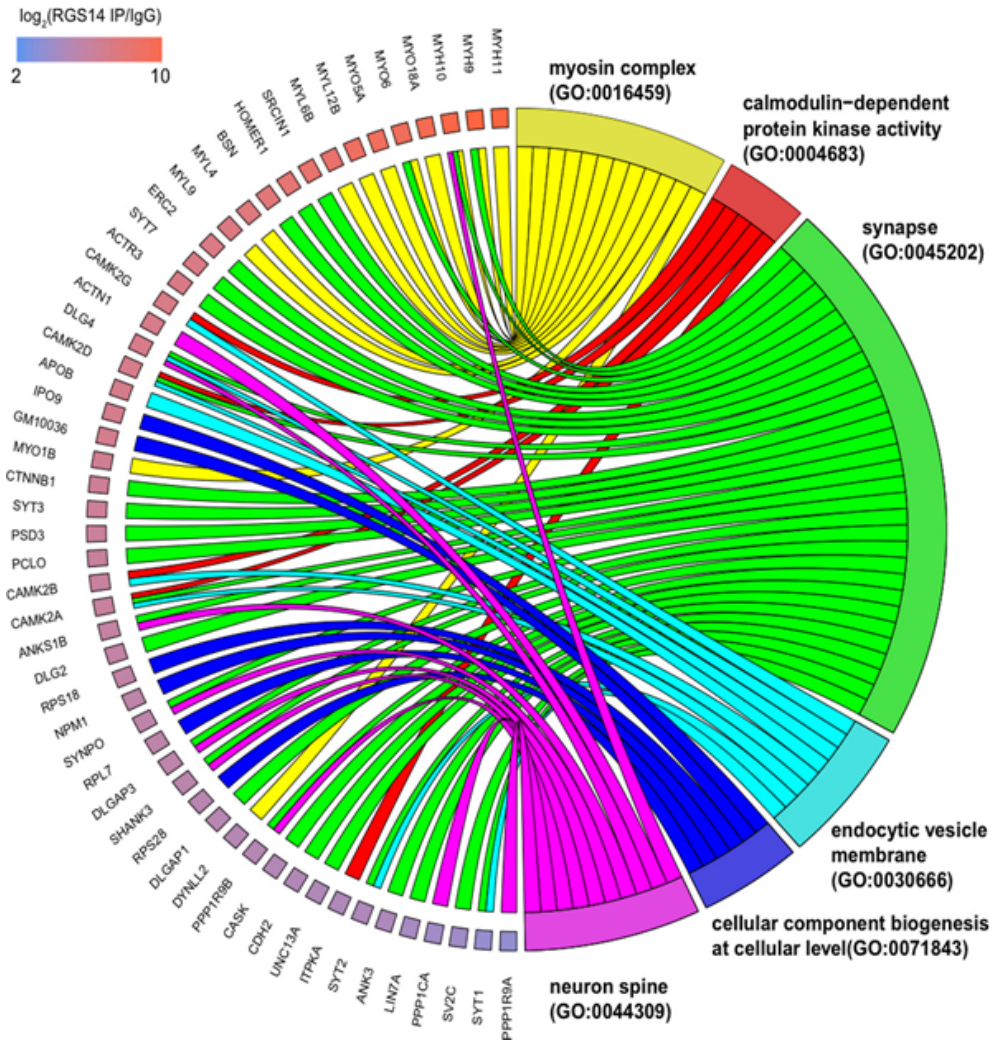

Figure 2.2. A circular view of RGS14 interactor overlap across selected ontologies. A color scale for individual genes depicts the log2(RGS14 IP/IgG) enrichment, which is the sort order for the genes around the semicircle, from highest (top) to lowest (bottom).

2.4 Discussion

Here, we present a comprehensive RGS14 interactome from mouse brain showing a clear localization of RGS14 at the synapse and neuron spine based on its interacting partners where it can regulate post-synaptic signaling to suppress LTP in CA2 hippocampal neurons. The most prominent binding partners for RGS14 in mouse brain appear to be myosins and other actin-binding proteins as well as proteins involved in calmodulin-dependent protein kinase activity. These groups provide two exciting new avenues of research that may allow us to elucidate the exact mechanism by which RGS14 suppresses plasticity.

RGS14 is known to suppress plasticity in CA2 hippocampal neurons but the proteins that RGS14 interacts with to perform this function in the cell are unknown. Furthermore, the precise location at which RGS14 is acting to suppress LTP is unknown as well. RGS14 is capable of being found throughout the neuron including the axon terminal, post-synaptic spine (Squires et al. 2018), and nucleus (Squires et al. 2018; Gerber, Squires, and Hepler 2018; Shu et al. 2007; Branch and Hepler 2017). Our interactome data shows that the majority of proteins that RGS14 interacts with in mouse brain are associated with the synapse and the post-synaptic spine (Fig. 2). These findings support the idea that RGS14 is acting post-synaptically in the spines of CA2 hippocampal neurons to suppress LTP, with additional potential functions in the nucleus and axon terminal. While it is possible that RGS14 interacts with completely different proteins depending on its subcellular localization, it is more likely that RGS14 interacts with the same types of proteins throughout the cell to perform different functions in different areas. Myosins and other actin-binding proteins are capable of performing the same basic action within different cell and tissue types to lead to radically different outcomes. For example, myosin IIB, which crosslinks actin filaments (Vicente-Manzanares et al. 2009), is necessary for both the normal development of the heart(Tullio et al.

1997) as well as correct spine morphology and function(Ryu et al. 2006). RGS14 interacts with a wide variety of myosins and other actin binding proteins and it is likely that these interactions play an important role in RGS14's known function in suppressing LTP as well as other potential roles at the axon and nucleus.

Many of the myosins and actin-binding proteins we see interacting with RGS14 in mouse brain are already implicated in LTP. The class II nonmuscle myosins, myosin IIA (MYH9), IIB (MYH10), and IIC (MYH11) , all interact with RGS14. Notably, myosin IIB has been shown to be necessary for spine stability and maintenance of LTP with inhibition of its activity preventing LTP consolidation (Ryu et al. 2006; Bu et al. 2015). Myosin II interacts with another protein found in our RGS14 interactome, drebrin (Mizui et al. 2014). Drebrin is necessary for proper spine development and morphology, controlling targeting of PSD95 as well as NMDA receptors to the spine to allow for normal plasticity (Takahashi et al. 2003; Takahashi, Mizui, and Shirao 2006). Notably, myosin II activity is necessary for LTP mediated efflux of drebrin from the spine to allow for the structural plasticity that allows potentiation(Mizui et al. 2014). It is possible that RGS14 interferes with the function of either of these two proteins individually or even interferes with the interaction between them to suppress LTP in pyramidal neurons in area CA2.

RGS14 also interacts with two myosins in a separate class, myosin Va (MYO5A) and myosin VI (MYO6). Both of these myosins travel along actin filaments to deliver cargo to different parts of the cell, toward the plus end and minus end of the actin filament, respectively. Notably, myosin Va has been shown to be necessary for LTP, transporting AMPA receptors to spines to allow for greater response to incoming glutamate at the synapse(Correia et al. 2008). Myosin VI performs moves in the opposite direction, mediating AMPA receptor endocytosis (Osterweil, Wells, and Mooseker 2005). RGS14 may interfere with myosin Va's role of AMPA receptor insertion

following LTP induction or it may facilitate myosin V's role in AMPA receptor endocytosis, suppressing LTP in either case.

It is important to note that this RGS14 interactome from mouse brain includes both direct and indirect protein-protein interactions. Adding to the difficulty in interpreting this data, many of the proteins that RGS14 interacts with appear to be actin-binding proteins. It is likely that RGS14 is interacting directly with only a few of the many actin-binding proteins that we have identified in the interactome, carrying with them the rest of the actin cytoskeleton in the neuron spine and the many other proteins associated with it. Future studies will focus on promising individual targets with function significance that RGS14 may be interacting with directly such as the mysosins discussed above. Complimentary studies using techniques such as APEX2 fusion proteins to biotinylate proteins near RGS14 that can be purified directly without the need for maintaning protein-protein interactions may also shed light on the functional interacting partners that bind directly to RGS14.

This interactome provides a comprehensive overview of functional interacting partners with RGS14 in mouse brain. These proteins provide us with a better understanding of the environment in which RGS14 is acting to suppress LTP and aid efforts to understand the exact molecular mechanism by which RGS14 suppresses LTP in pyramidal neurons in area CA2. Through RGS14, we can move toward a better understanding of plasticity throughout the hippocampus and specifically, area CA2 and its role in hippocampal physiology and learning and memory.

Chapter 3:

Differential Proteomics and Systems Biology Approaches Reveal a Unique Hippocampal Area CA2 Proteome

3.1 Introduction

The hippocampus is well established as serving essential roles in the processing of learning and memory. Anatomically, this brain region is composed of the Cornu Ammonis (CA), a strip of pyramidal neurons, and the dentate gyrus (DG), which is composed of granule cells. The pyramidal cell-containing CA regions are further split into distinct areas based on anatomical differences, CA1, CA2, CA3. The original, anatomical definition of CA2 indicated the portion of the CA between CA1 and CA3 containing large pyramidal neurons that lacked thorny excrescences indicative of mossy fiber synapses onto CA3 neurons from the DG (Lorente de No 1934). However, the extent of DG axon projection into the CA regions appears to be unreliable for distinguishing CA3 from CA2 as it differs among species (Kohara et al. 2014; San Antonio et al. 2014; Laurberg and Zimmer 1980). Indeed, in rodents DG neurons have been shown to not only project to CA3 but also to CA2 neurons (Kohara et al. 2014). A more reliable marker of the distinction between CA3 and CA2 has been the expression of proteins specific to CA2 (Dudek, Alexander, and Farris 2016). Many of these proteins have been identified including regulator of G protein signaling 14 (RGS14) (Lee et al. 2010; Evans et al. 2014; Squires et al. 2018), amigo-2 (Hitti and Siegelbaum 2014; Srinivas et al. 2017), Purkinje cell protein 4 (PCP4) (Srinivas et al. 2017; San Antonio et al. 2014), alpha-actinin 2 (ACTN2) (Wyszynski et al. 1998; Mercer, Trigg, and Thomson 2007), and striatum-enriched protein-tyrosine phosphatase (STEP) (Boulanger et al. 1995). These proteins have overlapping expression and many have been used to reliably identify a large proportion of CA2 neurons in functional studies examining physiology (Srinivas et al. 2017) and behavior (Hitti and Siegelbaum 2014) associated with CA2.

Notably, until recently, CA2 was largely ignored in many functional studies of the hippocampus. Within the hippocampus, the trisynaptic circuit between DG, CA3, and CA1 has

been extensively examined in the context of learning and memory, with many studies focusing on long-term potentiation (LTP) and synaptic plasticity at CA3-CA1 synapses (Malenka and Bear 2004). CA3 neurons also project to area CA2, where LTP is absent at proximal synapses under the same conditions that elicit LTP in CA1 (Lee et al. 2010; Zhao et al. 2007). This lack of LTP in CA2 has been shown to be due to both the selective expression of RGS14(Lee et al. 2010), and the unusually robust calcium buffering properties of CA2 pyramidal cells (Simons et al. 2009), though the exact causes are unclear. One of the most notable differences between CA2 and surrounding regions is the resistance of CA2 neurons to cell death following a variety of insults. Area CA2 is resistant to cell loss in temporal lobe epilepsy as well as status epilepticus. CA2 neurons are resistant to cell death following ischemia (Kirino 1982; Sadowski et al. 1999; Yang et al. 2000) and traumatic brain injury (Maxwell et al. 2003; Kotapka et al. 1992). However, the mechanism(s) by which area CA2 resists injury following such insults is unknown.

In order to better understand the differences between CA2 and its neighboring and better understood hippocampal regions, we initiated studies to define differences in protein expression between CA2 and CA1. Multiple proteins identified to be enriched in CA2 have already been shown to mediate unique aspects of CA2 signaling and physiology including aggrecan (Carstens et al. 2016) and RGS14 (Lee et al. 2010) which each serve roles in the suppression of LTP in CA2. Additionally, the vasopressin 1b receptor (Pagani et al. 2014) and adenosine A1 receptor (Simons et al. 2012) have been shown to mediate potentiation and inhibition, respectively, of postsynaptic signaling in CA2. To further our understanding of area CA2, it is vital to know what proteins are preferentially expressed in this region. While multiple studies have focused on differences between the CA3 and CA1 regions of the hippocampus (Gozal et al. 2002; von Ziegler et al. 2018), to date,

there has been no published study focused on either the transcriptome or proteome of the CA2 region.

Here we provide a differential proteomic analysis focused on proteins enriched in the CA2 region over CA1. Using reporter mice expressing enhanced green fluorescent protein (eGFP) under the Amigo-2 promoter, a known marker for area CA2, as a guide, we dissected out dorsal CA2 and CA1 and subjected them to LC-MS/MS. Of the 3000+ proteins surveyed, we identified over 100 proteins with consistently and robustly higher expression in CA2 (vs. CA1) including many established markers of area CA2. Furthermore, we identify nine separate co-expression networks that positively correlate with CA2 (vs. CA1) identity. These networks contain proteins already known to be expressed highly in CA2 as well as new targets that merit further study. By combining the differential expression data with the co-expression networks, we reveal a specific CA2 (vs. CA1) proteome that can be used to identify functional protein networks that contribute to CA2's unique physiology and signaling.

3.2 Experimental Procedures

Mouse model for hippocampus dissections

C57B6 mice heterozygous for GFP expression under the CA2-selective amigo-2 promoter were used for the experiment. Mice were deeply anesthetized with Fatal-Plus before brains were removed and dissected on dry ice. Hippocampi were isolated and the dorsal portion of the hippocampus was used to collect tissue from areas CA1 and CA2, with CA2 being identified through GFP expression. The dissection method for experiments 1 and 3 (n=8 each) was pooling of coronal slabs, while dissection for experiment 2 (n=6) relied upon dissection along the whole length of the hippocampus. Experiment 2 mice were 4-month old females whereas the mice dissected for experiments 1 and 3 were 2-month old males.

Tissue homogenization and digestion

Procedures for tissue homogenization were performed essentially as described(Seyfried et al. 2017). In total, 22 samples for either of the two regions of hippocampus were analyzed; all 11 CA1 samples were matched to the corresponding 11 CA2-derived tissue samples. Approximately 100 mg (wet tissue weight) of brain tissue was homogenized in 8 M urea lysis buffer (8 M urea, 100 mM $NaHPO_4$, pH 8.5) with HALT protease and phosphatase inhibitor cocktail (ThermoFisher) using a Bullet Blender (NextAdvance). Each Rino sample tube (NextAdvance) was supplemented with ~100 µL of stainless steel beads (0.9 to 2.0 mm blend, NextAdvance) and 500 µL of lysis buffer. Frozen samples were then placed into the bullet blender (in 4 °C cold room). The samples were homogenized for 2 full 5 min cycles and the lysates were transferred to new Eppendorf Lobind tubes. Each sample was then sonicated for 3 cycles consisting of 5 s of active sonication at 30% amplitude followed by 15 s on ice. Samples were then centrifuged for 5 min at 15 000 g and the supernatant was transferred to a new tube. Protein concentration was determined by bicinchoninic acid (BCA) assay (Pierce). For protein digestion, 100 µg of each sample was aliquoted and volumes normalized with additional lysis buffer. Samples were reduced with 1 mM dithiothreitol (DTT) at room temperature for 30 min, followed by 5 mM iodoacetamide (IAA) alkylation in the dark for another 30 min. Samples were then 8-fold diluted with 50 mM triethylammonium bicarbonate (TEAB). Lysyl endopeptidase (Wako) at 1:100 (w/w) was added and digestion continued overnight. Trypsin (Promega) was then added at 1:50 (w/w) and digestion was carried out for another 12 h. The peptide solutions were acidified to a final concentration of 1% formic acid (FA) and 0.1% triflouroacetic acid (TFA) and desalted with a C18 Sep-Pak column (Waters). Each Sep-Pak column was activated with 1 mL of methanol, washed with 1 mL of 80% acetonitrile, and

equilibrated with 2×1 mL 0.1% TFA. The samples were then loaded and each column was washed with 2×1 mL 0.1% TFA. Elution was performed with 2 rounds of 400 µL of 50% acetonitrile. Peptides were recovered by drying eluates under vacuum with a chilled vapor trap (Labconco).

Liquid-chromatography coupled to mass spectrometry (LC-MS/MS) for 2 label free quantitation (LFQ) experiments

For experiments 1 and 2, tryptic peptides (2 µg) from CA1 and CA2-specific samples were resuspended in peptide loading buffer (0.1% formic acid, 0.03% trifluoroacetic acid, 1% acetonitrile) containing 0.2 pmol of isotopically labeled peptide calibrants (ThermoFisher, #88321). Peptide mixtures were separated on a self-packed C18 (1.9 um Dr. Maisch, Germany) fused silica column (25 cm x 75 µM internal diameter; New Objective, Woburn, MA) by a NanoAcquity UHPLC (Waters, Milford, FA) and monitored on a Q-Exactive Plus mass spectrometer (ThermoFisher Scientific, San Jose, CA). Elution was performed over a 140-minute gradient at a rate of 400 nL/min with buffer B ranging from 3% to 80% (buffer A: 0.1% formic acid and 5% DMSO in water, buffer B: 0.1 % formic and 5% DMSO in acetonitrile). The mass spectrometer cycle was programmed to collect one full MS scan followed by 10 data dependent MS/MS scans. The MS scans [m/z ranges 400-1600 (experiment 1) and 400-1500 (experiment 2), 400,000 AGC, 50 ms maximum ion collection time] were collected at a resolution of 120,000 at m/z 200 in profile mode and the MS/MS spectra [0.7 m/z isolation width, 30% HCD collision energy, 10,000 AGC target, with maximum ion time of 35 ms (experiment 1) and 60 ms (experiment 2)] were acquired at a resolution of 15,000 (experiment 1) or 30,000 (experiment 2) at m/z 200. Dynamic exclusion was set to exclude previous sequenced precursor ions and their isotopes for 30 seconds within a 10 ppm window. Precursor ions with +1, and +8 or higher charge

states were excluded from sequencing. Experiment 1 RAW files are provided [Data Link 1: SAGE Bionetworks https://dx.doi.org/10.7303/syn16805615]; as are experiment 2 RAW files [Data Link 2: SAGE Bionetworks https://dx.doi.org/10.7303/syn16805616]. One technically replicated RAW file derived from peptide re-injection in experiment 2 (ca1_31_B.RAW) was generated and analyzed in downstream MaxQuant analysis, but not considered further.

MaxQuant for label-free proteome quantification

Experiment 1 and 2 RAW data files for the 14 samples plus one technical replicate were analyzed using MaxQuant v1.5.2.8 with Thermo Foundation 2.0 for RAW file reading capability. RAW files for each experiment were analyzed and summarized in separate runs of MaxQuant, but with the same database and search parameters as follows. The search engine Andromeda was used to build and search a concatenated target-decoy UniProt Knowledgebase (UniProtKB) peptide database containing both Swiss-Prot and TrEMBL mouse reference protein sequences (54,490 target sequences), plus 245 contaminant proteins included as a parameter for Andromeda search within MaxQuant (Cox et al. 2011). Methionine oxidation (+15.9949 Da) (up to 5 allowed each per peptide), and protein N-terminal acetylation (+42.0106 Da) were variable modifications; cysteine was assigned a fixed carbamidomethyl modification (+57.0215 Da). Only fully tryptic peptides were considered with up to 2 miscleavages in the database search. A precursor mass tolerance of ±10 ppm was applied prior to mass accuracy calibration and ±4.5 ppm after internal MaxQuant calibration. Other search settings included a maximum peptide mass of 6,000 Da, a minimum peptide length of 6 residues, 0.05 Da tolerance for high resolution MS/MS scans. The false discovery rate (FDR) for peptide spectral matches, proteins, and site decoy fraction were all set to 1 percent. Quantification settings were as follows: re-quantify with a second peak finding attempt after protein identification has completed; match full MS1 peaks between runs; a 0.7 min

retention time match window was used after an alignment function was found with a 20 min retention time search space. The label free quantitation (LFQ) normalization algorithm in MaxQuant (Cox et al. 2014b; Luber et al. 2010) was used for protein quantitation. The quantitation method only considered razor and unique peptides for protein level quantitation. All tab-separated text MaxQuant outputs, parameters, and summary files are available for experiment 1 [Data Link 3: SAGE Bionetworks https://dx.doi.org/10.7303/syn16805840], and experiment 2 [Data Link 4: SAGE Bionetworks https://dx.doi.org/10.7303/syn16805857]. The FASTA UniprotKB database used for all 3 experiments is provided [Data Link 5: SAGE Bionetworks https://dx.doi.org/10.7303/syn17056501.1].

Tandem mass tag (TMT) peptide labeling

For experiment 3, complete digestion of all samples was assumed and an aliquot equivalent to 20 µg was taken from each of the coronal slab-dissected, pooled samples and combined to make a global internal standard (GIS) for mixed CA1 and CA2 regions of mouse hippocampus. All peptide mixtures were dried down under vacuum. One batch using the 10-plex TMT kit (ThermoFisher) was used to label the 8 samples and 2 GIS mixture replicates. Sample arrangement by reporter channel is as follows: 127N: CA1_WT; 127C: CA1_540; 128N: CA1_542; 128C: CA1_545; 129N: CA2_WT; 129C: CA2_540; 130N: CA2_542; 130C: CA2_545. TMT channels 126 and 131 were used to label global internal standard (GIS) replicates. Labeling was performed according to manufacturer's protocol. Briefly, each sample (80 µg of peptides per sample/channel) was resuspended in 100 µL of 100 mM TEAB buffer. The TMT labeling reagents were equilibrated to room temperature and 41 µL anhydrous acetonitrile was added to each reagent channel and softly vortexed for 5 min. Peptide suspensions were transferred to the corresponding TMT channels and incubated for 1 h at room temperature. The reaction was quenched with 8 µl of

5% hydroxylamine. To ensure complete labeling, select channels from each batch were analyzed by LC-MS/MS according to previously published methods (Pichler et al. 2010). All 10 channels were then combined and dried by vacuum to~500 µL. Sep-Pak desalting was performed and the elution was dried to completeness.

Electrostatic repulsion-hydrophilic interaction chromatography (ERLIC) fractionation for 10-plex TMT

Dried samples were resuspended in 100 µL of ERLIC buffer A (90% acetonitrile with 0.1% acetic acid) and loaded onto a PolyWAX LP column (20 cm by 3.2 mm packed with 300 Å 5 µm beads from PolyLC Inc) as reported previously (Wingo et al. 2017). An Agilent 1100 HPLC system consisting of a degasser, a binary pump, an autosampler, a microflow UV detector, and a fraction collector was used to carry out the fractionation. The gradient was from 0 to 50% ERLIC buffer B (30% ACN with 0.1% FA) over 45 min. A total of 44 fractions were collected and then combined to 22 fractions. Final fractions 1 to 21 consisted of alternating combinations (1 and 21, 2 and 22, etc.) and fraction 22 consisted of the last fractions (43 to 44) similar to the method previously described (Wingo et al. 2017).

LC-MS/MS and TMT data acquisition on an orbitrap fusion mass spectrometer

Assuming equal distribution of peptide concentration across all 22 ERLIC fractions, 40 µL of loading buffer (0.1% TFA) was added to each of the fractions and 2 µL (2 µg equivalent) was separated on 25 cm long 75 µm internal diameter fused silica columns (New Objective, Woburn, MA) packed in-house with 1.9 µm Reprosil-Pur C18-AQ resin (Dr Maisch). The LC-MS platforms consisted of a Dionex RSLCnano UPLC coupled to an Orbitrap Fusion mass spectrometer with a Flex nano-electrospray ion source (ThermoFisher). Sample elution was performed over a gradient of 3 to 30% Buffer B (0.1% formic acid in ACN) over 140 min, from 30 to 60% B over 20 min,

and from 60 to 99% B over 5 min at 300 nl. The column was reconditioned with 99% B for 15 min at a flow rate of 500 nl/min and equilibrated with 1% B for 15 min at a flow rate of 350 nl/min. The Orbitrap Fusion (Thermo Scientific) was operated in positive ion data-dependent mode with synchronous precursor selection (SPS)-MS^3 analysis for reporter ion quantitation. The full scan was performed in the range of 380–1500 m/z at nominal resolution of 120 000 at 200 m/z and AGC set to 2×10^5, followed by selection of the most intense ions above an intensity threshold of 5,000 for collision-induced dissociation (CID)-MS^2 fragmentation in the linear ion trap with 35% normalized collision energy and 30 000 resolution. The isolation width was set to 1.5 m/z with a 0.5 m/z offset. Each of the top 10 fragment ions for each peptide MS^2 was notched out with an isolation width of 2 m/z and co-fragmented to produce MS^3 scans analyzed in the Orbitrap at a nominal resolution of 60,000 after higher-energy collision dissociation (HCD) fragmentation at a normalized collision energy of 65%. All resulting raw files (n=22) are provided [Data Link 6: SAGE Bionetworks https://dx.doi.org/10.7303/syn16805617].

TMT Protein identification and quantification

Raw data files from Orbitrap Fusion were processed using Proteome Discover (version 2.1). MS/MS spectra were searched against the same UniProtKB mouse proteome database as used for LFQ (54,489 total sequences plus EGFP). We chose to include both Swiss-Prot and TrEMBL sequences in the database as the additional depth provided by ERLIC fractionation enables the sequencing of rare protein isoforms (i.e., proteoforms) that may not be appreciated in mouse brain. The respective FASTA database used in this study is deposited on Synapse (https://www.synapse.org). SEQUEST parameters were specified as: trypsin enzyme, two missed cleavages allowed, minimum peptide length of 6, TMT tags on lysine residues and peptide N-termini (+ 229.162932 Da) and carbamidomethylation of cysteine residues (+ 57.02146 Da) as

fixed modifications, oxidation of methionine residues (+ 15.99492 Da) and deamidation of asparagine and glutamine (+0.984 Da) as a variable modification, precursor mass tolerance of 20 ppm, and a fragment mass tolerance of 0.6 Daltons. Peptide spectral match (PSM) error rates were determined using the target-decoy strategy coupled to Percolator(Käll et al. 2007) modeling of true and false matches. Reporter ions were quantified from MS^3 scans using an integration tolerance of 20 ppm with the most confident centroid setting. An MS^2 spectral assignment false discovery rate (FDR) of less than 1% was achieved by applying the target-decoy strategy. Following spectral assignment, peptides were assembled into proteins and were further filtered based on the combined probabilities of their constituent peptides to a final FDR of 1%. In cases of redundancy, shared peptides were assigned to the protein sequence with the most matching peptides, thus adhering to principles of parsimony. The search results and TMT quantification are provided [Data Link 7: SAGE Bionetworks https://dx.doi.org/10.7303/syn16805770].

Statistics for comparison of CA2 to CA1 quantification across three experiments

LFQ or TMT normalized abundances summarized for protein-level quantification based on parsimoniously assembled razor plus unique peptides in MaxQuant or Proteome Discoverer, respectively, were considered for statistical comparisons of CA1 to CA2 sample abundances within experiment. For the TMT normalized abundances, the ratio of the sample channel normalized reporter abundance to that of the average for the two GIS channels was calculated prior to log2-transformation. Likewise, LFQ abundances were log2-transformed. Then Student's T-test was performed for each of the three within-experiment comparisons using two tails and assuming equal variance for the two sample groups. Log_2(CA1 mean / CA2 mean) was also calculated for each experiment. To get a meta-analysis statistic across all three experiments, Fisher's negative log sum/Chi^2 was calculated in R using the survcomp::combine.test function with method="fisher"

parameter. The alternate method for calculating meta-p, "z.transform", was also used separately (Master Supplemental Table). Meta-p was only calculated if all available experiments' measurements of $\log_2$(CA2)-$\log_2$(CA1) mean log2 abundance ratio were equivalent in sign, or direction of change, and at least two of the three experiments measured the protein. Fisher's meta-p was minus-$\log_{10}$-transformed and used for volcano calculations. Of 2,947 proteins measured in at least 2 experiments, 1,625 (55%) were consistent in directionality; and more importantly, the standard deviation from mean of 0.000 for inconsistent proteins was only 0.107 $\log_2$ units, whereas for consistently measured proteins, the SD was 0.306; SD increased further to 0.384 for the 740 Fisher meta-p significant (meta-p < 0.05) proteins measured consistently in at least 2 experiments. Thus, the volcano fold-change cutoff for proteins with a meta-p calculation was set to <-0.3219 or >0.3219, which corresponds to a 25% fold enrichment minimum in CA1 or CA2, and which is more than 1.96xSD for inconsistently measured proteins, and more than 1.96xSD of all null TMT measurements, SD[$\log_2$(GIS2/GIS1)]=0.137. Greater than 1.96-fold of these SD represent a probability of <0.05 that Gaussian population tails overlap with markers deemed reliable, defining an upper bound on the false positive rate for the CA2-enriched markers determined by Fisher's meta-p. Finally, statistics for a large number of proteins only measured in the deeper TMT experiment relied on the T-test and are summarized in Supplemental Table (ORANGE TAB IN MASTER).

Data Normalization and Batch Correction for WGCNA

A 3,758-protein by 22-sample matrix was assembled for all common Uniprot identifiers across the data sets representing proteins with 10 or fewer (<50%) missing measurements. LFQ abundance data was downsampled, dividing by the lowest non-missing LFQ abundance in both experiment 1 and experiment 2, and further dividing all abundances by 5. Then all normalized

abundances including TMT normalized abundances were log_2-transformed, prior to R impute::impute.knn imputation, and sva::ComBat Bayesian batch effect removal, modelling hippocampus region as a common, protected variable, and removing inter-experiment systematic variance. Then originally missing values were returned to the matrix following ComBat.

WGCNA

A protein network was built using the above corrected log_2-abundance matrix after finding scale free toplogy at power Beta=6.6 using WGCNA::pickSoftThreshold function. WGCNA::blockwiseModules was used to automate network building with the following parameters, mergeCutHeight=0.07, replaceMissing=TRUE, minimum module size 17, deepSplit=4, corType="bicor", networkType="signed", PAMstage=TRUE, pamRespectsDendro=TRUE, reassignThreshold=0.05, and maxBlockSize greater than the number of proteins in the network. Resulting module eigenproteins were then correlated to hippocampus region as a binary trait, and selected module structures were drawn as iGraphs as previously published(Seyfried et al. 2017), and mapping edges which had been curated in the BioGRID interactome database previously, much as previously published(Umoh et al. 2018b).

3.3 Results

Previous studies have identified amigo-2 as a marker for the CA2 region of the hippocampus(Hitti and Siegelbaum 2014; Srinivas et al. 2017; Dudek, Alexander, and Farris 2016; Evans, Parra-Bueno, et al. 2018). Using mice expressing eGFP under the amigo-2 promoter, we isolated dorsal CA2 and CA1 from mouse hippocampus using two different approaches. One approach isolated the hippocampal regions by cutting along the length of the hippocampus while the other approach cut the hippocampus into slabs resembling coronal slices, pooling the CA2 and CA1 tissue fragments from the slabs for each sample (Fig. 1A). CA2 and paired CA1 tissue

samples were homogenized, digested, and analyzed by label free mass spectrometry. Following label free quantification, 3,257 unique proteins were well-quantified across samples obtained by dissection method 1 and 2,737 proteins were quantified in the samples obtained by dissection method 2, with 2,304 proteins overlapping between the two dissection methods (Fig. 1B). To dive deeper into these isolated tissue preparations, the samples collected via the hippocampal slab method (dissection method 2) were subjected to tandem mass tag (TMT) labeling, followed by extensive orthogonal prefractionation, and a batch of LC-MS^3 runs. This allowed us to identify more peptides in the samples and therefore, a more extensive proteome. In the TMT-labeled samples we identified 6,365 proteins compared to 3,690 total proteins identified in any of the LFQ samples with 2,333 proteins overlapping (Fig. 1C).

Comparing the proteins found in areas CA2 and CA1 from both dissection methods and the TMT enrichment, we identified 101 proteins enriched in CA2 and 85 proteins in CA1 that met the criteria of having a meta p-value less than 0.01 and a greater than 1.25-fold change in expression. These proteins are shown in a volcano plot (Fig. 2A) with CA2 enriched proteins on the right and CA1 enriched proteins on the left.

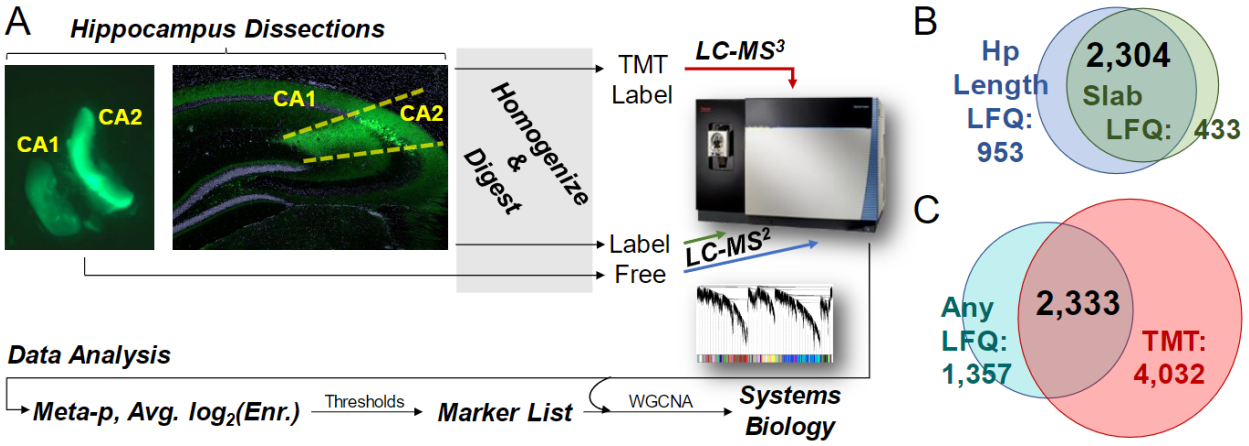

Figure 3.1. Dissection and analysis workflow. (A) Areas CA2 and CA1 of dorsal sections of excised mouse hippocampi were isolated with the aid of eGFP expression in area CA2 under the amigo-2 promoter. Tissue dissected out along the length of the hippocampus was processed and CA1 and CA2 proteomes were identified via LC-MS/MS. Coronal slab samples were not only analyzed by LC-MS/MS but also LC-MS^3 following TMT labeling. Following quantification samples were analyzed through differential expression as well as WGCNA, a systems biology approach examining networks of co-expressed proteins. (B) A comparison of dissection methods of areas CA1 and CA2 show that dissection via coronal slabs led to quantification of 2737 proteins with dissection along the length of the hippocampus yielding 3257 with 2304 overlapping proteins. (C) TMT labeling and orthogonal prefractionation of coronal slab samples followed by LC-MS^3 quantified 6365 proteins compared to 3690 in any of the LFQ samples with 2333 proteins overlapping.

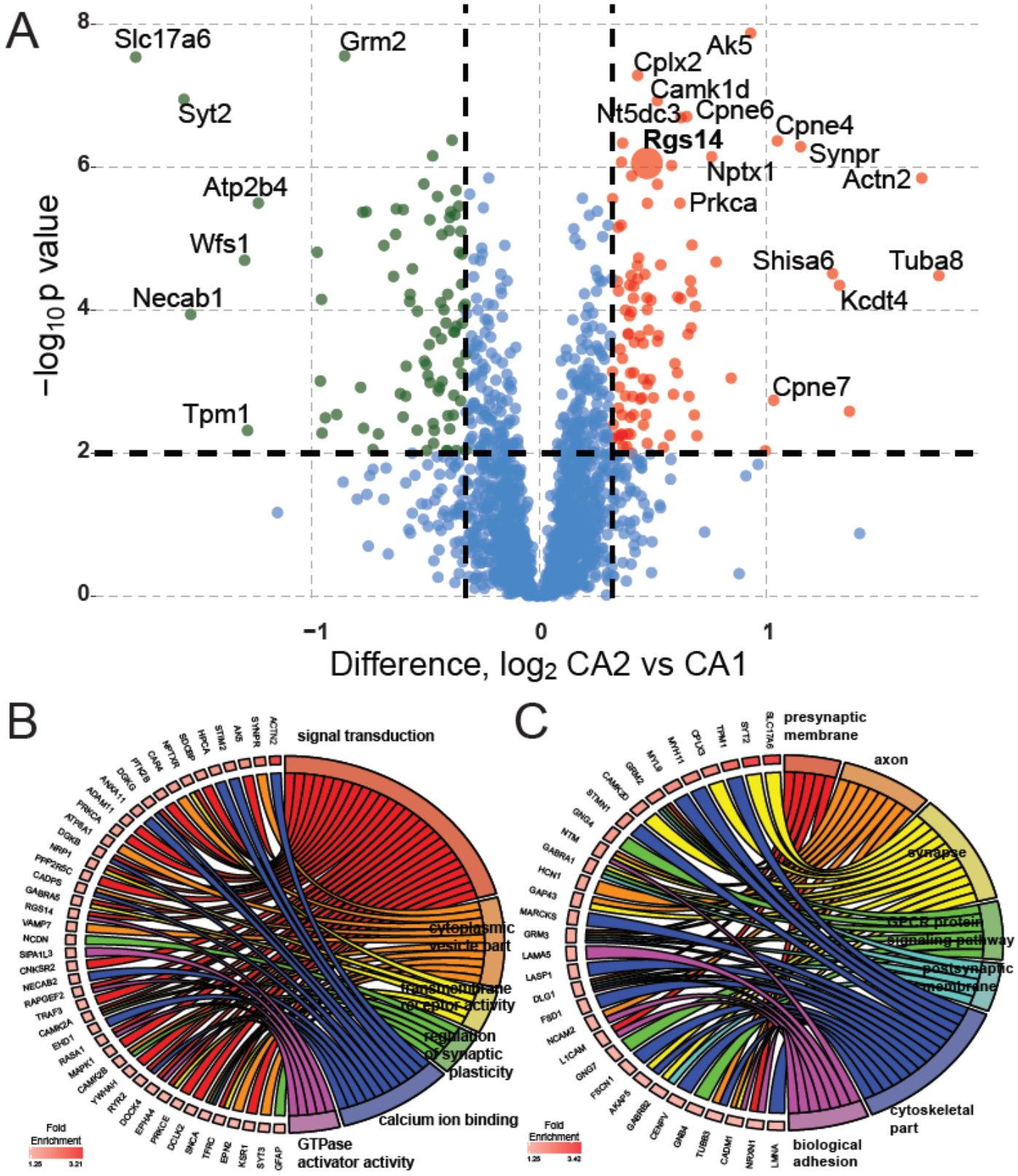
A
Slc17a6
Grm2
Syt2
Atp2b4
Wfs1
Necab1
Tpm1
Ak5
Cplx2
Camk1d
Nt5dc3
Cpne6
Cpne4
Rgs14
Synpr
Nptx1
Actn2
Prkca
Shisa6
Tuba8
Kcdt4
Cpne7
−log10 p value
Difference, log2 CA2 vs CA1
B
signal transduction
cytoplasmic vesicle part
transmembrane receptor activity
regulation of synaptic plasticity
calcium ion binding
GTPase activator activity
Fold Enrichment
C
presynaptic membrane
axon
synapse
cytoskeletal part
biological adhesion
postsynaptic membrane
Fold Enrichment

Figure 3.2. Differential expression and GO analysis reveal distinct CA1 and CA2 proteomes. (A) Volcano plot comparing differential expression of proteins in areas CA2 and CA1 across all dissection methods and mass spectrometry modalities. 101 proteins are enriched in CA2 (red) and 85 in CA1 (green) based on the criteria of a meta p-value < 0.01 and greater than 1.25-fold change in expression for each protein. (B) Chord plot linking specific proteins to associated gene ontology terms for proteins enriched in area CA2. (C) Chord plot linking specific proteins to associated gene ontology terms for proteins enriched in area CA1. Proteins are listed from most to least fold-enrichment in (B) and (C) from top to bottom counterclockwise.

The CA2-enriched proteins include well-known markers for area CA2, including RGS14 (Evans et al. 2014; Lee et al. 2010; Squires et al. 2018) and α-actinin 2 (Ratzliff and Soltesz 2001; Wyszynski et al. 1998). A gene ontology (GO) analysis of the CA2 enriched proteins is shown as a circle plot (Fig. 2B) with gene names of the 101 CA2 enriched proteins linked to their associated GO terms. Notably, the gene ontology terms regulation of synaptic plasticity and calcium ion binding are associated with proteins enriched in CA2, which is known to be distinctly different from CA1 in these functions(Zhao et al. 2007; Lee et al. 2010; Simons et al. 2009; Evans and Hepler 2012; Evans, Gerber, et al. 2018). We also created a chord plot with selected CA1 enriched proteins linked to their respective gene ontology terms (Fig. 2C).

While examining differential expression is common and useful when comparing two proteomes, many proteins of interest are excluded due to variance in expression across samples or small fold-changes between area CA1 and CA2. To fully take advantage of our data, we performed a meta-analysis taking into account the expression of all proteins quantified across all of our samples. In order to identify proteins that have coherent patterns of abundance across the 22 CA1- and CA-2 specific dissection samples, we performed weighted co-expression network analysis (WGCNA) following batch correction of the abundances from the 3 replicate experiments. Out of 47 distinct modules of co-expressed proteins, we found nine distinct co-expression patterns (module eigenproteins) that were significantly positively correlated with CA2 (vs. CA1) identity (M11, M10, M12, M14, M21, M20, M28, M2, and M1) (Fig. 3A). One network of particular interest is M11 (Fig. 3B). This module contains 15 out of the 101 differentially expressed CA2 (vs. CA1) markers; these markers verified across 3 experiments, and distinctly co-express across 22 samples with strong enrichment of the M11 module

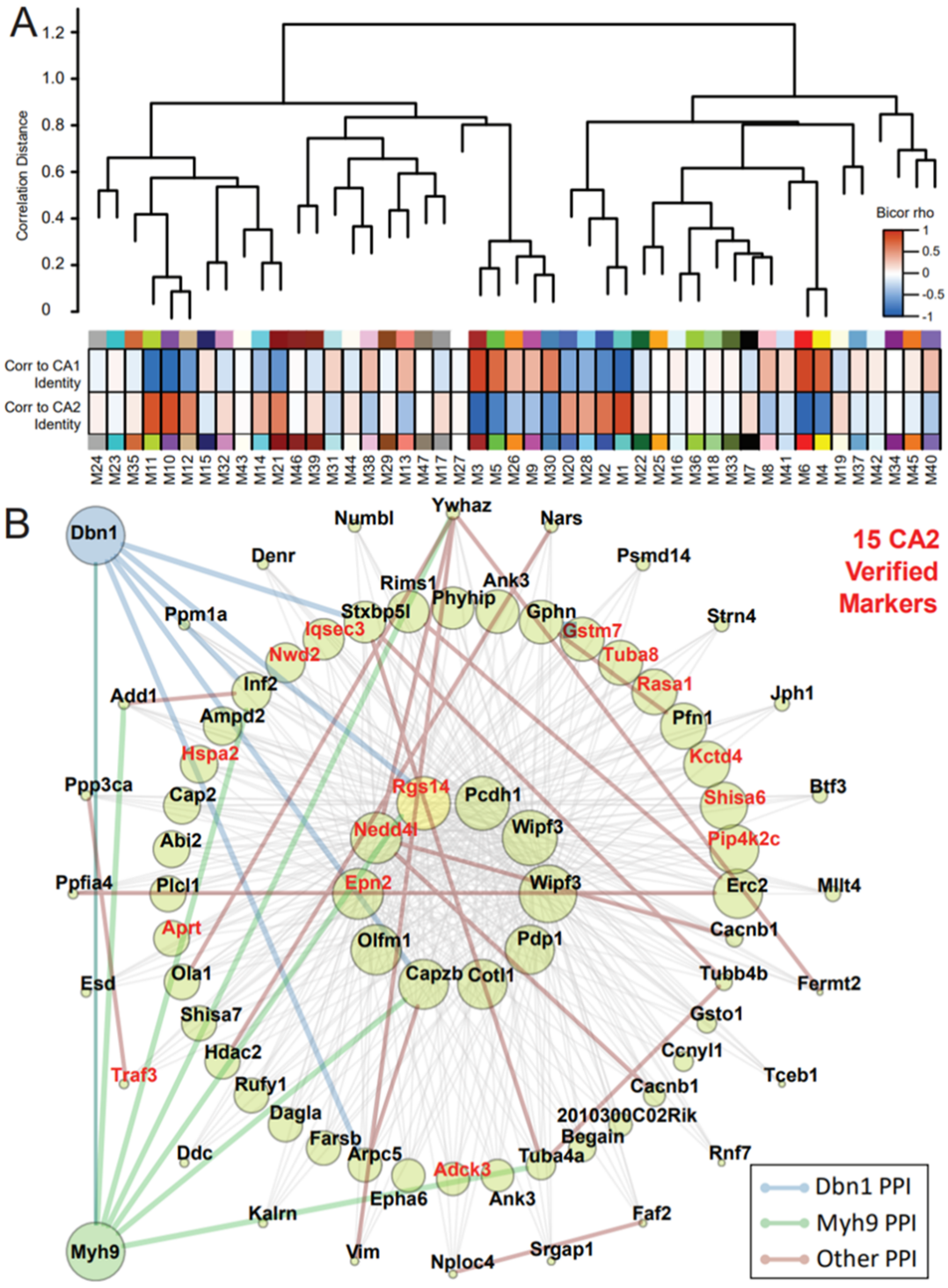

Figure 3.3. WGCNA reveals protein networks correlated with CA2 identity and provides context to known interactions. (A) A dendrogram displays relationships between protein co-

expression networks. Out of 47 distinct modules of co-expressed proteins, we found nine distinct co-expression patterns (module eigenproteins) that were positively correlated with CA2 (vs. CA1) identity (M11, M10, M12, M14, M21, M20, M28, M2, and M1) as indicated by the heatmap. (B) Proteins we found to be enriched in CA2 are highlighted in red in network M11. One of these proteins, RGS14, has been shown to interact with Dbn1 and Myh9. This network provides a context for these interactions through the PPIs shown throughout the network as blue (Dbn1 interactions), green (Myh9 interactions), or brown (all other interactions) lines as indicated.

eigenprotein in CA2 samples (gene symbols highlighted in red). Among the top 10 hubs enriched for drivers of M11 co-expression in the center of Fig 3B, is RGS14 (highlighted yellow node), a known marker of CA2 that regulates synaptic plasticity in CA2 pyramidal cells (Lee et al. 2010; Evans and Hepler 2012). Examining GO terms associated with proteins in this module, we find that this module is associated with regulation of actin filament polymerization and actin binding. Notably, RGS14 was recently shown to interact with multiple actin binding proteins in mouse brain (Evans, Gerber, et al. 2018).

To gain insight into functional protein-protein interactions (PPIs) between the RGS14-driven subnetwork of CA2-enriched markers and the multiple actin binding proteins in this module, known PPIs from BioGRID database and from our own RGS14 interactome(Evans, Gerber, et al. 2018) were added as edges in the subnetwork graph. We also checked for PPIs among M11 members and actin binding proteins we had previously shown to interact with RGS14, and found that Drebrin 1 (Dbn1), and myosin IIA (Myh9) PPIs were present among M11 members (Fig. 2B, added blue and green nodes), but not among CA1-specific modules, including M4, M8, and M9 (*data not shown*), which had other myosins as high correlation-ranked members (M4: Myo5a, Myh10; M8: Myo6; M9: Myl6). Our network/systems approach has thus identified more (and less) CA2-relevant actin-binding protein PPIs that connect the M11 hub Rgs14 and other co-expressed proteins' functions and that merit further study.

Gene Symbol	Protein name	Validation by mRNA	Validation by Protein	Known Function in neurons
DGKG	Diacylglycerol kinase gamma	Yes (Lein et al. 2007)	N/A	N/A
MCU	Mitochondrial Calcium Uniporter	Yes (Lein et al. 2007)	N/A	Main component of the protein complex that mediates mitochondrial calcium uptake (Baughman et al. 2011)
NECAB2	N-terminal EF-hand calcium-binding protein 2	Yes (Zimmermann et al. 2013)	Yes (Zimmermann et al. 2013)	Interacts with and modulates the activity of the adenosine 2A receptor (Canela et al. 2007) and metabotropic glutamate receptor 5 (Canela et al. 2009)
ACTN2	Alpha-actinin 2	N/A	Yes (Wyszynski et al. 1998; Ratzliff and Soltesz 2001)	Mediates spine morphology and assembly of the post-synaptic density in hippocampal neurons, (Hodges et al. 2014) anchoring PSD-95 at post-synaptic sites (Matt et al. 2018)
SMS	Spermine synthase	Yes (Lein et al. 2007)	N/A	Converts spermidine to spermine, a polyamine which has multiple effects (Pegg 2014) including modulation of NMDA receptor function (Hackos and Hanson 2017)
PRKCE	Protein kinase C ε	N/A	Yes (Kaasinen et al. 2002)	Activation and increased expression of this kinase mediates neuroprotection following oxygen and glucose deprivation (Cohan et al. 2017)
SLC25A22	Mitochondrial glutamate carrier 1	Yes (Lein et al. 2007)	N/A	Transports glutamate into the inner mitochondrial membrane (Fiermonte et al. 2002)
RGS14	Regulator of G protein signaling 14	Yes (Lein et al. 2007)	Yes (Lee et al. 2010; Evans et al. 2014; Squires et al. 2018)	Natural suppressor of LTP in the CA2 region of the hippocampus (Lee et al. 2010) through modulation of calcium signaling (Evans

				and Hepler 2012; Evans, Gerber, et al. 2018)
OSTF1	Osteoclast-stimulating factor 1	Yes (Lein et al. 2007)	Yes (Vermeren et al. 2017)	N/A
CADPS	Calcium-dependent secretion activator 1	Yes (Lein et al. 2007)	N/A	Essential factor for synaptic vesicle priming in hippocampal neurons (Jockusch et al. 2007)
GPC1	Glypican-1	Yes (Lein et al. 2007)	N/A	N/A
PPFIA2	Liprin-alpha 2	No(Zurner et al. 2011)	Yes (Spangler et al. 2011)	Controls synaptic output by regulating synaptic vesicle pool size (Spangler et al. 2013)
KCTD4	Potassium channel tetramerization domain containing 4	Yes (Lein et al. 2007)	N/A	N/A
RYR2	Ryanodine receptor 2	No (Lein et al. 2007)	Yes (Shimizu et al. 2008; Kaya et al. 2013)	Mediates calcium-induced calcium release from intracellular calcium stores (Tully and Treistman 2004), affecting cognitive function and hippocampal synaptic plasticity in chronically stressed mice (Liu et al. 2012)
ATP8A1	ATPase phospholipid transporting 8A1	Yes (Lein et al. 2007)	N/A	Deficiency in this flippase is associated with externalization of phosphatidylserine in hippocampal neurons, delaying hippocampal-dependent learning (Levano et al. 2012)
NRP1	Neuropilin 1	Yes (Lein et al. 2007)	N/A	Interacts with semaphoring 3 and VEGF to mediate axon guidance and angiogenesis respectively (Parker, Guo, et al. 2012)
ANXA11	Annexin A11	Yes (Lein et al. 2007)	N/A	Participates in ER-to-Golgi trafficking, modulating the early secretory pathway (Shibata et al. 2015)

CLVS2	Clavesin 2	Yes (Lein et al. 2007)	N/A	Regulates late endosome/lysosome morphology (Katoh et al. 2009)

Table 3.1. Previously validated CA2-enriched proteins. Here, we list expression (mRNA and protein) and known function of proteins that we found to have robustly enriched expression in CA2 (vs. CA1). These 18 proteins have been previously shown in the literature to be enriched in CA2 through examination of mRNA and/or protein expression and provide external validation of the methods used to isolate and analyze areas CA1 and CA2 for this study.

To further validate our findings, we compiled a list of proteins that show previous higher expression in area CA2 over CA1 (Table 1). A function for each protein in brain is also listed to provide context. Out of 101 proteins shown to be enriched in CA2, 18 already have been shown to be enriched in CA2 compared to CA1 either by mRNA or protein levels. These 18 proteins include RGS14 and alpha-actinin 2, known markers for the CA2 region (Lee et al. 2010; Evans et al. 2014; Squires et al. 2018; Wyszynski et al. 1998; Ratzliff and Soltesz 2001) that are not highly enriched in any other CA region of the hippocampus.

3.4 Discussion

Here, we provide evidence of a CA2-enriched proteome distinct from that of CA1 mouse hippocampus. Of the 3000+ proteins surveyed, we identified over 100 proteins with consistently and robustly higher expression in CA2 (vs. CA1) including established markers of area CA2, including RGS14 (Lee et al. 2010; Evans et al. 2014; Squires et al. 2018) and alpha-actinin 2 (Wyszynski et al. 1998; Ratzliff and Soltesz 2001). Gene ontology (GO) terms associated with these CA2-enriched proteins include "regulation of neuronal synaptic plasticity" and "calcium ion binding," both of which have been shown to be functionally different between CA2 from CA1 in the current literature (Lee et al. 2010; Matsuzaki et al. 2004; Zhao et al. 2007; Evans, Parra-Bueno, et al. 2018; Simons et al. 2009). Our findings identify nine distinct co-expression networks positively correlated with CA2 (vs. CA1) identity. These networks contain proteins already known to be expressed highly in CA2 as well as newly validated proteins that can be used potentially to identify functional protein networks that contribute to area CA2's unique physiology and signaling.

While area CA1 of the hippocampus has been extensively studied, much less effort has been directed toward understanding area CA2 (Dudek, Alexander, and Farris 2016). This is due to

the fact that CA2 has long been thought to be outside of the classical DG-CA3-CA1 trisynaptic pathway, and perhaps because CA2 is small compared with the surrounding CA regions with undefined boundaries, making it more difficult to study. Recently identified CA2-specific marker proteins (Dudek, Alexander, and Farris 2016) have helped to make the hippocampal region more accessible to investigators, including our use of amigo2-GFP here. Physiologically, the CA1 region has been of interest to researchers in part because it displays LTP at synapses from CA3, which is tied to hippocampal-dependent learning and memory (Nicoll 2017). Notably, LTP is absent in CA2 pyramidal neurons under the same conditions in which it is elicited in CA1 (Zhao et al. 2007). This lack of LTP can be overcome through select interventions including knockout of RGS14 (Lee et al. 2010) and increasing extracellular calcium to overcome the robust calcium buffering properties in CA2 pyramidal cells (Simons et al. 2009). In relation to disease, the hippocampus has been of interest due to its susceptibility to damage from a variety of insults including temporal lobe epilepsy (Sloviter 1991; Haussler et al. 2016), traumatic brain injury (Kotapka et al. 1992; Maxwell et al. 2003), and ischemia (Kirino 1982; Sadowski et al. 1999; Yang et al. 2000). However, area CA2 is resistant to cell death following each of these forms of damage compared to area CA1 (Kirino 1982; Sadowski et al. 1999; Yang et al. 2000; Sloviter 1991; Haussler et al. 2016; Kotapka et al. 1992; Maxwell et al. 2003). The mechanism of this protection of the CA2 region is unknown and highlights the need for a comprehensive understanding of the proteins controlling signaling and physiology within this region to better understand how CA2 is different from CA1 and the rest of the hippocampus.

We identified over 100 proteins that are robustly and reliably enriched in CA2 (vs. CA1). While many of these proteins have not been previously shown to be enriched in CA2, we were able to identify 18 proteins that had been shown to be preferentially expressed in CA2 (vs.CA1)

via either mRNA or protein expression levels (Table 1). Considering these proteins that are validated not only by our own results but also outside findings, many of these targets merit further research in the context of CA2 function. Alpha-actinin 2, a known marker for area CA2, has been shown to mediate spine morphology and assembly of the post-synaptic density in hippocampal neurons (Hodges et al. 2014; Matt et al. 2018), which are known to affect synaptic plasticity. Notably, alpha-actinin 2 is calcium insensitive, providing a mechanism by which CA2 neurons may be able to control spine morphology under conditions in which calcium levels are heavily buffered. Spermine synthase may also be involved in post-synaptic plasticity in CA2. This enzyme converts spermidine to spermine, which can modulate the activity of multiple ion channels including inwardly rectifying potassium channels, NMDA receptors, AMPA receptors, and kainite receptors (Pegg 2014; Hackos and Hanson 2017). All of these ion channels have been shown to play a role in synaptic plasticity, and higher levels of spermine is CA2 due to spermine synthase may play a role in CA2's relative lack of plasticity compared to area CA1. MCU, a mitochondrial Ca^{++} uniporter, and ryanodine receptor 2 each control intracellular calcium levels(Baughman et al. 2011; Tully and Treistman 2004). Both may be involved in area CA2's enhanced calcium buffering properties with MCU already having been shown to buffer cytoplasmic calcium levels in other cell types by importing calcium into mitochondria (Drago et al. 2012).

Many of the proteins we found to be enriched in CA2 (vs. CA1) have been shown to control presynaptic signaling or function including neuropilin 1 (Nrp1) (Parker, Guo, et al. 2012), liprin-alpha 2 (Ppfia2) (Spangler et al. 2013), and calcium-dependent secretion activator 1 (Cadps) or CAPS-1 (Jockusch et al. 2007). While these proteins have been shown to be enriched in CA2 by other methods, it is worth noting that these and other presynaptic proteins may be enriched in area CA2 partially due to their expression in other areas that project to the CA2 region including CA3

(Zhao et al. 2007; Lee et al. 2010), the DG (Kohara et al. 2014), and the entorhinal cortex (EC) (Chevaleyre and Siegelbaum 2010; Srinivas et al. 2017). Also, CA2 neurons project into CA1 potentially obscuring identification of additional presynaptic proteins preferentially expressed in CA2. These limitations could be addressed by future studies using RNA sequencing to examine differential expression in CA2 and CA1 though mRNA has also been shown to be transported throughout the axon as well (Sahoo et al. 2018).

Area CA2 is also noteworthy for its remarkable resistance to cell loss following injury. CA2 is resistant to damage from temporal lobe epilepsy, ischemia, and traumatic brain injury. Among the proteins we identified as enriched in CA2 (vs. CA1) that have been previously shown to be high in CA2 (Table 1), protein kinase C-ε (PRKCE) and ATPase phospholipid transporting 8A1 (ATP8A1) are known to have neuroprotective effects. Protein kinase C-ε activation has been shown to mediate neuroprotection following oxygen and glucose deprivation as is the case during ischemia (Cohan et al. 2017). ATP8A1 deficiency in hippocampal neurons is associated with externalization of phosphatidylserine in hippocampal neurons (Levano et al. 2012), which is associated with apoptosis (Fadok et al. 2000). Enhanced ATP8A1 expression in CA2 pyramidal cells may decrease phosphatidylserine externalization and subsequent programmed cell death following injury, providing a mechanism of neuroprotection. In addition to proteins with known neuroprotective functions, we find proteins that should be studied further to investigate a possible role in neuroprotection in CA2. MCU may help to buffer calcium levels in CA2 by importing calcium into mitochondria, inhibiting excitotoxic cell death as a result. RGS14 has been shown to modulate calcium in CA2 pyramidal neurons, restricting post-synaptic calcium elevations and inhibiting LTP (Evans, Parra-Bueno, et al. 2018). This suppression of spine calcium likely prevents

excitotoxic cell death due to high intracellular calcium levels linked to excessive glutamate stimulation.

Beyond these individual proteins that show preferential expression in CA2 (vs. CA1), we have identified entire networks of proteins with correlated expression with 9 of these networks correlating with CA2 sample identity (Fig. 3A). Furthermore, one of these networks contains 15 proteins we find to be enriched in CA2 (vs. CA1) via differential expression with RGS14 as a hub protein of the module. While RGS14 has never been shown to directly affect the actin cytoskeleton, the GO terms associated with the proteins in this module include "regulation of actin filament polymerization," "actin binding," and "cytoskeleton." However, RGS14 recently has been shown to exist in brain with multiple myosin heavy chains and actin binding proteins (Evans, Gerber, et al. 2018). These interactors include drebrin 1 (Dbn1) and myosin IIA (Myh9), which interact with multiple other proteins in the same module as RGS14 (Fig. 3B), providing evidence for a potential functional interaction between RGS14 and these two actin binding proteins as well as other actin binding proteins within the module. Related to RGS14's known role as a suppressor of LTP in area CA2, drebrin 1 has been shown extensively to be important for spine formation and plasticity (Takahashi et al. 2003; Takahashi, Mizui, and Shirao 2006; Koganezawa et al. 2017; Mizui et al. 2014). Drebrin forms a stable structure with actin in dendritic spines but following NMDA receptor activation, drebrin exits spines, presumably allowing F-actin polymerization associated with plasticity (Mizui et al. 2014). Furthermore, this removal of drebrin from spines is actually mediated by myosin II (Mizui et al. 2014), which has been shown to be necessary for maintenance of LTP (Ryu et al. 2006). Based on the known functions of drebrin and myosin II as well as the network enrichments for PPIs that implicate these proteins as relevant RGS14 interactions in CA2, RGS14 appears likely to interact functionally with these new targets. RGS14 may act on either drebrin 1

or myosin II or both to prevent their interaction to disrupt actin dynamics and suppress LTP in CA2 pyramidal neurons, providing an example of how this network analysis can be used to narrow focus for CA2-relevant PPIs in future studies.

Our findings here identify over 100 proteins enriched in CA2 that are involved in synaptic signaling and plasticity. Most of these proteins have never been shown to be highly expressed in CA2 (vs. CA1) and merit further research to determine how their selective expression may affect the unique physiology and signaling observed in this hippocampal subregion. In addition to a wealth of newly identified proteins of interest, we have created networks of proteins with correlated expression, with nine of these networks being significantly correlated with CA2 sample identity. These networks can be used to provide context for expression of proteins within the same module and help identify and sharpen focus on potential functional interactions as we have shown with RGS14. Future studies will focus on newly identified CA2-enriched (vs. CA1) proteins with known functions that appear to explain aspects of area CA2's unique physiology and signaling.

Chapter 4:

14-3-3γ binds RGS14 at distinct sites to inhibit the RGS14:Gαi-AlF_4^- signaling complex and RGS14 nuclear localization

This chapter contains figures and text that have been modified from the published manuscript: Gerber, K. J., Squires, K. E., and Hepler, J. R. (2018) 14-3-3gamma binds regulator of G protein signaling 14 (RGS14) at distinct sites to inhibit the RGS14:Galphai-AlF4(-) signaling complex and RGS14 nuclear localization, *The Journal of biological chemistry 293*, 14616-14631.

4.1 Introduction

The regulator of G protein signaling (RGS) and RGS-like family of proteins (nearly 40 members) are characterized by their GTPase activating protein (GAP) activity on G protein alpha (Gα) subunits (Ross and Wilkie 2000; Hollinger and Hepler 2002). One RGS protein family member, RGS14, is an unusual brain scaffolding protein that integrates G protein and MAPKinase signaling pathways to regulate synaptic plasticity relating to hippocampal-based learning and memory (Lee et al. 2010). RGS14 integrates signaling through multiple GTPases by binding active Gαi/o subunits (Hollinger et al. 2001), inactive Gαi1 and Gαi3, (Shu et al. 2007) as well as small GTPases including active H-Ras (Vellano et al. 2013; Willard et al. 2009) and Rap2 (Traver et al. 2000). Besides binding Gαi/o at its RGS domain, RGS14 also interacts with GDP-bound Gαi1/3 subunits at its G protein regulatory (GPR) motif (Shu et al. 2007; Brown et al. 2015; Brown, Lambert, and Hepler 2016; Hollinger et al. 2001). While RGS14 was originally discovered as a Rap-binding protein via its R1 Raf-like Ras/Rap binding domain, studies suggest that RGS14 likely interacts preferentially with active H-Ras in cells (Vellano et al. 2013; Willard et al. 2009). RGS14 also interacts with both GPCRs and the non-receptor guanine nucleotide exchange factor, Ric-8A, in a G protein-dependent manner (Vellano, Maher, et al. 2011; Vellano et al. 2013; Brown, Lambert, and Hepler 2016). Whereas RGS14 interacts with multiple signaling proteins at the plasma membrane, we and others have shown that RGS14 is also a nucleo-cytoplasmic shuttling protein (Shu et al. 2007; Branch and Hepler 2017; Squires et al. 2018; Cho, Kim, and Kehrl 2005), suggesting it serves as yet undefined roles in the nucleus.

While RGS14 binds to a variety of signaling GTPases, other regulatory protein binding partners have not been identified. Members of the 14-3-3 family of proteins are ubiquitous regulatory proteins abundant in brain (Aitken 1995). They consist of seven distinct isoforms in mammals, though differences in their function are largely unclear, with all 14-3-3 isoforms often referred to generally as 14-3-3 proteins (Fu, Subramanian, and Masters 2000; Yaffe 2002; Qiao et al. 2014; Tzivion, Shen, and Zhu 2001). These proteins exist as dimers (Tzivion, Luo, and Avruch 1998; Yuan, Michelsen, and Schwappach 2003), with each monomer capable of interacting with a distinct 14-3-3 binding site (Yaffe et al. 1997; Petosa et al. 1998), typically centered at a phosphorylated serine or threonine (Molzan and Ottmann 2012; Muslin et al. 1996; Yaffe et al. 1997), though there are exceptions (Abramow-Newerly, Ming, and Chidiac 2006; Campbell et al. 1997; Fu, Coburn, and Collier 1993; Masters et al. 1999; Alam et al. 1994; Clark et al. 1997). In some cases, 14-3-3 can bind to poorly defined protein sequences in a phosphorylation-independent manner (Abramow-Newerly, Ming, and Chidiac 2006; Campbell et al. 1997; Fu, Coburn, and Collier 1993; Masters et al. 1999; Alam et al. 1994; Clark et al. 1997). Upon binding, 14-3-3 proteins exert multiple effects on their substrates including changes in conformation, masking of binding sites for other proteins (Abramow-Newerly, Ming, and Chidiac 2006), and changes in subcellular localization (Abramow-Newerly, Ming, and Chidiac 2006; Nufer and Hauri 2003; Obsil et al. 2001; O'Kelly et al. 2002; Yuan, Michelsen, and Schwappach 2003; Yaffe 2002). 14-3-3 has been shown to interact with multiple RGS proteins including RGS4, RGS5, RGS16 (Abramow-Newerly, Ming, and Chidiac 2006), RGS3 (Benzing et al. 2000; Niu et al. 2002; Rezabkova et al. 2010; Rezabkova et al. 2011), and RGS7 (Benzing et al. 2000; Benzing et al. 2002). In many of these cases, 14-3-3 association with phosphorylated residues within the RGS domain results in inhibition of GAP activity (Benzing et al. 2000; Abramow-Newerly, Ming, and

Chidiac 2006; Rezabkova et al. 2010; Rezabkova et al. 2011), providing a mechanism through which posttranslational modification can negatively regulate the impact of an RGS protein on G protein signaling. Additionally, 14-3-3 proteins are reported to affect the subcellular localization of RGS4, sequestering it in the cytoplasm and preventing its recruitment to the plasma membrane by active Gα (Abramow-Newerly, Ming, and Chidiac 2006).

While RGS14 interaction with Gαi-GTP has been shown to be enhanced by phosphorylation (Hollinger, Ramineni, and Hepler 2003), no clear mechanism for the negative regulation of RGS14 interactions with Gαi has been identified. Here, we report that native RGS14 forms a stable complex with 14-3-3 in hippocampus, where RGS14 has been shown to negatively regulate synaptic plasticity and consequently, learning and memory (Lee et al. 2010). 14-3-3 binds RGS14 at two distinct sites, one phosphorylation-dependent and the other phosphorylation-independent. In HEK 293 cells, we find that RGS14 binds 14-3-3γ selectively, and that this interaction is markedly potentiated by downstream active H-Ras signaling. This interaction is phosphorylation-dependent, and complex formation between RGS14 and 14-3-3 occurs directly, independent of any other interacting partners. 14-3-3 binding is centered at phosphorylated serine 218, and binding at that site inhibits active Gαi binding at the RGS domain of RGS14 without affecting inactive Gαi interaction with the GPR motif or active H-Ras binding at the R1 domain. In hippocampal neurons, the cell type in which RGS14 is natively expressed in the brain (Evans et al. 2014; Squires et al. 2018), we report 14-3-3 also binds at a second site in a phosphorylation-independent manner. This 14-3-3 binding is distinct from that at phospho-serine 218. RGS14 is a nucleo-cytoplasmic shuttling protein (Shu et al. 2007; Branch and Hepler 2017; Cho, Kim, and Kehrl 2005), and 14-3-3 prevents RGS14 nuclear import in hippocampal neurons independent of binding to phospho-Ser 218.

Overall, our findings provide clear evidence for distinct phosphorylation-dependent and phosphorylation-independent binding sites for 14-3-3 on RGS14. Binding of 14-3-3 at these sites negatively regulates RGS14 interaction with active Gαi at the RGS domain and nuclear import, respectively, demonstrating two distinct mechanisms through which 14-3-3 modulates RGS14 function and subcellular localization in hippocampal neurons.

4.2 Experimental Procedures

Plasmids and Antibodies

Rat RGS14 cDNA (GenBankTM accession number U92279) used throughout this study was obtained as previously described (4). The plasmids encoding full length FLAG-RGS14 in pcDNA3.1 (Invitrogen) as well as FLAG-RGS14 truncation mutants encompassing residues 1-202, 205-490, 371-544, and 444-544 were created as previously described (5). The plasmid encoding rat RGS14 cDNA was used to generate Luciferase (Luc)-RGS14 and RGS14-Luc constructs in the phRLucN2 vector as described previously (6). The plasmid encoding H6-MBP-TEV-RGS14 in a pLIC-MBP vector was obtained as previously described (9). H6-MBP-TEV-RGS14(300-C) cloned into the pLIC-MBP vector using ligation-independent cloning with the primers : forward, 5'-TAC TTC CAA TCC AAT GCG ATG AAG TAC TGC TGC GTG TAT CTA CC-3'; reverse, 5'-TTA TCC ACT TCC AAT GCG CTA TGG AAG GAC CAG GTC CTC TTT GCG-3'. H6-MBP-TEV-RGS14(N-298) was created by inserting a stop codon at residue 299 of full length RGS14 in the same vector using the QuickChange kit (Stratagene) with the following primers: forward, 5'- AGC GAA AGC CGG CCC TAG AAG TAC TGC TGC GTG-3'; reverse, 5'- CAC GCA GCA GTA CTT CTA GGG CCG GCT TTC GCT-3'. The RGS14(R333L), which demonstrates decreased binding to active H-Ras at the R1 domain, was created as previously described (45). The FLAG-RGS14 (S258A) construct used to probe for a potential 14-3-3 binding

site was generated with the QuickChange kit (Stratagene) using the following primers: forward, 5'-GCC CTG CGA CGA GAG GCT CAG GGA TCC CTG AAT TCT TCC GCG-3'; reverse, 5'-CGC GGA AGA ATT CAG GGA TCC CTG AGC CTC TCG TCG CAG GGC. The FLAG-RGS14 (S286A) construct used to probe for a potential 14-3-3 binding site was generated using the QuickChange kit (Stratagene) and the following primers: forward, 5'- GTG AGC AGC AAA TCC GAG AGC CAC CGA AAG GCC CTT GGA AGT GGA GAG GGT GAG-3'; reverse, 5'-CTC ACC CTC TCC ACT TCC AAG GGC CTT TCG GTG GCT CTC GGA TTT GCT GCT CAC-3'. The FLAG-RGS14 (S218A) construct in which serine 218 was replaced with phospho-null alanine to prevent binding of 14-3-3 at that residue was generated with the QuickChange kit (Stratagene) using the following primers: forward, 5'- CCA AAG CTG AAG CCT GGA AAG GCA CTG CCG CTC GGT GTG GAA GAG-3'; reverse, 5'- CTC TTC CAC ACC GAG CGG CAG TGC CTT TCC AGG CTT CAG CTT TGG-3'. The Luc-RGS14 (S218A) and YFP-RGS14 (S218A) constructs were created using the same primers and QuickChange kit (Stratagene). The FLAG-RGS14 truncation from residues 1-380 was created by mutating the codon for leucine 381 to a stop codon using the QuickChange kit (Stratagene) and the following primers: forward, 5'-GCT GGA GTT GGT CGG CTA GGA GCG TGT GGT ACG GAT CTC TGC TAA GCC C-3'; reverse, 5'- GGG CTT AGC AGA GAT CCG TAC CAC ACG CTC CTA GCC GAC CAA CTC CAG C-3'. The FLAG-RGS14 truncation from residues 1-300 was created by mutating the codon for tyrosine 301 to a stop codon using the QuickChange kit (Stratagene) and the following primers: forward, 5'- CGG CCC GGG AAG TAA TGC TGC GTG TAT C-3'; reverse, 5'- GAT ACA CGC AGC ATT ACT TCC CGG GCC G-3'. Rat YFP-Gαi1 in pcDNA3.1 was generated by Dr. Scott Gibson (72). 3xHA-tagged (N-terminus) wild type H-Ras plasmid and inactive (S17N) mutant as well as untagged active H-Ras(G12V) were purchased from the cDNA Resource Center

(Bloombsburg, PA). 14-3-3γ, β, τ, and ζ cDNA constructs in pcDNA3.1 were graciously provided by Dr. Haian Fu (Emory University) along with the binding-incompetent 14-3-3γ(K50E) construct. Anti-sera used include: anti-penta-His (Qiagen), anti-14-3-3 (Santa Cruz Biotechnologies Inc.), anti-14-3-3γ (Santa Cruz Biotechnologies Inc.), anti-H-Ras (Santa Cruz Biotechnologies Inc.), anti-P-p44/42 MAPK (Cell Signaling Technology, Inc.), HRP-conjugated anti-FLAG (Sigma), HRP-conjugated goat anti-mouse IgG (Rockland Immunochemicals), HRP-conjugated goat anti-rabbit IgG (BioRad), and AlexaFluor 546 goat anti-mouse IgG (ThermoFisher).

Immunoblotting

Protein samples in Laemmli buffer were loaded onto 11% acrylamide gels and proteins were resolved via SDS-PAGE before being transferred onto a nitrocellulose membrane. Membranes were blocked at room temperature for 1 hor at 4°C overnight in buffer containing 5% nonfat milk (w/v), 0.1% Tween-20, and 0.02% sodium azide in 20mM Tris-buffered saline, pH 7.6. Membranes were then incubated with primary antibody in the same buffer, except for anti-FLAG, for 2 hours at room temperature or overnight at 4°C. Membranes were washed three times for eight minutes with Tris buffered saline containing 0.1% Tween-20 (TBST) before being incubated with either anti-mouse or anti-rabbit HRP-conjugated secondary antibody diluted in TBST (1:5,000 and 1:25,000 respectively) for 45 minutes at room temperature. Membranes being blotted for FLAG were incubated with anti-FLAG HRP-conjugated primary antibody for 45 minutes immediately after blocking. Following incubation with HRP-conjugated primary or secondary antibody, membranes were washed three times for eight minutes each in TBST before visualizing protein bands using enhanced chemiluminescence and exposing membranes to X-ray films.

Ponceau red stain stock was made from 20 mg/mL Ponceau S in water. Membranes were stained in a 1:100 stock to water dilution for 5 minutes before being rinsed in water and imaged.

Cell culture and transfection

HEK 293 cells were incubated in 1x Dulbecco's modified Eagle's medium with phenol red pH indicator supplemented with 10% fetal bovine serum and 100 units/mL each of penicillin and streptomycin. Cells were maintained at 37 °C in 5% CO2. Transfections were carried out using polyethyleneimine (PEI) as previously described (73).

Our protocol for culturing neurons was adapted from Beaudoin et al. 2012 (74). Brains were removed from E18-19 embryos obtained from a timed pregnant Sprague-Dawley rat (Charles River). All animal housings and procedures were approved by the Emory University Institutional Animal Care and Use Committee (IACUC) and all procedures were approved by IACUC protocol. The meninges were removed and the hippocampi were isolated in calcium and magnesium free HBSS (Invitrogen) supplemented with 1x sodium pyruvate (Invitrogen), 0.1 percent glucose (Sigma-Aldrich), and 10 mM HEPES (Sigma-Aldrich) pH 7.3. Isolated hippocampi were washed with the HBSS solution then dissociated using the same buffer containing 0.25 percent trypsin (Worthington) for minutes at 37°C. Trypsinized hippocampi were washed two times with the same HBSS buffer before being triturated 5-6 times with a fire-polished glass Pasteur pipette in BME (Invitrogen) supplemented with 10 percent FBS (VWR), 0.45 percent glucose (Sigma-Aldrich), 1x sodium pyruvate (Invitrogen), 1x Glutamax (Invitrogen), and 1x penicillin/streptomycin (HyClone). Neurons were counted and plated at a density of 80,000 cells/cm2 in the BME-based buffer on coverslips that had been etched with 70 percent nitric acid (Sigma-Aldrich) before being coated with 1 mg/mL poly-L-lysine (Sigma-Aldrich) in borate buffer. Cells were allowed to adhere for 1-3 hours before media was changed to Neurobasal (Invitrogen) supplemented with 1x B27

(Invitrogen) and 1x Glutamax (Invitrogen). Neurons were kept in a 37°C, 5 percent CO2 incubator and half of the media was replaced with new Neurobasal every 3-4 days until neurons were used for experiments.

Neurons were transfected using a calcium phosphate transfection kit (Clontech) with a protocol adapted from Jiang and Chen (75). Briefly, calcium solution containing DNA was slowly added to an equal volume of HBS to form calcium phosphate precipitate containing the DNA. This precipitate was added to neurons on coverslips that had been placed in new wells in new media. Neurons were incubated with precipitate for an hour and a half before dissolving the precipitate with slightly acidified media that had been equilibrated in a 10% CO2 incubator for 15-20 minutes. Cells were placed back in the 5% CO2 incubator. After this incubation, coverslips were placed back in their original well in their original culture media.

RGS14 immunoprecipitation from mouse hippocampus

Brains from C57BL6 wild-type mice were removed and hippocampi were isolated by dissection. Hippocampi were homogenized using a Dounce homogenizer in lysis buffer containing 50mM Tris pH 7.05, 150mM NaCl, 1mM EDTA, 2mM DTT, 5mM MgCl2, 1 EDTA-free cOmplete mini protease inhibitor tab (Roche) at 1x concentration, 1x Halt phosphatase inhibitor cocktail (Thermo Scientific), and 1% Triton X-100. Brain lysate was incubated on a rotator at 4°C for 1 hour then cleared by spinning it down at 13,000 rpm for 10 minutes. Protein G sepharose beads (GE healthcare) were pre-blocked with 3% BSA before lysate was added. Half of the brain lysate was incubated with 50 uL of pre-blocked beads in the absence of RGS14 antibody while the other half of the lysate was incubated with 50uL of beads along with 5uL (1.63ug) anti-RGS14 (Proteintech) antibody for 2 hours on a rotator at 4°C. Immunocomplexes were then washed four times with PBS containing 0.1% Tween-20 before being boiled off the beads in 2x Laemmli buffer

for 5 minutes. Samples were then resolved via SDS-PAGE and subjected to immunoblotting for analysis. All animal housings and procedures were approved by the Emory University Institutional Animal Care and Use Committee (IACUC) and all procedures were approved by IACUC protocol.

FLAG-Immunoprecipitation

Twenty-four hours following transfection, cells were washed twice in ice cold PBS and collected in lysis buffer of the same composition used for RGS14 immunoprecipitation from mouse brain. Lysates were rotated at 4°C for 1 hour. Lysates were cleared by spinning down samples at 13,000 rpm for 10 minutes, with 30uL put aside to determine total cell lysate expression of proteins of interest while the remaining supernatant was incubated with ANTI-FLAG M2 affinity gel (Sigma), which was previously blocked in 3% bovine serum albumin (BSA) in PBS for 1 hour. Cleared lysates were rotated at 4°C for 1.5 hours. Immunocomplexes were then washed three times with 1mL PBS containing 0.1% Tween-20 before being suspended in 2x Laemmli buffer, boiled for 5 minutes, resolved by 11% SDS-PAGE, and transferred to a nitrocellulose membrane for immunoblotting.

Purification of recombinant proteins

RGS14 and truncated RGS14 (N-298 and 300-C) were expressed in E. coli and partially purified as previously described (9). Recombinant hexahistidine-14-3-3γ was expressed from a pDEST17-based plasmid in BL21 (DE3) E. coli cells and purified using Ni2+ affinity chromatography in the manner described previously (76) with minor modifications. Specifically, cells were lysed using sonication instead of a French pressure cell press. Purified protein was snap frozen in liquid nitrogen and stored in aliquots at -80°C until use.

Lambda phosphatase treatment of lysates

FLAG-immunoprecipitation was performed as described above with the exception of the addition of 1x Halt phosphatase inhibitor cocktail (Thermo Scientific). Before washing the immunocomplexes and eluting samples, the anti-FLAG affinity gel was resuspended in fresh lysis buffer with the addition of 2mM MnCl2 and 900 units of Mn2+-dependent lambda phosphatase and rotated at room temperature for 1 hour to cleave phosphate groups from potentially phosphorylated serine and threonine residues. Following treatment with phosphatase, lysates were washed, eluted, and analyzed as described above.

Blot overlay "Far-Western blot"

HEK 293 cells were transfected with FLAG-RGS14 in the presence or absence of active H-Ras using polyethyleneimine (PEI). Twenty-four hours after transfection, FLAG-RGS14 and associated proteins were isolated via FLAG-immunoprecipitation, resolved with SDS-PAGE, and transferred to a nitrocellulose membrane. The membrane was then treated with pure his-tagged 14-3-3γ at 7.5 ug/mL in a buffer containing 50mM Tris, 50mM NaCl, and 2mM DTT on a rocking incubator at 4°C overnight. The membrane was then immunoblotted as described above for 14-3-3 to determine whether 14-3-3 directly bound the RGS14 in the membrane.

Bioluminescence Resonance Energy Transfer (BRET)

BRET experiments were performed as described previously (6,9). Briefly, HEK 293 cells were transfected with a donor and acceptor as well as any additional constructs using PEI. To determine whether 14-3-3 affects active H-Ras association with RGS14, we expressed H-Ras (G12V)-Venus with RGS14-Luc or RGS14 (S218A)-Luc in the presence or absence of 14-3-3γ. To measure YFP-Gαi1 interactions with the RGS14 RGS domain, Luc-RGS14 was expressed, while YFP-Gαi1 interactions with the RGS14 GPR motif were measured using RGS14-Luc as the RGS domain and GPR motif are closer to the N- and C-termini of RGS14, respectively. Luc-

RGS14 S218A was used as a negative control to determine the effect of 14-3-3 interaction with RGS14 on active YFP-Gαi1 binding at the RGS domain. Twenty-four hours after transfection, cells were suspended in Tyrode's solution containing 140 mM NaCl, 5 mM KCl, 1 mM MgCl2, 1 mM CaCl2, 0.37 mM NaH2PO4, 24 mM NaHCO3, 10 mM HEPES, and 0.1% glucose, pH7.4. Cells treated with AlF4- were harvested in Tyrode's solution containing the addition of 10 mM NaF, 9 mM MgCl2, and 30 uM AlCl3 for 30 minutes before readings were taken. Cells were plated onto white 96-well Optiplates (PerkinElmer Life Sciences). Acceptor expression was determined by measuring fluorescence using a TriStar LB 941 plate reader (Berthold Technologies) with 485 nm and 530 nm excitation and emission filters, respectively. BRET was measured using 485 nm and 530 nm emission filters after a 2 minute application of 5 um coelenterazine H (Nanolight Technologies). The change in BRET (Net BRET) was determined by dividing the 530 nm (YFP) signal by the 485 nm (Luc) signal and subtracting the signal from Luc-RGS14 or RGS14-Luc alone. All data were collected using MikroWin 2000 software and analyzed in Microsoft Excel followed by GraphPad Prism.

Kinase inhibitor treatments

HEK 293 cells were treated with the MEK inhibitor U0126 (Sigma) at 10 uM, the PI3K inhibitor LY294002 (Sigma) at 50 uM, or the CaMKII inhibitor KN-93 (Sigma) at 100 uM for 2 hours before cells were collected and lysed. Samples were then submitted to FLAG-immunoprecipitation before being analyzed via immunoblot.

EGF treatment of cells

HEK 293 cells were treated with EGF (Sigma) at 100 ng/mL for 0, 10, 60, or 120 minutes before being collected and lysed for FLAG-immunoprecipitation.

Leptomycin B treatment of cells and immunocytochemisty

Primary hippocampal neurons were treated with leptomycin B (LMB) (Sigma) at 40 ng/mL or vehicle, 70% ethanol, for 2 hours before being fixed 15 minutes in 4% paraformaldehyde in 1x PBS. Cells were then permeabilized for 10 minutes in PBS containing 0.1% Triton X-100 in PBS and incubated in 8% BSA in PBS blocking buffer for 1 hour before being incubated with primary antibody in 4% BSA in PBS for 2 hours. Following 3 washes with 0.05% Triton X-100 in PBS, coverslips were incubated with secondary antibody in 4% BSA in PBS for 1 hour before being stained with 1.6 μM Hoechst dye (Thermofisher) for 4 minutes. Coverslips were then washed 3x in PBS before being mounted on slides using ProLong Diamond Antifade mountant (ThermoFisher). Images were taken on an Olympus FV1000 inverted confocal microscope at 100x then processed using ImageJ software. Approximately ten images per condition were obtained and representative images are shown.

4.3 Results

Previous work reported that 14-3-3 regulates the functions of several RGS proteins (Benzing et al. 2000; Benzing et al. 2002; Niu et al. 2002; Abramow-Newerly, Ming, and Chidiac 2006; Rezabkova et al. 2010; Rezabkova et al. 2011). To explore the possibility that 14-3-3 might bind to and regulate the function of RGS14, we immunoprecipitated native RGS14 out of mouse brain and subsequently probed for interactions with 14-3-3 proteins via immunoblot (Fig. 1). Because RGS14 is highly and selectively expressed in the CA2 area of the hippocampus (Evans et al. 2014), we used isolated hippocampi as a tissue source for these studies. 14-3-3γ was highly enriched in samples in which RGS14 was specifically immunoprecipitated as opposed to the beads only condition where RGS14 was not enriched (Fig. 1). In combination, these data show that endogenously expressed 14-3-3 specifically interacts with native RGS14 from the CA2 region of the mouse hippocampus.

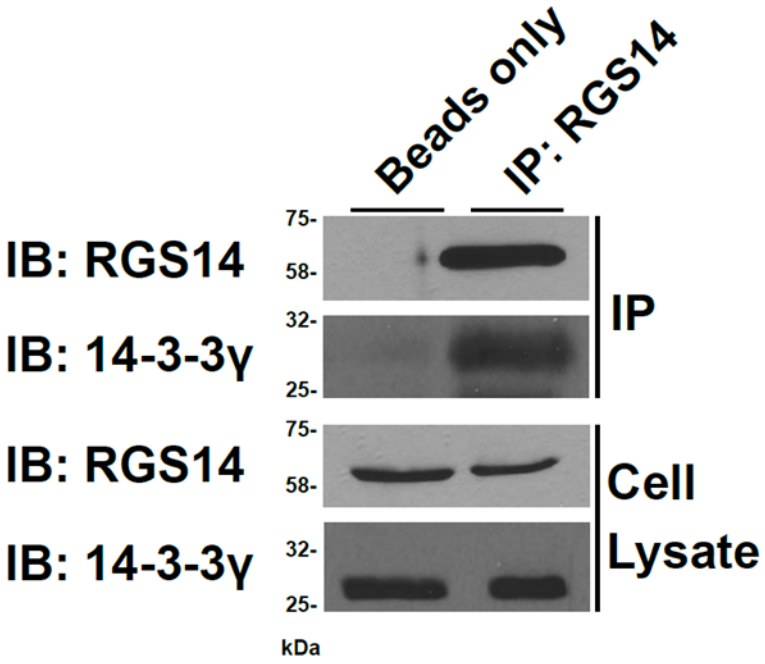

Figure 4.1. Native RGS14 interacts with endogenous 14-3-3γ in mouse hippocampus. Both hippocampi from an adult mouse were isolated and homogenized with lysis buffer to generate cell lysate. Half of the lysate was incubated with anti-RGS14 antibody (IP: RGS14) and protein G sepharose beads while the other half was incubated with the beads alone (Beads only). Beads were then washed and recovered proteins were resolved using SDS-PAGE before being subjected to immunoblotting. The cell lysate immunoblots represent 2% of the whole cell lysates used for the IP.

In order to better understand the subcellular signaling events that affect and control the interaction between RGS14 and 14-3-3, we transitioned to the more manipulation-friendly system of transient transfection in HEK 293 cells. Following FLAG-immunoprecipitation from HEK 293 cells expressing FLAG-RGS14 and 14-3-3γ, we saw little or no interaction between RGS14 and 14-3-3 (Fig. 2A) when compared to a baseline condition in which the immunoprecipitation was performed in the absence of RGS14 and the presence of 14-3-3. However, when RGS14's binding partner at the R1 domain, active H-Ras(G12V) (Willard et al. 2009; Vellano et al. 2013), is expressed along with RGS14 and 14-3-3γ, we observe a clear interaction. The specificity of this interaction is further validated by the inclusion of a condition in which 14-3-3γ(K50E), which contains a mutation in the amphipathic helix of 14-3-3 that significantly decreases affinity for known 14-3-3 substrates (Zhang et al. 1997; Jin et al. 2006), is expressed. As expected, 14-3-3γ(K50E) shows decreased binding when compared to the wild type protein (Fig. 2A), indicating that induction of 14-3-3 association with RGS14 by active H-Ras is specific.

Because active H-Ras has been reported to interact directly with RGS14 (Snow et al. 1997; Willard et al. 2009; Shu, Ramineni, and Hepler 2010; Vellano et al. 2013), it was unclear whether downstream H-Ras signaling or direct H-Ras binding to RGS14 was responsible for its induction of a 14-3-3γ:RGS14 complex. In order to parse out the role of active H-Ras in relation to 14-3-3γ and RGS14, we used a mutation of RGS14 (R333L) that has been shown to greatly reduce binding of H-Ras at the R1 domain (Shu, Ramineni, and Hepler 2010; Vellano et al. 2013). Using RGS14(R333L), any observed enhancement of the RGS14:14-3-3γ interaction by active H-Ras can be attributed only to downstream signaling of H-Ras and not direct interaction with RGS14.

We saw no difference in 14-3-3γ binding to RGS14 or RGS14(R333L) in the presence of active H-Ras (Fig. 2B), indicating that H-Ras induces RGS14 association with 14-3-3γ through a downstream signaling mechanism.

To further confirm that downstream signaling by active H-Ras is necessary to promote 14-3-3γ interaction with RGS14 in HEK 293 cells, we immunoprecipitated FLAG-RGS14 and probed for an interaction with 14-3-3γ in the presence of active H-Ras(G12V), wild type H-Ras, and a dominant negative mutant of H-Ras(S17N). As expected, only H-Ras(G12V) greatly enhanced 14-3-3 binding to RGS14 (Fig. 2C), indicating that downstream signaling through active H-Ras is necessary for the potentiation of the interaction between RGS14 and 14-3-3.

To test for possible specific interactions between RGS14 and distinct 14-3-3 isoforms, we performed a screen of multiple 14-3-3 isoforms (β,γ,τ, and ζ), in the presence of H-Ras(G12V). We blotted for the hexahistidine tag on each of the 14-3-3 isoforms following immunoprecipitation of FLAG-RGS14 so that all of the isoforms could be compared equally. Besides 14-3-3γ, 14-3-3ζ also appeared to interact with RGS14, with 14-3-3γ appearing to interact most strongly (Fig. 2D). Therefore, our subsequent studies focused on the specific interaction between RGS14 and 14-3-3γ.

14-3-3 proteins typically bind substrates at specific motifs centered at a phosphorylated serine or threonine (Muslin et al. 1996; Molzan and Ottmann 2012). However, 14-3-3 proteins are also capable of binding target proteins at non-phosphorylated residues as well (Abramow-Newerly, Ming, and Chidiac 2006; Campbell et al. 1997; Fu, Coburn, and Collier 1993; Masters et al. 1999; Alam et al. 1994; Clark et al. 1997). In order to determine whether the H-Ras-potentiated 14-3-3γ interaction with RGS14 was phosphorylation-dependent, we overexpressed

FLAG-RGS14 and 14-3-3γ and immunoprecipitated RGS14 from HEK 293 cells in the presence or absence of constitutively active H-Ras(G12V).

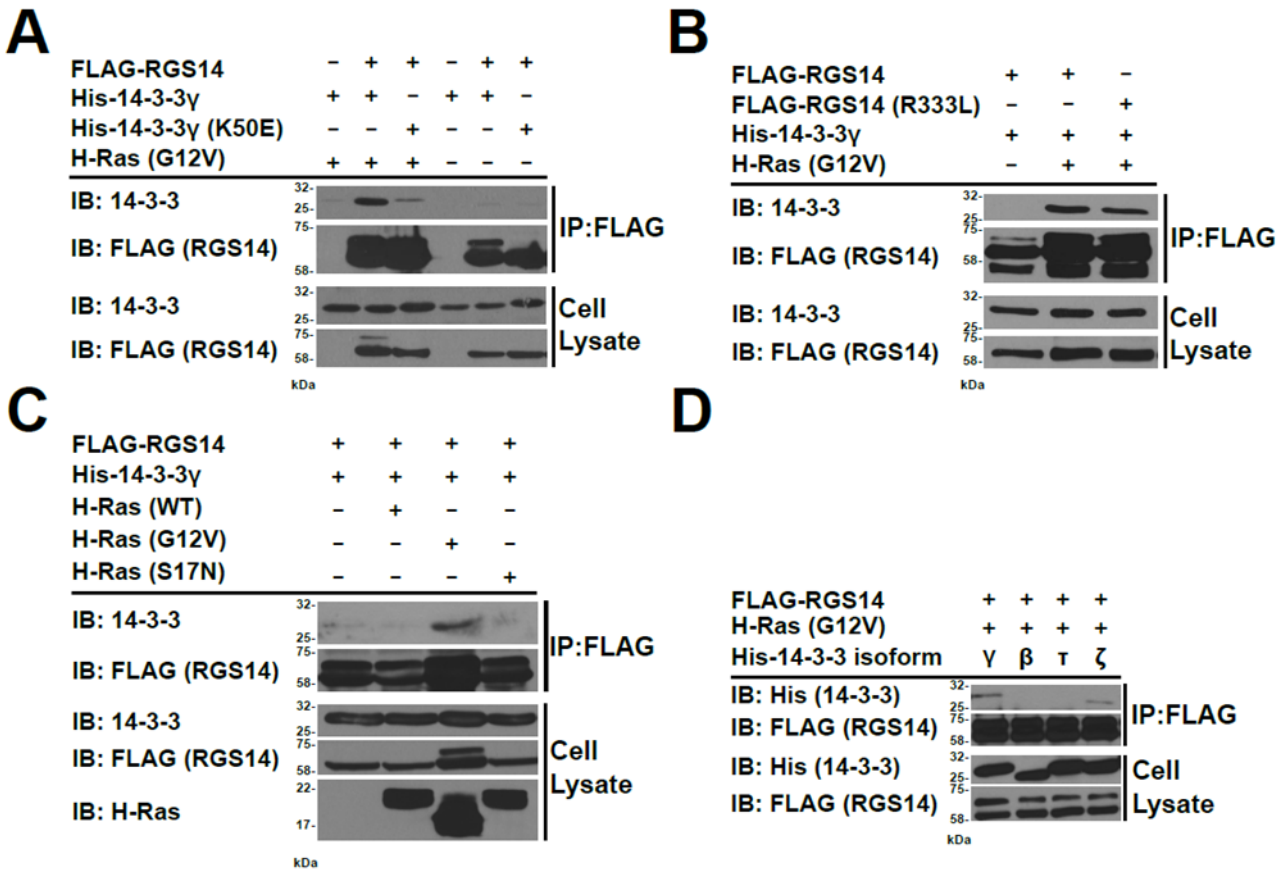

Figure 4.2. RGS14 specific association with 14-3-3γ is promoted by signaling events downstream of active H-Ras. (A) Active H-Ras enhances RGS14 association with 14-3-3γ. 10 cm dishes of HEK 293 cells were transfected with 1.5 μg FLAG-tagged RGS14 (FLAG-RGS14), 3 μg His-tagged 14-3-3γ (His-14-3-3γ), 3 μg of a binding-incompetent mutant of 14-3-3γ (14-3-3γ(K50E)), and/or 1.5 μg of constitutively active H-Ras (H-Ras(G12V)) as indicated. Whole cell

lysates were subjected to FLAG immunoprecipitation (IP: FLAG) and recovered proteins subjected to SDS-PAGE followed by immunoblotting. (B) Active H-Ras does not influence 14-3-3 binding through direct interaction with RGS14. HEK 293 cells were transfected with 1.5 μg FLAG-RGS14, 3 μg His-tagged 14-3-3γ, 1.5 μg active H-Ras, and/or a 1.5 μg of a point mutant of RGS14 that demonstrates greatly decreased binding to Ras (FLAG-RGS14(R333L)). Samples were collected and subjected to FLAG immunoprecipitation, run on SDS-PAGE, and analyzed via immunoblotting. (C) H-Ras must be active to potentiate RGS14:14-3-3 interaction. 1.5 μg FLAG-RGS14 and 3 μg His-tagged 14-3-3γ were transfected into in HEK 293 cells along with either 1.5 μg empty vector, 1.5 μg wild type (WT), 1.5 μg constitutively active (G12V), or 1.5 μg dominant negative (S17N) H-Ras. RGS14 and associated proteins were isolated via FLAG immunoprecipitation and run via SDS-PAGE before being analyzed using immunoblotting. (D) RGS14 selectively interacts with the gamma isoform of 14-3-3. HEK 293 cells were transfected overnight with FLAG-RGS14, H-Ras(G12V), and his-tagged 14-3-3γ, β, τ, or ζ. Samples were then lysed and subjected to FLAG-immunoprecipitation before being run on SDS-PAGE and analyzed for 14-3-3 interactions with RGS14 by immunoblotting for the hexahistidine tag on the 14-3-3 isoforms**.** The cell lysate immunoblots represent 2% of the whole cell lysates used for the IP. These findings are representative of three independent experiments.

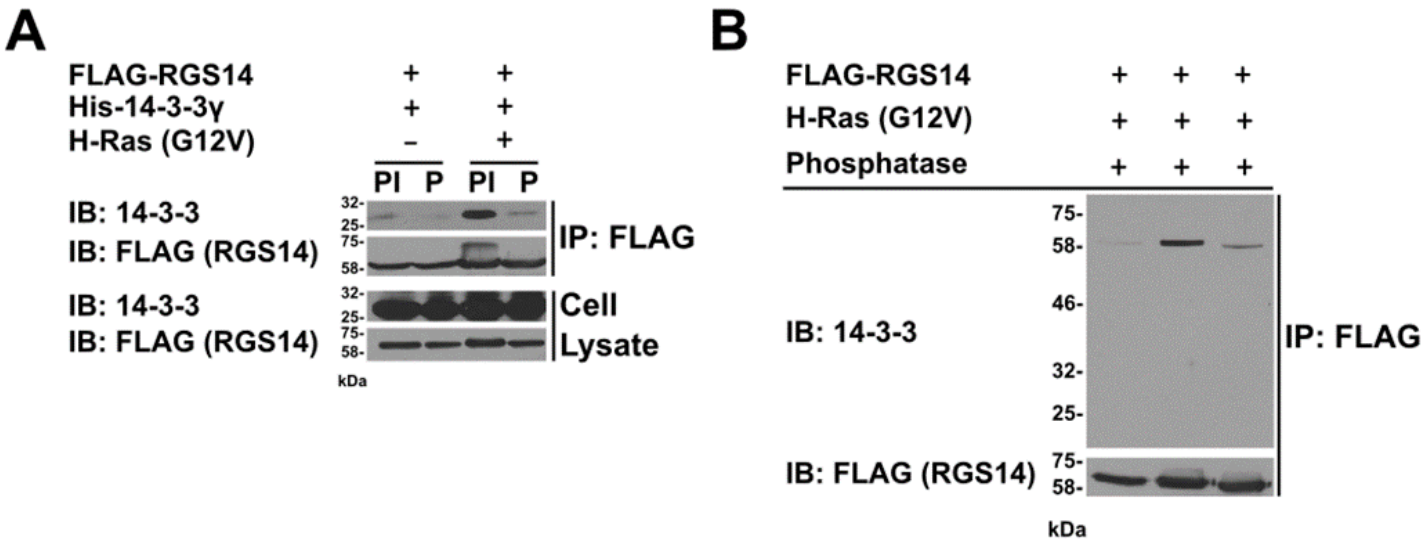

Figure 4.3. 14-3-3γ directly binds RGS14 in a phosphorylation-dependent manner. (A) 14-3-3 binds RGS14 in a phosphorylation-dependent manner. HEK 293 cells were transfected with 1.5 μg FLAG-RGS14 and 3 μg His-tagged 14-3-3γ either in the presence or absence of 1.5 μg overexpressed H-Ras(G12V). Samples were either lysed in buffer containing a phosphatase inhibitor cocktail (PI) or treated with lambda phosphatase following lysis (P). All samples were then incubated with ANTI-FLAG M2 affinity gel to pull down any proteins associated with FLAG-RGS14. The gel was washed and samples were denatured in Laemmli buffer before being

subjected to SDS-PAGE and immunoblotting. (B) 14-3-3 interacts directly with RGS14 in a far-Western blot. HEK 293 cells were transfected with FLAG-RGS14 either in the presence or absence of overexpressed H-Ras(G12V). All samples were then incubated with ANTI-FLAG M2 affinity gel to separate RGS14 from the whole cell lysate. Samples were then either denatured in Laemmli buffer or treated with lambda phosphatase. They were then subjected to SDS page and transferred to a nitrocellulose membrane which was incubated with pure His-tagged 14-3-3γ overnight and probed for interactions between RGS14 and 14-3-3 via immunoblot for 14-3-3. The cell lysate immunoblots represent 2% of the whole cell lysates used for the IP. These findings are representative of three independent experiments.

Samples were either collected in the presence of a phosphatase inhibitor cocktail to preserve phosphorylation sites or treated with lambda phosphatase to dephosphorylate any phosphorylated residues on RGS14. While little interaction between RGS14 and 14-3-3γ is seen in the absence of active H-Ras, the sample collected in the presence of both the phosphatase inhibitor cocktail and H-Ras(G12V) shows a robust interaction between RGS14 and 14-3-3γ. Notably, the sample collected in the absence of phosphatase inhibitor cocktail and treated with lambda phosphatase shows a greatly reduced interaction compared to the positive control (Fig. 3A), indicating that 14-3-3γ interacts with RGS14 through a phosphorylated serine or threonine.

One major caveat of using co-immunoprecipitation from whole cells as a technique to examine protein-protein interactions is the inability to determine whether an interaction between two proteins is direct or indirect. In the case of RGS14, it was imperative to determine if 14-3-3γ binding to RGS14 was direct because RGS14 is reported to interact with Raf in an active H-Ras-dependent manner (Shu, Ramineni, and Hepler 2010) and Raf is a well-known binding partner of 14-3-3 (Li et al. 1995; Clark et al. 1997; Zhang et al. 1997; Tzivion, Luo, and Avruch 1998; Roy et al. 1998; Light, Paterson, and Marais 2002; Fischer et al. 2009; Molzan and Ottmann 2012). Therefore, we used a far-Western blot overlay experiment to determine whether 14-3-3γ is capable of binding to RGS14 directly under the same conditions in which it interacts with RGS14 using co-immunoprecipitation (Fig. 3B). FLAG-RGS14 expressed in HEK 293 cells in the presence or absence of H-Ras(G12V) was immunoprecipitated to enrich the RGS14 in each sample. The samples were denatured, run on SDS-PAGE, and transferred to a nitrocellulose membrane, which was incubated overnight with pure 14-3-3γ protein. 14-3-3γ binding to RGS14 was detected by

immunoblotting of the nitrocellulose membrane. We find that purified 14-3-3γ interacts directly with the denatured RGS14 bands in the membrane at the correct size, 61kD (14-3-3γ is approximately 28kD), in the same manner as predicted by previous co-immunoprecipitation experiments. Active H-Ras greatly increased 14-3-3γ binding to RGS14 while treatment of an identical sample with lambda phosphatase greatly decreased this interaction (Fig. 3B). This indicates that 14-3-3γ interacts directly with phosphorylated RGS14, with no other protein necessary as part of a complex to mediate the interaction.

Knowing that 14-3-3γ interacts directly with RGS14 at a typical 14-3-3 binding motif centered at a phosphorylated serine or threonine, we created truncations of RGS14 to map the location of the 14-3-3γ binding site (Fig. 4A). All truncated proteins were created with an N-terminal FLAG tag so that they could be immunoprecipitated equally and their expression could be directly compared. Full length FLAG-RGS14 and the four truncations were expressed in HEK 293 cells with 14-3-3γ and active H-Ras and subjected to FLAG-immunoprecipitation. Notably, only RGS14 constructs that contain the linker region between the RGS domain and the tandem RBDs (constructs 1, 3 and 4) co-immunoprecipitate with 14-3-3γ (Fig. 4B), indicating that 14-3-3γ binds a site within that linker region including RGS14 residues 186-301 (Fig. 4).

Having mapped the possible 14-3-3γ binding site to the linker region between the RGS and R1 domains, we submitted the RGS14 amino acid sequence to Scansite3 to identify possible 14-3-3γ binding motifs (Obenauer, Cantley, and Yaffe 2003). At low stringency, Scansite3 predicted seven possible 14-3-3 binding motifs throughout RGS14, with three of those sites included within residues 205-301, the region determined to contain the 14-3-3γ binding site by the truncations. While mutation of serines 258 and 286 to phospho-null alanines had no effect on 14-3-3γ

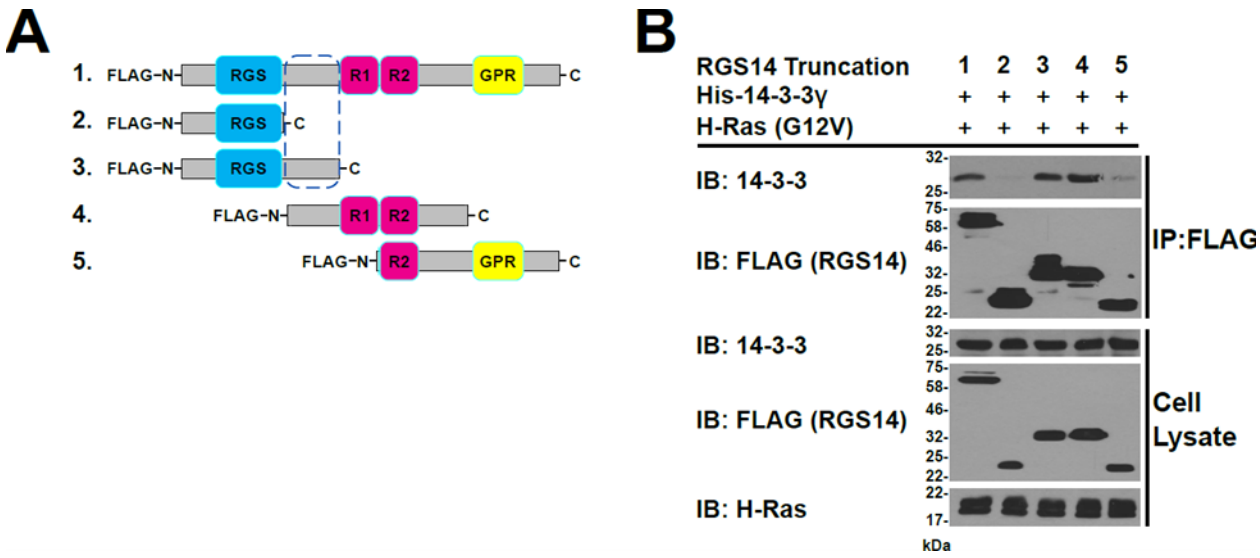

Figure 4.4. 14-3-3γ binds the linker region between the RGS and tandem R1/R2 domains of RGS14. (A) Truncation mutants of RGS14 with FLAG tags on the N-terminal end of the protein were made to determine the 14-3-3 binding site. "1" is full-length rat RGS14 composed of 544 amino acids discounting the FLAG tag. Mutant 2 contains the RGS domain and encodes for amino acids 1-202 of RGS14. Mutant 3 contains the RGS domains as well as the linker region between the RGS domain and R1, ending at residue 300. Mutant 4 contains both Raf-like Ras binding domains (R1 and R2) and contains residues 205-490. Mutant 4 consists of amino acids 371-544 and contains both the R2 and GPR domains. HEK 293 cells were transfected with these constructs (1.5 μg), 3 μg His-tagged 14-3-3γ, and 1.5 μg H-Ras(G12V). (B) Samples were collected and incubated with ANTI-FLAG M2 affinity gel to pull down the FLAG-RGS14 and associated proteins. These samples were then subjected to SDS-PAGE and immunoblotting with the indicated antibodies. The cell lysate immunoblots represent 2% of the whole cell lysates used for the IP. These findings are representative of three independent experiments.

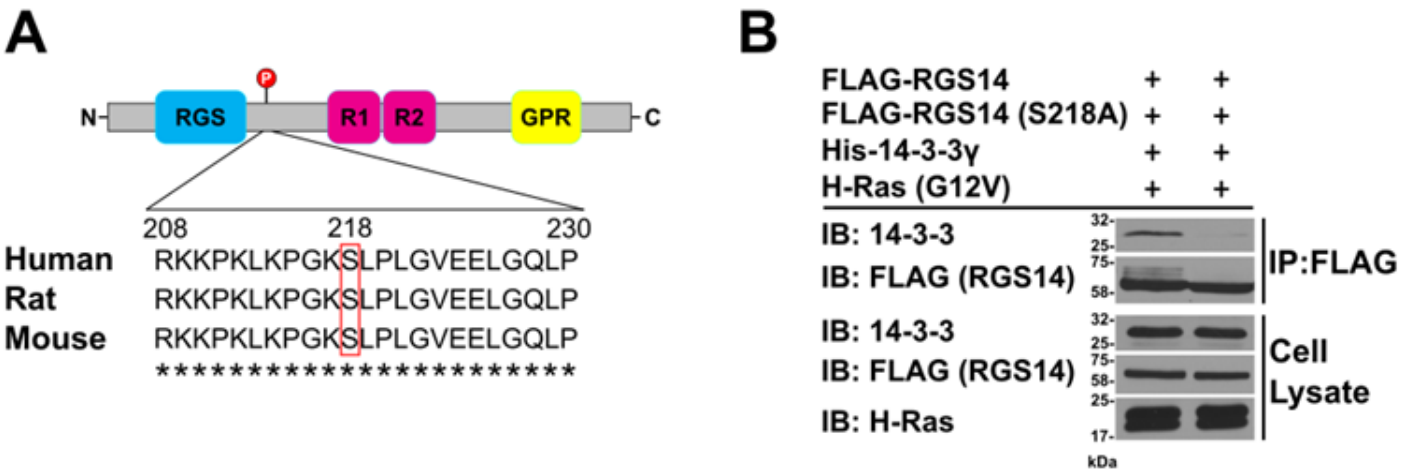

Figure 4.5. 14-3-3γ binds RGS14 at serine 218. (A) Alignment of the human, rat, and mouse RGS14 amino acid sequences show complete conservation of serine 218 (S218) and surrounding amino acids. (B) Mutation of serine 218 of RGS14 to a phospho-null alanine decreases RGS14's association with 14-3-3. 1.5 μg WT RGS14 or 1.5 μg RGS14 S218A were expressed in HEK 293 cells in the presence of 3 μg his-tagged 14-3-3γ and 1.5 μg active H-Ras. Lysates were collected and subjected to FLAG immunoprecipitation before being analyzed by SDS-PAGE followed by immunoblotting. The cell lysate immunoblots represent 2% of the whole cell lysates used for the IP. These findings are representative of three independent experiments.

association with RGS14 (Supp. Fig. 1), mutation of serine 218 to alanine (RGS14(S218A)) greatly decreased H-Ras-potentiated binding of 14-3-3 to RGS14 (Fig. 5B). Furthermore, serine 218 and the surrounding region is completely conserved through human, rat, and mouse RGS14 (Fig. 5A) and has been shown to be phosphorylated in multiple mass spectrometry experiments (Hornbeck et al. 2015), with peptides unique to RGS14 being found to contain phospho-S218 of RGS14 from rat (Demirkan et al. 2011; Lundby et al. 2012), mouse (Pinto et al. 2015), and human (Mayya et al. 2009) cells. Taken together, these findings show that RGS14 contains a conserved 14-3-3γ binding motif centered at serine 218.

Knowing the specific site at which 14-3-3 binds RGS14, we next attempted to determine the kinase that phosphorylates serine 218 of RGS14 to better understand the role that 14-3-3 interaction with RGS14 plays in relation to both RGS14 and 14-3-3 signaling. We focused on MEK, Akt, and CaMKII as possible kinases that could phosphorylate serine 218 since all of these kinases are downstream of active H-Ras signaling, and also because Akt and CaMKII are both predicted to phosphorylate serine 218 by Scansite3 (Obenauer, Cantley, and Yaffe 2003) under the minimum stringency. Following treatment of HEK 293 cells expressing FLAG-RGS14, 14-3-3γ, and H-Ras(G12V) with selective inhibitors of either MEK (U0126), PI3K (LY294002), or CaMKII (KN-93) for two hours, cells were collected and subjected to FLAG-immunoprecipitation, and probed for RGS14:14-3-3 interactions. However, none of the kinase inhibitors had any effect (Supp. Fig. 2A) indicating that ERK, Akt, and CaMKII are not responsible for the phosphorylation of serine 218 of RGS14.

We next tested if acute activation of endogenous H-Ras is sufficient to promote 14-3-3γ binding to RGS14 or whether long-term activation is necessary. To activate endogenous Ras acutely, HEK 293 cells expressing FLAG-RGS14 and 14-3-3γ were treated with EGF for 0, 10,

60, or 120 minutes. EGF treatment did not markedly enhance RGS14 pull-down of 14-3-3γ at the earlier time points, but increased interaction was evident at the two hour time point, indicating that prolonged H-Ras signaling is necessary (Supp. Fig. 2B). This suggests that changes at a protein translation level are likely necessary to enhance the RGS14:14-3-3 interaction in HEK cells. These findings indicate that the kinase responsible for phosphorylating serine 218 of RGS14 is unlikely to be directly downstream of active H-Ras, making the kinase responsible immensely difficult to predict and identify. Therefore, in subsequent efforts to identify a function for 14-3-3γ interaction with RGS14, we focused on the functional consequences of 14-3-3γ binding to RGS14 rather than the specific phosphorylation site and responsible kinase.

14-3-3 has been shown to interact with multiple RGS proteins (Benzing et al. 2000; Abramow-Newerly, Ming, and Chidiac 2006; Rezabkova et al. 2010; Rezabkova et al. 2011), competing with Gα for binding at the RGS domain and consequently inhibiting GTPase activity (Benzing et al. 2000; Abramow-Newerly, Ming, and Chidiac 2006). Interestingly, even 14-3-3 binding near, but outside of the RGS domain of RGS3 has been shown to block G protein binding (Niu et al. 2002). Due to the relatively close proximity of the 14-3-3γ binding site on RGS14 to the RGS domain (33 amino acids away), we examined the effect of 14-3-3γ binding to RGS14 on its interactions with active H-Ras(G12V) at the R1 domain as well as active Gαi1 binding at the RGS domain. For this, we examined protein:protein interactions in live cells using bioluminescence resonance energy transfer (BRET).

To determine whether 14-3-3γ binding to RGS14 affects H-Ras(G12V) interaction with RGS14 at the R1 domain, we used BRET to measure the interaction of H-Ras(G12V)-Venus with RGS14-Luc in the presence of increasing expression of 14-3-3γ. As a control for specific 14-3-3γ binding to RGS14, we compared active H-Ras binding to wild-type RGS14 to H-Ras interaction

with RGS14(S218A). We see no difference in H-Ras(G12V)-Venus interaction with RGS14-Luc or RGS14(S218A)-Luc at any level of 14-3-3γ expression (Fig. 6), indicating that 14-3-3γ does not affect active H-Ras(G12V) binding to RGS14.

We next sought to determine whether 14-3-3 affects active Gαi1 binding at the RGS domain of RGS14. Following incubation of HEK 293 cells expressing H-Ras(G12V), Luc-RGS14, and Gαi1-YFP with AlF_4^-, a nonspecific activator of heterotrimeric Gα subunits, we measured binding of Gαi1 at the RGS domain of RGS14. With the addition of overexpressed 14-3-3γ, the maximum measured interaction between Gαi1:AlF_4^- and RGS14 was decreased by approximately 50 percent (Fig. 7A), indicating that binding of 14-3-3γ to RGS14 inhibits G protein binding at the RGS domain. We also performed this experiment with Luc-RGS14(S218A) to confirm that 14-3-3γ binding centered at serine 218, as opposed to a possible off-target effect, was responsible for inhibition of active Gαi1 binding at the RGS domain. Using this Luc-RGS14(S218A) point mutant, we saw no effect on maximal G protein binding when 14-3-3γ was overexpressed (Fig. 7B). Furthermore, to examine whether 14-3-3γ inhibition of Gαi1 interaction with RGS14 is specific to the RGS domain, we performed the same experiment in the absence of AlF_4^- with RGS14-Luc to measure any contributions that 14-3-3γ binding to RGS14 might have to Gαi1 binding to the GPR motif at the C-terminal end of the protein. In this case, expression of 14-3-3γ had no effect (Fig. 7C), indicating that 14-3-3γ binding to RGS14 only decreases active Gαi1 interaction with the RGS domain.

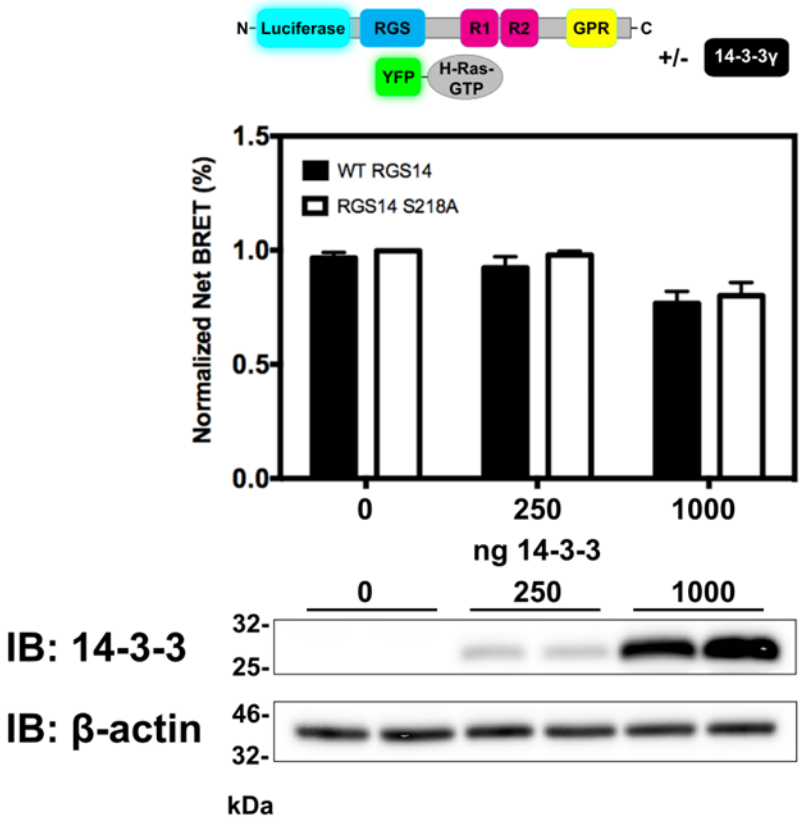

Figure 4.6. RGS14:14-3-3γ interaction does not affect H-Ras binding at the R1 domain. 6-well plates of HEK 293 cells were transfected with 500 ng H-Ras(G12V)-Venus and 10 ng wild type or S218A RGS14-Luciferase with increasing amounts of 14-3-3γ (0, 250, or 1000 ng of plasmid). BRET ratios for the interaction between H-Ras(G12V) and RGS14-Luc or RGS14(S218A)-Luc were recorded and the net BRET signal was calculated by subtracting the BRET signal from RGS14-Luc or RGS14(S218A) alone respectively. Net BRET was normalized with maximum net BRET (0.0978) given a value of 1 and plotted against the acceptor (Venus)/Donor (Luciferase) ratio. Data shown are the pooled mean ± S.E. of three separate experiments, each with triplicate determinations**.** Representative immunoblots showing expression levels of 14-3-3γ are shown below along with a β-actin loading control.

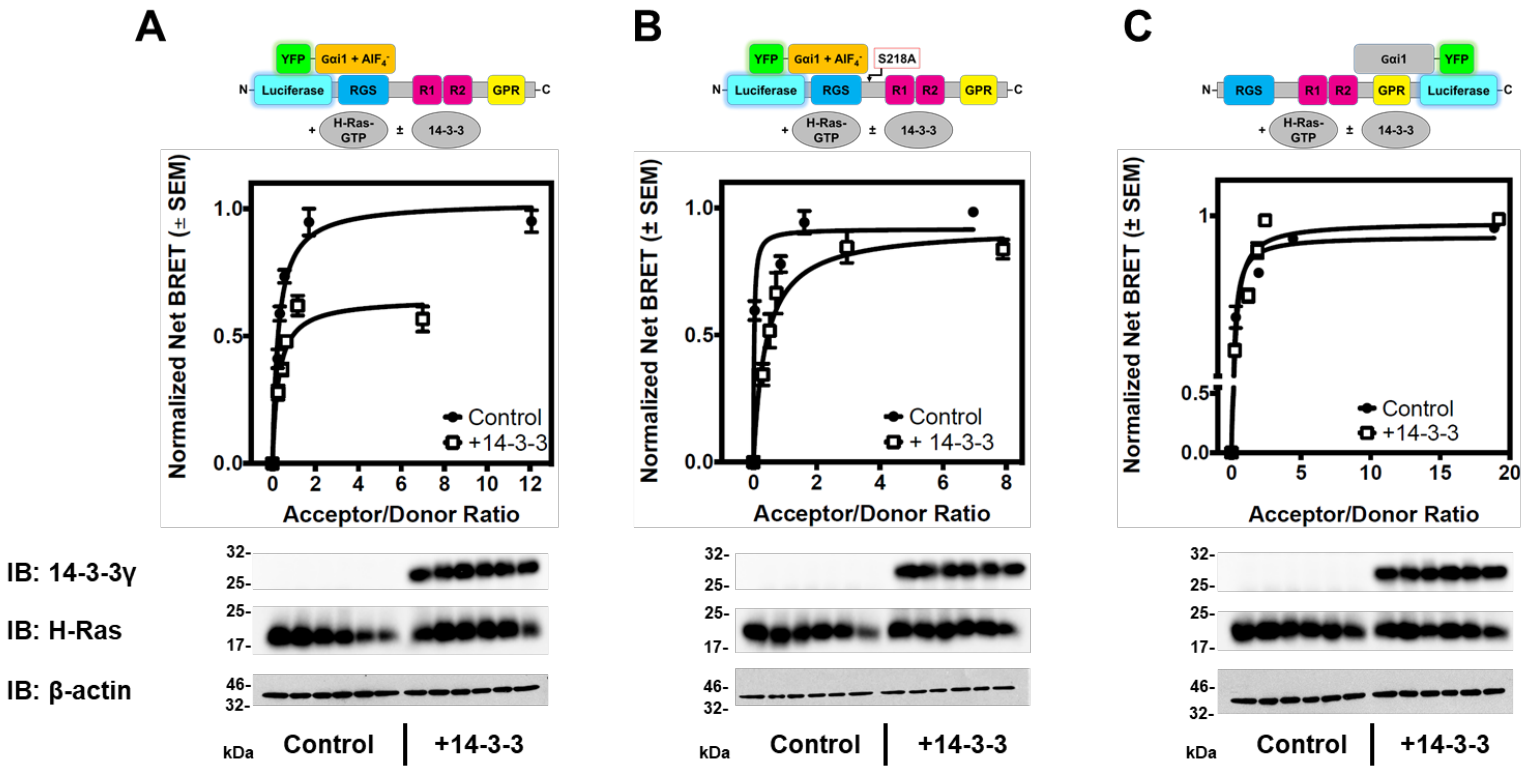

Figure 4.7. 14-3-3γ blocks Gαi1 binding to the RGS14 RGS domain. (A+B) HEK 293 cells were transfected with 5 ng Luciferase-RGS14 or 5 ng Luciferase-RGS14 S218A, increasing amounts of YFP-Gαi1 (0 ng, 25 ng, 50 ng, 100 ng, 250 ng, 500 ng), and 250 ng active H-Ras in the presence or absence of 500 ng 14-3-3γ. Gαi1 was activated with AlF_4^- for 30 minutes before BRET was measured. (C) HEK 293 cells were transfected with 5 ng RGS14-Luciferase, increasing amounts of YFP-Gαi1 (0 ng, 25 ng, 50 ng, 100 ng, 250 ng, 500 ng), and 250 ng active H-Ras in the presence or absence of 500 ng 14-3-3γ and Gαi1 was not activated. For all experiments, BRET ratios were recorded and the net BRET signal was calculated by subtracting the BRET signal from Luciferase-RGS14 (A+B) or RGS14-Luciferase (C) alone. Net BRET was normalized with maximum net BRET (0.0668 for (A), 0.2768 for (B), and 0.0607 for (C)) given a value of 1 and plotted against the acceptor (YFP)/Donor (Luciferase) ratio. Data shown are the pooled mean ±

S.E. of three separate experiments, each with triplicate determinations. Representative immunoblots showing expression levels of unlabeled proteins relevant to the experiments, H-Ras and 14-3-3γ, are shown below each BRET plot along with a β-actin loading control.

After demonstrating that 14-3-3 specifically affects Gαi1 binding to the RGS domain of RGS14, we next sought to examine the effect of 14-3-3 on RGS14 subcellular localization since 14-3-3 proteins have been shown to often affect the distribution of binding partners within the cell (Abramow-Newerly, Ming, and Chidiac 2006; Yaffe 2002; Yuan, Michelsen, and Schwappach 2003). We and others have previously shown that while RGS14 is predominantly cytosolic, it is nonetheless a nucleo-cytoplasmic shuttling protein (Branch and Hepler 2017; Squires et al. 2018; Shu et al. 2007) is demonstrated by the fact that treatment of HEK cells with leptomycin B (LMB), which inhibits nuclear export, leads to a build up of RGS14 in the nucleus as it is constantly being imported but unable to be shuttled out of the nucleus (Shu et al. 2007; Branch and Hepler 2017). Here, we show that YFP-RGS14 shuttles in and out of the nucleus in primary hippocampal neurons, the cell type in which RGS14 is natively expressed in the adult brain (Evans et al. 2014) (Figure 8). Notably, coexpression of 14-3-3γ prevents RGS14 translocation into the nucleus over the course of a two hour treatment with LMB. Furthermore, coexpression of a binding-null mutant 14-3-3γ(K50E) with RGS14 still allows RGS14 to be transported into the nucleus (Fig. 8), indicating that 14-3-3γ is binding specifically to substrates in the cell, presumably RGS14, to block RGS14 nuclear localization.

Next, we tested RGS14(S218A) to determine whether 14-3-3's interaction with RGS14 at that specific site contributed to its effect on RGS14's nuclear localization. Quite unexpectedly, RGS14(S218A) behaved identically to wild type RGS14 in the presence of 14-3-3γ following treatment with LMB. 14-3-3γ was still able to prevent transport of RGS14(S218) into the nucleus (Fig. 9), suggesting the possibility of a second 14-3-3γ binding site on RGS14 with its own distinct function.

To explore this idea of a second 14-3-3 binding site, and in an effort to make sense of 14-3-3's effect on RGS14 nuclear localization, we re-examined previous data (Fig. 3B) noticing faint bands in the control conditions in the far-Western. These findings were consistent with direct 14-3-3 binding to RGS14, thus providing evidence of a potential second, phosphorylation-independent binding site on RGS14 for 14-3-3γ. To test this idea, we again performed a far-Western experiment (Fig. 10), this time comparing 14-3-3 binding to RGS14 immunoprecipated from HEK cells (not treated with constitutively active H-Ras and therefore not strongly phosphorylated at serine 218), and RGS14 purified from E.coli, which is assured to be unphosphorylated by mammalian kinases. Notably, 14-3-3γ directly binds RGS14 in both of these conditions (Fig. 10A), confirming the presence of a phosphorylation-independent 14-3-3 binding site on RGS14. To confirm that we were looking at a 14-3-3 binding site that is completely separate from the one that is centered at Ser218 of RGS14, we created two truncation mutants of RGS14, RGS14(N-298) and RGS14(300-C), and partially purified them out of E.coli. We then performed a far-Western comparing direct binding of 14-3-3 to these truncations as well as full length RGS14. 14-3-3γ interacts with full length RGS14 and RGS14(300-C) but does not interact with RGS14(N-298) (Fig. 10B), confirming the presence of a second, phosphorylation-independent 14-3-3 binding site on RGS14 that is separate from the phosphorylation-dependent 14-3-3 binding site that requires Ser218 phosphorylation.

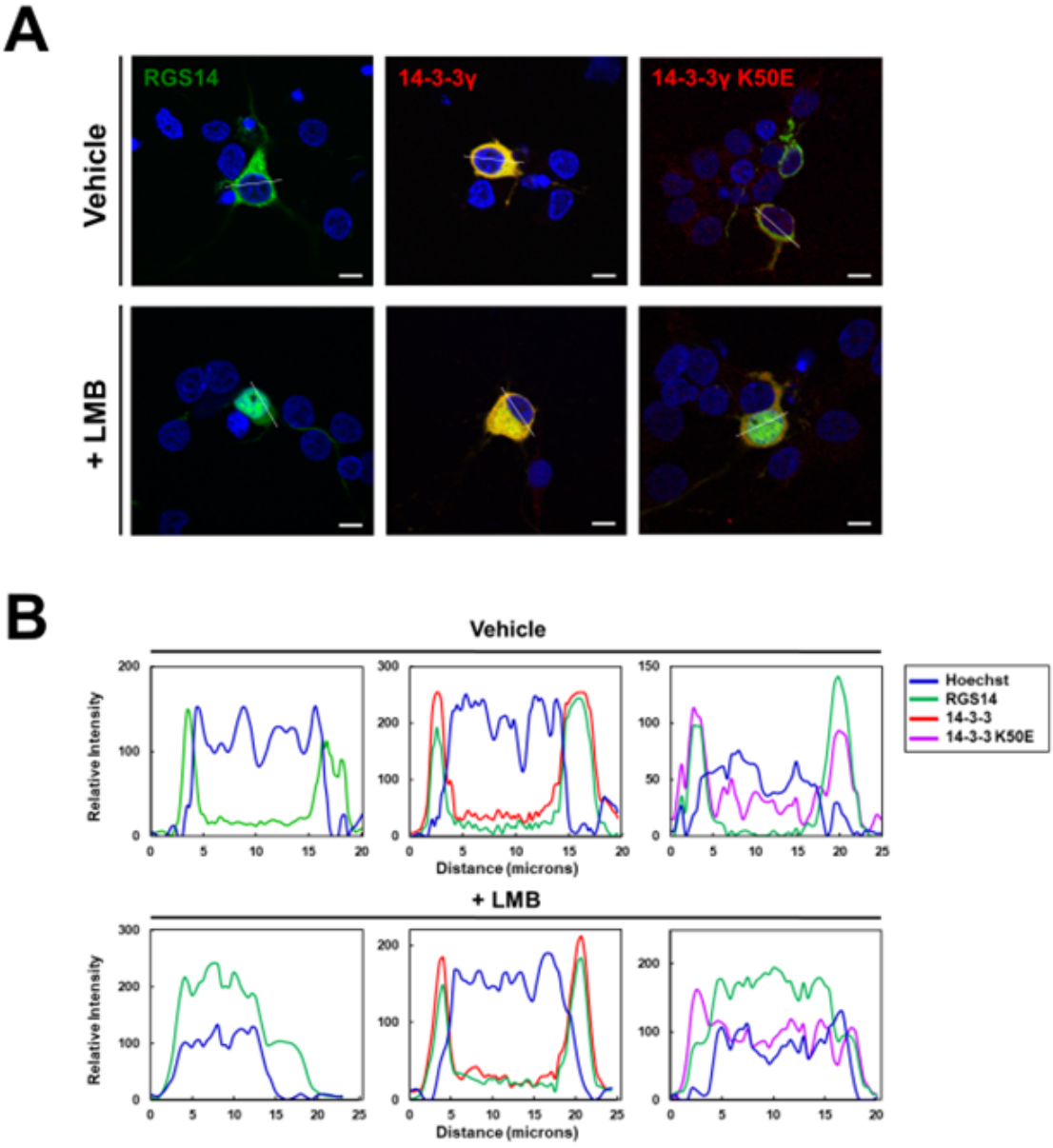
A
RGS14
14-3-3γ
14-3-3γ K50E
Vehicle
+ LMB
B
Vehicle
+ LMB
Relative Intensity
Distance (microns)
Hoechst
RGS14
14-3-3
14-3-3 K50E

Figure 4.8. 14-3-3γ blocks RGS14 import into the nucleus of hippocampal neurons. (A) Primary neurons were transfected with 1 μg YFP-RGS14 and 1 μg empty vector, 1 μg His-tagged 14-3-3γ, or 1 μg His-tagged 14-3-3γ(K50E) per coverslip. Twenty-four hours later, neurons were treated with 40 nM leptomycin B (+LMB) or vehicle for 2 hours before being fixed in 4% paraformaldehyde in PBS. YFP-RGS14 was visualized by the intrinsic fluorescence of YFP (green). 14-3-3γ immunostaining was performed using an anti-14-3-3γ primary antibody and alexa fluor 546 (red) secondary antibody while nuclei were visualized by staining DNA with Hoechst 33258 (blue). Images are representative of at least three separate experiments. Scale bars represent 10 μm. (B) Relative fluorescence intensity of YFP-RGS14, 14-3-3, and nuclear staining was measured through a cross-section of each cell as indicated by the white line through each cell in (A).

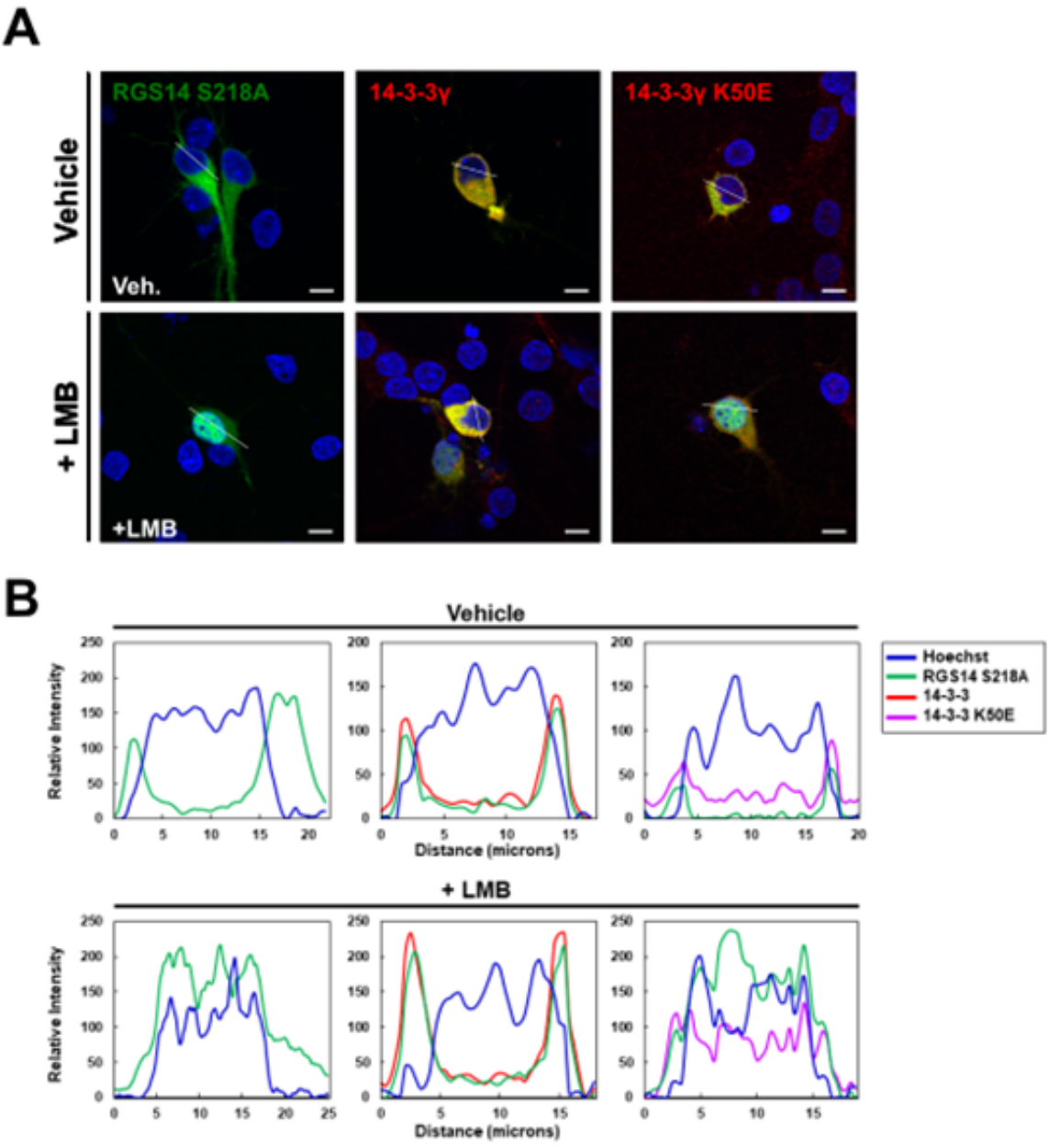
A
RGS14 S218A
14-3-3γ
14-3-3γ K50E
Vehicle
+ LMB
Veh.
+LMB
B
Vehicle
+ LMB
Relative Intensity
Distance (microns)
Hoechst
RGS14 S218A
14-3-3
14-3-3 K50E

Figure 4.9. 14-3-3γ does not bind at serine 218 of RGS14 to block RGS14 import into the nucleus of hippocampal neurons. (A) Primary neurons were transfected with 1 μg YFP-RGS14 and 1 μg empty vector, 1 μg His-tagged 14-3-3γ, or 1 μg His-tagged 14-3-3γ(K50E) per coverslip. 24 hours later, neurons were treated with 40 nM leptomycin B (+LMB) or vehicle for 2 hours before being fixed in 4% paraformaldehyde in PBS. YFP-RGS14(S218A) was visualized by the intrinsic fluorescence of YFP (green). 14-3-3γ immunostaining was performed using an anti-14-3-3γ primary antibody and AlexaFluor 546 (red) secondary antibody while nuclei were visualized by staining DNA with Hoechst 33258 (blue). Images are representative of at least three separate experiments. Scale bars represent 10 μm. (B) Relative fluorescence intensity of YFP-RGS14(S218A), 14-3-3, and nuclear staining was measured through a cross-section of each cell as indicated by the white line through each cell in (A).

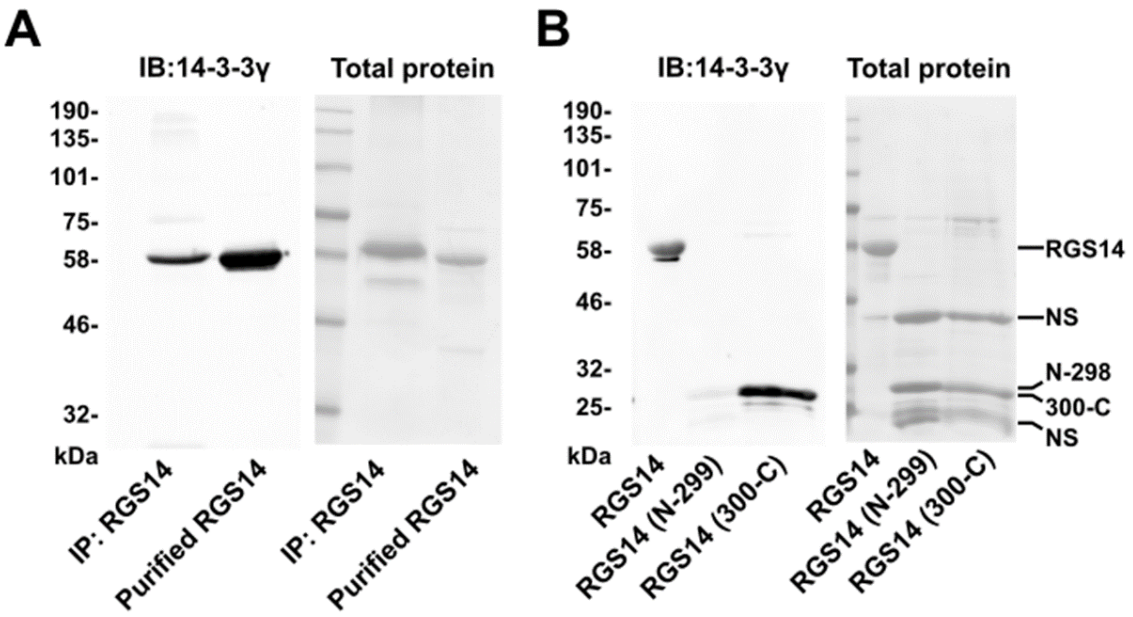

Figure 4.10. 14-3-3γ interacts with RGS14 at a unique binding site in a phosphorylation-independent manner. (A) 9 μg Flag-RGS14 was expressed in HEK 293 cells and recovered by immunoprecipitation (IP-RGS14). 30% of the IP-RGS14 sample and 5 μg of purified recombinant RGS14 expressed in E. coli (Purified RGS14) were subjected to SDS-PAGE and then transferred to a nitrocellulose membrane. The membrane (left panel) was incubated with pure His-tagged 14-3-3γ overnight and probed for interactions between RGS14 and 14-3-3 via immunoblot for 14-3-3 (IB: 14-3-3γ). Equal amounts of the same protein samples were loaded in parallel on a separate gel and stained with Ponceau S (Right panel) to show the relative abundance of the proteins in the immunoblot. (B) 5 μg of RGS14, RGS14(N-298), and RGS14(300-C) partially purified from E. coli were subjected to SDS-PAGE then transferred to a nitrocellulose membrane. The membrane (left panel) was incubated with pure His-tagged 14-3-3γ overnight and probed for interactions

between RGS14 and 14-3-3 via immunoblot for 14-3-3 (IB: 14-3-3γ). Equal amounts of the same protein samples were loaded in parallel on a separate gel and stained with Ponceau S (Right panel) to show the relative abundance of the proteins in the immunoblot. Lines to the right of the right panel indicate the bands of RGS14 or truncations at the expected sizes in the Ponceau stained membrane as well as nonspecific, unidentified proteins (NS) in the partially purified preparations. These findings are representative of three independent experiments.

3.4 Discussion

Here, we provide evidence that RGS14 directly interacts with 14-3-3 in both a phosphorylation-dependent and phosphorylation-independent manner. The phosphorylation-dependent interaction is markedly enhanced by downstream signaling through active H-Ras and is mediated by phosphorylation of serine 218 of RGS14, located adjacent to the RGS domain, in the linker region between the RGS domain and the R1 domain. Functionally, this interaction blocks active Gαi binding at the RGS domain but does not affect H-Ras binding to RGS14. Meanwhile, the phosphorylation-independent binding of 14-3-3 is correlated with the blockade of nuclear import of RGS14, thereby trapping it in the cytosol. One or both of these interactions take place within the mouse hippocampus, suggesting that 14-3-3 plays a role in regulating RGS14's suppression of synaptic plasticity in the CA2 region of the hippocampus.

H-Ras signaling promotes the specific phosphorylation-dependent interaction between RGS14 and 14-3-3

Our findings (Fig. 2) demonstrate that the 14-3-3 interaction with RGS14 is promoted by downstream signaling of active H-Ras, independent of H-Ras binding directly to RGS14. As RGS14 interacts with Raf (Shu, Ramineni, and Hepler 2010), a well-known 14-3-3 binding partner (Li et al. 1995; Clark et al. 1997; Tzivion, Luo, and Avruch 1998; Roy et al. 1998; Petosa et al. 1998), it was unclear to us whether 14-3-3 interacts directly with RGS14 or through an indirect interaction bridged by Raf. However, analysis by far-Western blotting showed that 14-3-3 is able to interact directly with RGS14 in the absence of any other RGS14 interacting partners (Fig. 3B). Furthermore, decreased interaction between RGS14 and 14-3-3 following treatment with lambda phosphatase indicated that 14-3-3 binds at a motif centered at a phosphorylated serine or threonine on RGS14 (Fig. 3). Mapping of the 14-3-3 binding site with truncation mutants of RGS14 followed

by creation of phospho-null point mutants at potential 14-3-3 binding sites revealed a 14-3-3 binding site centered around serine 218 on RGS14 in the linker region between the RGS and R1 domains (Fig. 4 and 5). This serine and the surrounding sequence is fully conserved between human, rat, and mouse RGS14, making it a likely candidate for 14-3-3 interaction and subsequent regulation of RGS14 activity (Fig. 5).

We next attempted to determine the kinase downstream of H-Ras that facilitates the interaction of 14-3-3 and RGS14 through the phosphorylation of serine 218 of RGS14. While Scansite3 set on minimum stringency predicted the phosphorylation of serine 218 by CaMKII and Akt (Obenauer, Cantley, and Yaffe 2003), which are both activated downstream of H-Ras, treatment of cells with selective MEK, PI3K, and CaMKII inhibitors to block ERK, Akt, and CaMKII kinase activity respectively, had no effect (Suppl. Fig. 2A). Additional experiments showed that treatment of cells with EGF to activate kinases downstream of activated Ras, including ERK, does not begin to potentiate the interaction between RGS14 and 14-3-3 until approximately two hours after treatment, even though ERK activation occurs very rapidly (Suppl. Fig. 2B). Taken together, these data suggest that active H-Ras enhancement of the interaction between RGS14 and 14-3-3 likely takes place due to long-term H-Ras activation, likely independent of ERK signaling, that influences changes in transcription and translation in the cell. These data coupled with the failure of the most highly predicted kinases to phosphorylate the 14-3-3 binding site on RGS14 makes identification of a kinase that phosphorylates serine 218 of RGS14 extremely difficult. While the Scansite3 database takes many kinases into account, not all kinases are included, potentially excluding the kinase relevant to this discussion. Furthermore, there are many kinases for which there is no clear phosphorylation motif, making prediction of phosphorylation by those kinases difficult. H-Ras has many reported effectors that engage many more downstream kinases

(Rajalingam et al. 2007). Thus, at this time, we are unable to identify the kinase responsible for phosphorylating RGS14 at serine 218.

14-3-3 interaction with RGS14 inhibits active Gαi binding at the RGS domain

The interaction of 14-3-3 with target substrate proteins can elicit various effects including conformational change, change in subcellular localization, and/or enhancement or inhibition of protein-protein interactions (Tzivion, Shen, and Zhu 2001; Fu, Subramanian, and Masters 2000; Yaffe 2002). Looking specifically at RGS proteins, 14-3-3 has been shown in several cases to inhibit Gα binding at the RGS domain (Benzing et al. 2000; Abramow-Newerly, Ming, and Chidiac 2006). These previously reported effects of 14-3-3 on RGS functions, coupled with the proximity of the RGS14 14-3-3 binding site adjacent to the RGS domain, led us to examine effects of 14-3-3 binding on RGS14 interactions with its known binding partners active Gαi/o, as well as active H-Ras and inactive Gαi1. For these studies, ideally, we would examine the effects of 14-3-3 on direct protein-protein interactions using pure proteins to gain insight into the function of the RGS14:14-3-3 interaction. However, our inability to phosphorylate RGS14 *in vitro* with the appropriate kinase to promote 14-3-3 interaction limited this approach. In an attempt to mimic phosphorylation of RGS14 at serine 218, we replaced the residue with a phosphomimetic aspartate as well as glutamate. However, these phosphomimetic residues have been shown to be a poor mimic for a phosphate with respect to 14-3-3 binding (Johnson et al. 2010; Astuti and Gabrielli 2011; Muslin et al. 1996) and these residue changes failed to promote 14-3-3 binding to RGS14 (data not shown). Therefore, with such limited options, we were forced to analyze interactions between RGS14 and associated proteins in live cells using BRET.

We first determined the effect of 14-3-3 interaction on the binding of active Gαi at the RGS domain and found that 14-3-3 does indeed decrease active Gαi interaction with the RGS domain,

presumably inhibiting RGS14's negative regulation of Gαi downstream signaling. Because H-Ras signaling enhances 14-3-3 binding to RGS14 and 14-3-3 binds within the linker region between the RGS and Ras binding domains of RGS14, we also examined the effect of 14-3-3 on H-Ras interaction with RGS14. Here, we saw no effect, indicating that 14-3-3 interactions with RGS14 selectively inhibit only active Gαi binding at the RGS domain, leaving intact RGS14 interaction with H-Ras at the R1 domain and inactive Gαi at the GPR motif. This selective inhibition by 14-3-3 of active Gαi/o interaction could function as a regulatory mechanism in which RGS14 could promote or enhance signaling through interactions at the R1 domain and GPR motif, while selectively silencing RGS14 activity through the RGS domain.

RGS14 nuclear localization is prevented by phosphorylation-independent interaction with 14-3-3

A common function of 14-3-3 proteins is to affect the subcellular localization of their substrates (Yaffe 2002; Yuan, Michelsen, and Schwappach 2003; Nufer and Hauri 2003; O'Kelly et al. 2002). Because we have previously shown that RGS14 shuttles in and out of the nucleus (Cho, Kim, and Kehrl 2005; Shu et al. 2007; Branch and Hepler 2017), we wanted to examine the effect of 14-3-3 interaction on RGS14 nuclear localization. Surprisingly, we found that 14-3-3 prevents RGS14 from translocating to the nucleus but that 14-3-3 binding at the phosphorylation-dependent binding site at serine 218 is not responsible for this effect (Fig. 8 and 9). Further examination showed that 14-3-3 is able to interact with RGS14 in a phosphorylation-independent manner at a unique 14-3-3 binding site on RGS14 (Fig. 10B), providing a bifunctional mechanism by which 14-3-3 can modulate RGS14 nuclear localization at one binding site while regulating active Gαi binding at another (Fig. 11).

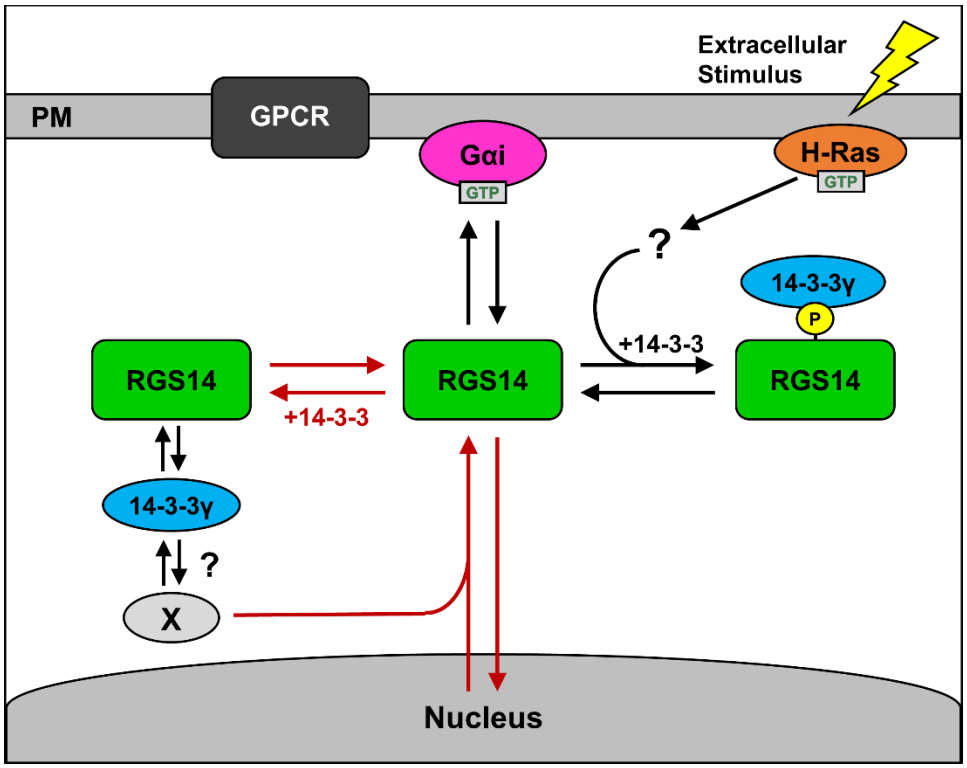

Figure 4.11. Proposed model showing bifunctional regulation of RGS14 by 14-3-3 contingent upon two different modes of binding. In resting cells, RGS14 exists in the cytoplasm, capable of shuttling in and out of the nucleus as well as interacting with active Gαi-GTP at the plasma membrane via its RGS domain. Long-term H-Ras activation following an extracellular stimulus leads to the upregulation and/or activation of an unidentified kinase, leading to phosphorylation of serine 218 of RGS14 and binding of 14-3-3γ at the motif centered around that residue. This phosphorylation-dependent binding disrupts RGS14 interaction with active Gαi at the plasma membrane, while leaving interaction with other binding partners and nuclear localization unaffected (black arrows). RGS14 also interacts directly with 14-3-3γ in a phosphorylation-independent manner, possibly interacting directly with RGS14 to prevent RGS14 nuclear localization while not affecting interaction with active Gαi-GTP (red arrows), though it is possible that 14-3-3 interacts with another binding partner to indirectly inhibit RGS14 nuclear localization.

However, we should note that the phosphorylation-independent binding of 14-3-3 is only correlated with blockade of RGS14 nuclear import, and we cannot rule out the possibility that 14-3-3 may be interacting with other proteins to indirectly inhibit RGS14 transport into the nucleus.

Because this RGS14:14-3-3 interaction is not mediated by phosphorylation of a typical 14-3-3 binding site, there remains the question of how this interaction is regulated in the cell. RGS14 levels in the CA2 region of the hippocampus increase into adulthood and remain stable (Evans et al. 2014). However, 14-3-3 expression has been shown to change based on conditions in the cell (Chen et al. 2007). It is possible that expression levels of 14-3-3 may be a unique mechanism by which RGS14 nuclear localization is regulated. Insight into the actual function of 14-3-3's blockade of RGS14 nuclear localization is limited at this time because a function for RGS14 in the nucleus has not yet been determined.

Endogenous RGS14 interacts with 14-3-3 in mouse hippocampus

Within the brain, RGS14 is selectively expressed in the CA2 subregion of the hippocampus (Evans et al. 2014), where it has been shown to suppress synaptic plasticity and associated learning and memory (Lee et al. 2010). Importantly, we find that endogenous RGS14 and 14-3-3 can form a stable complex in this part of the brain, as shown via co-immunoprecipiation of 14-3-3 with RGS14 from isolated mouse hippocampus (Fig. 1). 14-3-3γ, the 14-3-3 isoform that selectively interacts with RGS14 (Suppl. Fig. 1), is highly expressed in hippocampal neurons as well (Baxter et al. 2002), putting this isoform in position to regulate RGS14 function. Of note, 14-3-3 proteins are also linked to synaptic plasticity. Functional knockout of 14-3-3 has been shown to inhibit hippocampal LTP and associative learning and memory (Qiao et al. 2014). Additionally, 14-3-3 proteins have been shown to be necessary for activation of the Ras/Raf/MEK/Erk signaling pathway (Tzivion, Luo, and Avruch 1998; Roy et al. 1998), which we show here *indirectly*

promotes the phosphorylation-dependent interaction between RGS14 and 14-3-3. Furthermore, this signaling cascade has been shown to be necessary for normal synaptic plasticity and the expression of LTP (English and Sweatt 1997) behind mammalian associative learning (Atkins et al. 1998), which native RGS14 has been shown to suppress in the CA2 region (Lee et al. 2010). Additionally, it is unclear where and how RGS14 is acting to suppress LTP. Phosphorylation-independent interaction between RGS14 and 14-3-3 could regulate the balance of RGS14 in the cytoplasm and nucleus, changing RGS14's distribution to either reduce or enhance it's suppression of LTP in the hippocampus. Due to the effect of 14-3-3 on RGS14's subcellular localization (Fig. 8 and 9) and interaction with functional binding partners, we speculate that 14-3-3 interactions could regulate RGS14 suppression of synaptic plasticity.

Conclusions and Future Directions

Here, we show that RGS14 interacts with a novel binding partner, 14-3-3, in both a phosphorylation-dependent and phosphorylation-independent manner. The phosphorylation-dependent interaction is promoted by signaling downstream of activated H-Ras. This interaction specifically inhibits interaction of active Gαi/o at the RGS domain while leaving association with active H-Ras and inactive Gαi unperturbed. Meanwhile, 14-3-3 also binds within the C-terminal half of RGS14 in a phosphorylation-independent manner, and blocks (either directly or indirectly) RGS14 import into the nucleus of neurons. These interactions provide novel mechanisms of regulation of RGS14 interactions and localization respectively, that give us further insight into RGS14 function in its native environment, the hippocampus, where we demonstrated that endogenous RGS14 interacts with native 14-3-3. Furthermore, both H-Ras and 14-3-3 have been shown to play critical roles in the proper expression of LTP, with RGS14 suppressing this form of synaptic plasticity. Future studies will be directed at determining if and how H-Ras signaling in

CA2 pyramidal neurons functions to control phosphorylation-dependent RGS14:14-3-3 interactions. Of great interest also is understanding the role of RGS14 in the nucleus, and 14-3-3's role in blocking RGS14 localization there. To our knowledge, this is the first report demonstrating 14-3-3-mediated inhibition of RGS protein nuclear translocation, though the possibility has been suggested for other RGS proteins (Burchett 2003; Niu et al. 2002). Multiple other RGS proteins have been found in the nucleus including RGS3 (Dulin et al. 2000), RGS6 (Chatterjee and Fisher 2003), RGS7 (Rose et al. 2000; Witherow et al. 2000), RGS9-2 (Witherow et al. 2000), RGS10 (Lee and Tansey 2015; Burgon et al. 2001), and RGS12(Chatterjee and Fisher 2000, 2002). It is possible that 14-3-3 acts similarly on all of these RGS proteins, preventing their nuclear import. Future studies elucidating the conditions necessary for phosphorylation-dependent and -independent RGS14:14-3-3 complex formation will allow us to understand if and how 14-3-3 plays a definitive role in RGS14 regulation of synaptic plasticity.

Chapter 5:

Discussion

This chapter contains text that has been modified from: Squires, K. E., K. J. Gerber, J. F. Pare, M. R. Branch, Y. Smith and J. R. Hepler (2018). "Regulator of G protein signaling 14 (RGS14) is expressed pre- and postsynaptically in neurons of hippocampus, basal ganglia, and amygdala of monkey and human brain." Brain Struct Funct **223**(1): 233-253.

5.1 RGS14 is a complex scaffolding protein

RGS14 interacts with many different proteins, scaffolding them together to affect their activity toward each other to ultimately control cell signaling and the physiology mediated by those cells. At the RGS domain, RGS14 acts as a GAP toward active Gαi/o family members, terminating downstream signaling started by activation of a GPCR. Near the C-terminus of the protein, RGS14 interacts with inactive Gαi1 and 3. While this function was speculated to be a way for RGS14 to enhance Gβγ signaling while keeping Gα-mediating signaling pathways inactive, this was recently shown not to be the case (Brown et al. 2015). The current view is that RGS14's interaction with inactive Gαi1/3 anchors RGS14 at the plasma membrane, where it is optimally-positioned to manipulate signaling involved in synaptic plasticity.

In addition to RGS14's interactions with heterotrimeric Gα proteins, RGS14 also interacts with active H-Ras and Rap2 at its R1 domain, the first half of RGS14's tandem Raf-like Ras binding domains. While H-Ras and Rap2 have been shown to interact with R1, the binding partner for R2 is still unkown and the function of this tandem Ras binding domain is unclear. In addition to these proteins that have specific binding domains or motifs with which to interact on RGS14, many other RGS14 binding partners have been identified. Calmodulin has been shown to interact directly with RGS14 in a calcium-dependent manner and CaMKII phosphorylates RGS14 at multiple sites. PKA has also been shown to phosphorylate RGS14, enhancing RGS14's interaction with inactive Gαi at the GPR motif. In light of recent discoveries this is likely a mechanism to direct RGS14 to the plasma membrane where it is positioned to interact with its many binding partners and modulate synaptic plasticity.

5.2 RGS14 interaction with 14-3-3

RGS14 also interacts with with 14-3-3, a ubiquitously expressed phospho-serine and -threonine binding protein known for controlling many aspects of phosphorylation-dependent signaling throughout the cell. Notably, neither PKA nor CaMKII mediate RGS14's interaction with 14-3-3. RGS14 is capable of interacting with 14-3-3 in both a phosphorylation-dependent and -independent manner, which is unusual for 14-3-3 proteins. 14-3-3's more typical, phosphorylation-dependent interaction with RGS14 is centered at serine 218 of RGS14, in the linker region between the RGS and R1 domain. This interaction is enhanced by the presence of active H-Ras though direct binding of H-Ras to RGS14 is not necessary to potentiate binding. Furthermore, signaling downstream of H-Ras needs to be active for an extended period of time to potentiate this interaction, indicating that H-Ras is likely not activating a kinase that is phosphorylating RGS14 but that it is causing long-term transcriptional changes in the cell that facilitate phosphorylation of RGS14 at serine 218. This has made identification of the kinase responsible for phosphorylation of serine 218 difficult. These efforts included examining this 14-3-3 binding site for potential kinase phosphorylation motifs and testing the activity of multiple kinases at this site including PKA, CaMKII, PKC, and Erk(Gerber, Squires, and Hepler 2018). Future studies that are able to identify this kinase will be extremely useful in understanding regulation of RGS14 phosphorylation at this site as well as determining the context in which this 14-3-3 binding is taking place. 14-3-3 binding at this site inhibits active Gαi-GTP binding to the RGS domain of RGS14 but we still do not know how this specific interaction ties into the broader role of RGS14 as a suppressor of synaptic plasticity.

In addition to phosphorylation-dependent binding of 14-3-3 at serine 218 of RGS14, 14-3-3 is also capable of interacting with RGS14 is a phosphorylation-independent manner. This

interaction takes place at a separate site on RGS14, though the exact location is unclear. While binding of 14-3-3 to this separate, unique location on RGS14 does not affect Gαi binding, it does prevent RGS14 from translocating into the nucleus. Future work into understanding the function of RGS14 in the nucleus will help us understand the bifunctional role of 14-3-3 interaction with RGS14 and help us elucidate how this interaction is regulated. 14-3-3 expression levels or localization within the cell may change in order to enhance or diminish the phosphorylation-independent interaction as it is unaffected by kinase or phosphatase activity. Interestingly, RGS14 appears to only interact with 14-3-3γ, one of seven unique 14-3-3 isoforms. While differences between the different isoforms are largely unknown as they typically bind the same proteins and perform the same functions, it is likely that this preference for 14-3-3γ for RGS14 over the other isoforms is relevant to the function of the interaction. It may also be a method of regulation. Through changing levels of 14-3-3γ specifically while keeping expression of the other isoforms the same, the cell may be able to tilt the equilibrium of phosphorylation-independent binding toward interaction or dissociation, influencing binding to RGS14 and other proteins with which 14-3-3γ interacts with in a phosphorylation-independent manner. This mechanism of control would be possible with any 14-3-3 isoform and would provide a rational for the existence of so many distinct isoforms with seemingly overlapping functions.

5.3 Finding the functional interactions in the RGS14 interactome

While many interactions between RGS14 and its multiple binding partners have been examined and characterized, it is still unclear how RGS14 modulates cellular signaling through these interactions to suppress synaptic plasticity in the hippocampus. As a complex scaffold protein with many binding domains that integrate extensive signaling pathways within the cell, identification of the binding partners and associated signaling that mediate RGS14 suppression of

plasticity is a formidable challenge. In an effort to narrow our focus on necessary interactions for this distinct RGS14 function, we performed unpublished studies in which RGS14 was expressed in CA1 hippocampal neurons in organotypic slices, and showed that RGS14 suppressed LTP in CA1 in the same way that endogenous RGS14 suppresses LTP in CA2. This allowed us to express point mutants of RGS14 that did not interact with active Gαi/o-GTP at the RGS domain, active H-Ras and Rap2 at the R1 domain, and inactive Gαi1/3-GDP at the GPR motif in order to determine the contributions of these binding domains and their associated proteins to RGS14's ability to suppress hippocampal LTP. Unexpectedly, mutations in the RGS and R1 domains did not impact RGS14's effect on plasticity while preventing the GPR motif from interacting with inactive Gαi1/3 ablated RGS14's ability to suppress LTP.

Two obvious questions arise from these results: 1) What makes this interaction so important for RGS14's function and, 2) why does blockade of RGS14 interaction with active Gαi, H-Ras, and Rap2 not affect RGS14's ability to suppress LTP? One possible answer to the first question is that the GPR motif is important for proper RGS14 localization. Brown and co-workers propose a model in which an RGS14 signaling node is targeted and anchored to the PSD by inactive Gαi1/3, where it is positioned to intercept and modulate incoming signals from GPCRs or other membrane receptors or ion channels (Brown et al. 2015). The simplest answer to the second question of why blockade of RGS14 interaction with H-Ras and Rap2 as well as active Gαi/o does not affect suppression of LTP is that RGS14's interaction with them is simply not necessary for RGS14's suppression of learning and memory, or perhaps they play a more understated, regulatory role. Because these domains are highly conserved, though it suggests that these interactions are likely important for additional, unkown functions of RGS14 that have yet to be discovered. It is also worth noting that while the point mutation in R1 greatly decreases binding to Rap2 and H-

Ras, it does not completely ablate it (Shu, Ramineni, and Hepler 2010). This lower level of binding may still be enough for RGS14 to suppress LTP when it is being exogenously expressed once Gαi-GDP binding at the GPR motif has targeted RGS14 to the proper location in the cell.

The RGS14 interactome has been immensely helpful in determining potential functional RGS14 binding partners in an unbiased manner. While RGS14's domains dictate that it's most prominent interactors in hippocampal neurons are likely heterotrimeric and small GTPases, the interactome from mouse brain differs from these expectations. By far the most abundant protein-protein interactions that we see with RGS14 are actomyosin-binding proteins, and calcium-dependent kinases (Evans, Gerber, et al. 2018). RGS14's interaction with calmodulin (CaM) and CaM-dependent protein kinases has already been further examined. RGS14 directly interacts with CaM in a calcium-dependent manner and CaMKII is capable of phosphorylating RGS14 *in vitro*. Furthermore, another report revealed that RGS14 attenuates spine calcium elevations in area CA2 and that RGS14's suppression of LTP can be overcome by increasing extracellular calcium indicating a clear role for RGS14 regulation of calcium-signaling and handling in hippocampal neurons(Evans, Parra-Bueno, et al. 2018). It is important to note, though, that RGS14's interaction with CaM and CaMKII have not yet been shown to directly to be involved in it's effect on calcium handling in CA2.

While RGS14's interactions with proteins connected to calcium-dependent kinase activity have been examined, its interactions with proteins connected to actin/myosin binding are uninvestigated. Many of the actin-binding proteins from our RGS14 interactome are directly connected to control of plasticity and LTP. Two of the top interactors, myosin Va and myosin VI, have been studied in the context of LTP. These myosins travel along actin filaments to deliver cargo to different parts of the cell including the spine, moving toward the plus and minus end of

actin filaments, respectively. Myosin Va is actually necessary for LTP, as it is responsible for transporting AMPA receptors to spines so that these receptors can mediate the enhanced depolarization in the dendritic spine observed following LTP induction (Correia et al. 2008). As myosin Va is responsible for the transport of AMPA receptors to the synapse, it may also facilitate transport of RGS14, bringing with it RGS14 and any other proteins associated with RGS14 that may disrupt synaptic signaling and suppress LTP. Notably, we do not see AMPA receptor subunits in the RGS14 interactome, suggesting that RGS14 may disrupt the interaction between myosin Va and the AMPA receptor, inhibiting its transport. While myosin Va facilitates insertion of AMPA receptors into the synapse, myosin VI performs the opposite action, mediating AMPA receptor endocytosis (Osterweil, Wells, and Mooseker 2005). RGS14 may directly or indirectly facilitate myosin VI's function, thereby suppressing LTP.

RGS14 appears to interact not just with myosin Va and myosin VI but with a large number of other actin-binding proteins. This is likely due to all of these proteins being connected to each other through the actin cytoskeleton, with RGS14 interacting directly with only a select few to mediate its function at the dendritic spine. As is often the case with proteomic data, the problem is not obtaining enough data but sorting through a huge number of potential targets to identify those of greatest interest and relevance. To this end, a meta-analysis combining data from the RGS14 interactome and the CA2 proteome in which RGS14 is enriched is especially useful. Upon examining multiple networks of proteins with correlated expression in the hippocampus, we found that RGS14 is predictive of expression of an entire network of proteins that have enhanced expression in CA2 (vs. CA1). The GO terms associated with proteins in this module include "regulation of actin filament polymerization," "actin binding," and "cytoskeleton." Not only do the RGS14 interactome and coexpression network in CA2 independently implicate RGS14 in

regulation and control of the actin cytoskeleton, but these data can be combined to gain insight into the most relevant interactions between RGS14 and the extensive network of actin-binding proteins with which RGS14 interacts.

Two of the proteins found to be highly enriched in the RGS14 interactome, drebrin 1 and myosin IIA, also interact with multiple proteins in the RGS14 coexpression network, suggesting that these proteins may be direct, functional interactors with RGS14. Related to RGS14's known role as a suppressor of LTP in area CA2, drebrin 1 has been shown extensively to be important for spine formation and plasticity (Takahashi et al. 2003; Takahashi, Mizui, and Shirao 2006; Koganezawa et al. 2017; Mizui et al. 2014). Drebrin forms a stable structure with actin in dendritic spines but following NMDA receptor activation, drebrin exits spines, presumably allowing F-actin polymerization associated with plasticity (Mizui et al. 2014). Furthermore, this removal of drebrin from spines is actually mediated by myosin II (Mizui et al. 2014), which has been individually shown to be necessary for maintenance of LTP (Ryu et al. 2006). While myosin IIB specifically has been shown to be necessary for LTP, those results were obtained in CA1 neurons and dissociated hippocampal neuron cultures. It is possible that myosin IIA functions in CA2 in a similar manner as myosin IIB does in CA1 or that RGS14 interacts with myosin IIA in a manner that affects LTP even while myosin IIA is not critical for the maintenance of LTP by itself. It is worth noting that the RGS14 interactome shows that RGS14 interacts with myosin IIB as well but it is not implicated by the CA2 proteome data.

5.4 RGS14 does what where

Cell signaling events affect cellular function and physiology differently depending on timing, duration, and subcellular localization among other factors. RGS14's modulation of neuronal signaling is no different. RGS14 has been observed in many locations throughout the

neuron including dendritic spines, the cell body, the nucleus, and even axon terminals (Hollinger et al. 2001; Squires et al. 2018; Gerber, Squires, and Hepler 2018). At each of these locations, RGS14 is likely performing different functions through interactions with either the same or different binding partners.

The most apparent question based on current knowledge of RGS14 function is: where is RGS14 acting to suppress LTP in CA2 hippocampal neurons? RGS14 inhibits LTP at the point in which it is consolidated through post-translational modifications coupled with the movement of receptors and ion channels that have already been made prior to its onset. These changes take place at the level of the dendritic spine and do not require signaling back to the nucleus and translation of additional proteins there, indicating that RGS14 is likely working at the level of the dendritic spine to suppress plasticity. Furthermore, RGS14 interacts with multiple calcium-dependent kinases and actin-binding proteins that are necessary for onset and maintenance of LTP (Evans, Gerber, et al. 2018), with expression of RGS14 controlling calcium dynamics in the spines of hippocampal neurons (Evans, Parra-Bueno, et al. 2018). While substantial evidence points to RGS14 directly interacting with proteins in the neuron spine to suppress LTP, it is also possible that expression of RGS14 changes proteomic profile of the cell through manipulation of nuclear transcription such that LTP is no longer supported. This potential outcome could be addressed by expressing a mutant of RGS14 with a nonfunctional nuclear localization sequence and testing its effect on LTP. If this mutant RGS14 is still capable of suppressing LTP in hippocampal neurons, we know that RGS14 is certainly not working in the nucleus to suppress plasticity and is likely functioning in the neuron spine.

What then, is RGS14 doing in the nucleus? RGS14 has long been known to have the capacity to translocate into the nucleus, first being shown to accumulate there following mild heat

stress in HeLa cells (Cho, Kim, and Kehrl 2005). RGS14 nuclear localization has since been examined in multiple publications. While RGS14 usually appears to be predominantly cytosolic in localization, treatment of cells with leptomycin B, which blocks nuclear export, leads to accumulation of RGS14 in the nucleus, revealing that RGS14 is constantly being actively transported in and out of this cellular compartment (Gerber, Squires, and Hepler 2018; Shu et al. 2007). Gαi1-GDP and Gαi3-GDP anchor RGS14 to the membrane through its GPR motif, preventing its translocation to the nucleus (Shu et al. 2007). 14-3-3γ blocks RGS14 translocation to the nucleus in hippocampal neurons over an extended period of time, providing clear evidence of regulation of nuclear localization in RGS14's native environment (Gerber, Squires, and Hepler 2018). Endogenous RGS14 has been examined in the nucleus as well. In primate brain, electron microscopy images show RGS14 in the nucleus of striatal projection neurons (Squires et al. 2018), indicating that RGS14's nuclear localization is likely relevant to its function in the human brain. In B35 neuroblastoma cells, native RGS14 has been shown to behave in the same manner as the exogenously expressed protein following treatment with leptomycin B (Branch and Hepler 2017). Nuclear RGS14 in these cells forms puncta in chromatin-rich regions of the nucleus with non-condensed DNA(Branch and Hepler 2017). Coupled with findings that expression of recombinant RGS14 can alter gene transcription (Cho, Kim, and Kehrl 2005), it appears likely that RGS14 plays a role in transcriptional regulation.

Upon examining our RG14 interactome in mouse brain we identified two proteins that RGS14 may interact with to control transcription, NAP1L1 and NAP1L4. Both of these proteins are expressed broadly throughout neurons in the brain including those in the hippocampus (Takahashi et al. 2014) and while they are mainly localized to the cytoplasm, much like RGS14, they also shuttle in and out of the nucleus (Okuwaki, Kato, and Nagata 2010). These proteins

mediate both nucleosome formation and disassembly, regulating histone dynamics and altering transcription by changing the availability of DNA to the RNA-synthesis machinery of the cell. Specific to neurons, NAP1L1 depletion has been shown to induce abnormal dendritic morphology (Qiao et al. 2018), likely affecting synaptic plasticity as well. Further research must be done to elucidate the function of this interaction between RGS14 and these two nucleosome assembly proteins.

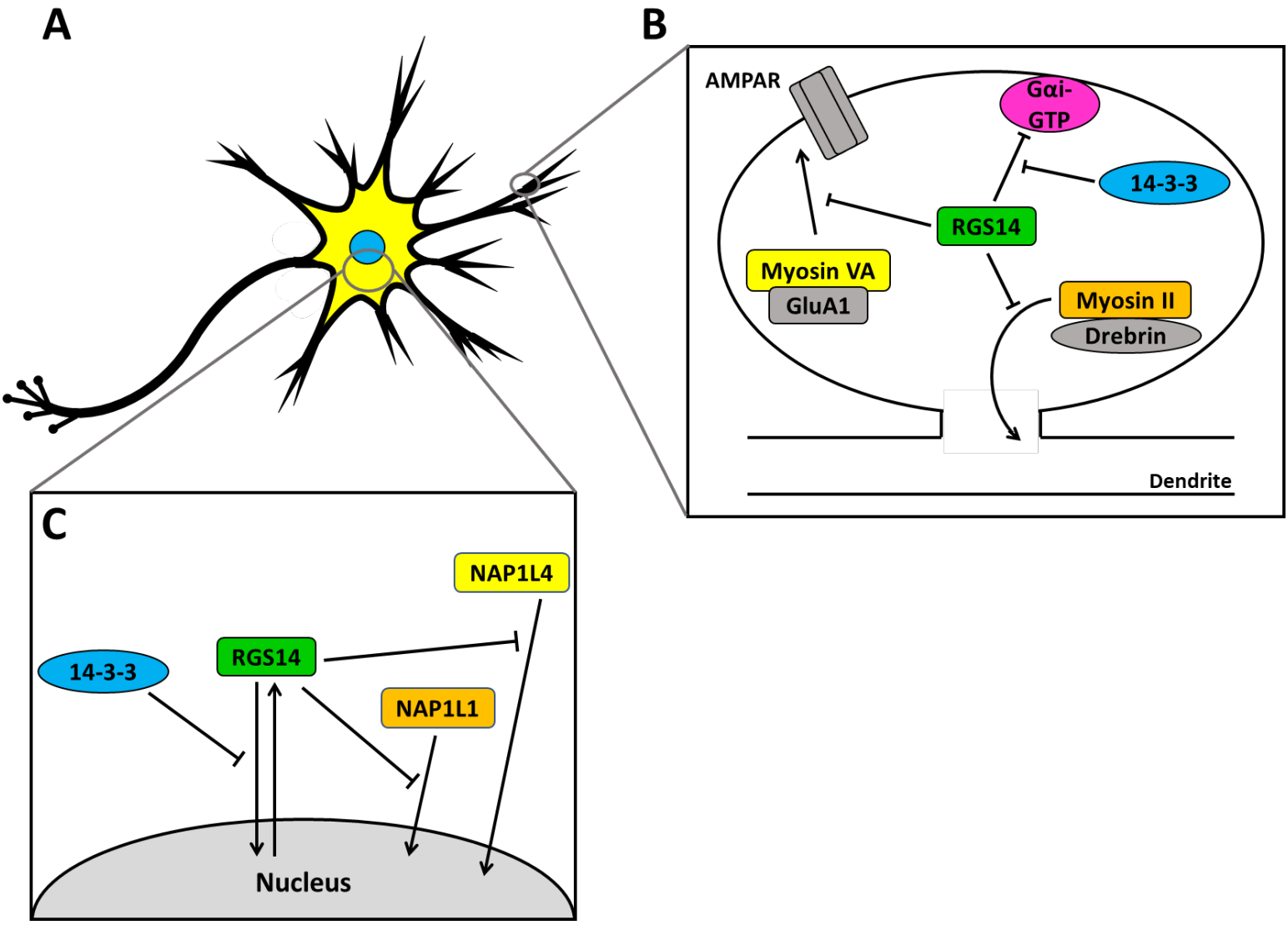

Figure 5.1. RGS14 interacts with what it wants, where it wants, when it wants. A) RGS14 is expressed in pyramidal neurons in area CA2 of the hippocampus. B) 14-3-3 inhibits RGS14 binding to active Gαi1-GTP at the plasma membrane. This regulation of RGS14 action on G protein signaling could be occuring in the neuron spine, modulation RGS14's effects on neurotransmission. RGS14 has also been shown to interact with myosin II and myosin Va. Through these interactions, RGS14 may suppress synaptic plasticity through blockade of myosin

II action on drebrin or myosin Va trafficking of AMPA receptor subunits to the synapse, both of which have been shown to be necessary for normal synaptic plasticity. C) At the cell body, RGS14 is constantly shuttling in and out of the nucleus. Transport of RGS14 into the nucleus is blocked by 14-3-3. Furthermore, RGS14 interactome data shows that RGS14 interacts with nucleosome assembly factors, NAP1L1 and NAP1L4, potentially blocking their translocation into the nucleus and altering neuronal transcription as a result.

While the role of RGS14 in the spine and nucleus have been heavily considered, little work has gone into understanding the potential role of RGS14 in the axon terminal, where the native protein was recently shown to localize in monkey brain via electron microscopy (Squires et al. 2018). Roles for presynaptic heterotrimeric G protein signaling are well established (Chen and Lambert 2000; Brown and Sihra 2008), with RGS proteins like RGS14 capable of modulating this axonal signaling. Active Gβγ subunits can inhibit voltage-gated calcium channels necessary for calcium-dependent neurotransmitter release following an action potential (Bormann 1988; Zamponi and Currie 2013) In this case, RGS proteins can antagonize the effects of Gβγ on N- and P/Q-type Ca_V channels ($Ca_V2.2$ and $Ca_V2.1$), facilitating neurotransmitter release (Kammermeier and Ikeda 1999; Mark, Wittemann, and Herlitze 2000; Jeong and Ikeda 2000). RGS2 has been shown to regulate presynaptic plasticity through this mechanism. (Han et al. 2006). Activation of Gαi/o leads to the dissociation of Gβγ subunits which can inhibit presynaptic voltage-gated $Ca_V2.2$ channels, preventing calcium influx necessary for neurotransmitter release (Ikeda 1996; Kajikawa, Saitoh, and Takahashi 2001). Decreased expression of RGS2 leads to increased Gβγ-mediated inhibition of calcium influx and decreased probability of neurotransmitter release from the synapse, leading to paired-pulse facilitation (PPF). This interpretation is strengthened by *in vitro* evidence showing RGS2-mediated facilitation of $Ca_V2.1$ calcium channels, which are also inhibited by Gβγ subunits (Mark, Wittemann, and Herlitze 2000). Conversely, expression of RGS14 has been shown to decrease calcium influx through voltage-gated calcium (Cav1) channels (Martin-Montanez et al. 2010) (A. Lee, J.R. Hepler, unpublished), though it is unknown if RGS14 modulates activity through pre-synaptic Cav2 channels. Examining the environment in which RGS14 is expressed, we see CA2 hippocampal neurons do not have notably different presynaptic properties compared to area CA1 but they do display slightly enhanced PPF at small intervals

(Zhao et al. 2007). If anything, this would suggest that RGS14 is potentially contributing to enhanced Gβγ signaling in the axon terminal. This could actually be possible through the activity of RGS14's GPR motif, which binds inactive Gαi1/3. Studies have shown that Gα binding to Gβγ and the GPR motif of RGS14 are mutually exclusive (Mittal and Linder 2006) (Shu et al. 2007), suggesting that RGS14 may prolong Gβγ signaling by interfering with the reformation of Gαβγ heterotrimers. This enhanced Gβγ signaling could inhibit voltage-gated calcium channels at the axon terminal and decrease the probability of synaptic vesicle release. However, studies have shown that RGS14 does not prolong Gβγ signaling following receptor activation in live HEK 293 cells (Brown, Lambert, and Hepler 2016). That being said, RGS14 may function differently in the environment of the axon terminal, in which it is natively expressed.

5.5 RGS14 function throughout the brain

While RGS14 has largely been studied in the context of its function as a natural suppressor of LTP in the CA2 region of the hippocampus, it is actually expressed in other brain regions during early development in rodents and in adult primates including humans (Evans et al. 2014; Squires et al. 2018). In mice during early postnatal development (P1-14), RGS14 immunoreactivity can been seen in the anterior olfactory nucleus, piriform cortex, orbital cortex, and entorhinal cortex, although this staining decreases, and area CA2 of the hippocampus demonstrates the strongest staining throughout the brain in adulthood (Evans et al. 2014). In adult primates, including humans, the staining pattern is much different. While primates still display strong staining in hippocampal area CA2, significant RGS14 immunoreactivity is seen outside the hippocampus as well. These areas include the striatum, basal ganglia, and amygdala (Squires et al. 2018), indicating that RGS14 plays much broader role in the brain than suppression of LTP in the hippocampus.

Light and electron microscopic immunohistochemical findings indicate that RGS14 is heavily expressed post-synaptically in dendrites and spines of striatal GABAergic projection neurons and, pre-synaptically in striatopallidal and striatonigral terminals of primates (Squires et al. 2018). Therefore, RGS14 is expressed along both the so-called direct and indirect GABAergic striatofugal pathways of the basal ganglia (Gerfen et al. 1990; Albin, Young, and Penney 1989; Kreitzer and Malenka 2008). Other RGS proteins, including RGS4, contribute to the dopamine-mediated regulation of long term depression (LTD) of corticostriatal glutamatergic synapses in indirect pathway neurons through modulation of postsynaptic mGluR1/5 and D2 dopamine receptors (Lerner and Kreitzer 2012). RGS9-2 and RGS7, which are also highly expressed in the striatum (Anderson, Lujan, and Martemyanov 2009) were similarly found to modulate dopamine signaling (Anderson et al. 2010; Rahman et al. 2003). RGS14 could possibly modulate synaptic signaling and plasticity in a similar manner to these other RGS proteins. However, multiple GPCRs and their associated downstream signals are implicated in synaptic plasticity in the basal ganglia (Kreitzer and Malenka 2008), providing many potential targets at which RGS14 could act in both indirect and direct pathway striatal projection neurons.

Specific RGS14 immunostaining is also observed within the basal and centrolateral nuclei of the monkey amygdala. Although this staining is slightly weaker than the robust basal ganglia and hippocampal immunoreactivity, significant cell body and neuropil labeling is expressed in the basomedial, basolateral and centrolateral nuclei, while the lateral nucleus is largely devoid of immunoreactivity. The amygdala is a central component of the limbic system which plays key roles in the processing of emotional memory, decision making and emotional responses to fear, anxiety and social aggression in primates and rodents (Knox 2016; Bocchio et al. 2016; Lamprecht 2016; Lee, Lee, and Kim 2016). Because the amygdala is made up of glutamatergic principal

neurons and various populations of GABAergic interneurons (Muller, Mascagni, and McDonald 2006; Mascagni and McDonald 2003; McDonald and Mascagni 2001), determining the exact cellular phenotype of RGS14-containing neurons requires further double labeling studies. However, based on morphological grounds and relative abundance, it is clear that some of the labeled cells belong to the population of amygdalofugal glutamatergic neurons. Whether RGS14 inhibits LTP linked to spatial and contextual learning and memory in the amygdala in a similar fashion as it does in CA2 hippocampal cells (Lee et al. 2010) is unknown. The possibility that RGS14 in the amygdala modulates neuronal plasticity and LTP associated with emotional learning and memory linked to human social anxiety and PTSD (Sheynin and Liberzon 2016; Minkova et al. 2017) remains a topic of great interest for future studies.

Is RGS14 interacting with the same proteins in each of these regions? The answer is likely yes and no. One way to begin to answer this question would be to dissect out specific regions of the brain and immunoprecipitate RGS14 from different areas to determine if RGS14's interactome changes in different parts of the brain. Our current RGS14 interactome is based on immunoprecipitation of RGS14 from whole brain, so it likely includes interactions that are taking place in the hippocampus as well as other brain regions. While the potential functional binding partners we have identified for RGS14 play important roles in the hippocampus, many of them have been shown to be essential for processes in other brain regions as well. CaMKII is known for being highly expressed in the hippocampus, where it is approximately 2% of total protein, but it is expressed throughout the brain including the striatum and amygdala (Erondu and Kennedy 1985). In the striatum, CaMKII controls levels of excitatory synapses and intrinsic excitability of medium spiny neurons(Klug et al. 2012), in which RGS14 is also expressed(Squires et al. 2018). In the amygdala, AMPA receptor activity selectively promotes alcohol self-administration in a CaMKII-

dependent manner, suggesting a role for CaMKII in control of AMPA receptor activity and plasticity in the amygdala that leads to behavioral changes. Myosin has also been shown to play a role in mediating changes in synaptic signaling in the amygdala that affect behavior. Myosin II motor activity in the lateral amygdala is required for fear memory consolidation(Gavin et al. 2012), mirroring its role in the hippocampus where it is necessary for consolidation of LTP (Ryu et al. 2006). In the striatum and amygdala, RGS14 may be interacting with myosin, CaMKII, and other proteins in the interactome to control plasticity and behavior linked to these brain reigons. While we know that RGS14 likely affects learning and memroy in primates, we do not know what role RGS14 may play in fear conditioning or drug self-administration experiments. Based on RGS14's expression and the known functions of it's interacting partners in these regions, these behaviors merit further study to determine if RGS14 plays a role in types of learning and memory mediated by brain regions outside the hippocampus.

5.6 Concluding Remarks

Overall, my findings presented in this thesis have progressed our understanding of not only what proteins RGS14 may be interacting with to mediate its unique regulation of synaptic plasticity but also the environment in which RGS14 is interacting with these proteins. While RGS14's characterized binding domains indicate that it integrates multiple aspects of G protein signaling, the RGS14 interactome from mouse brain shows that RGS14 also interacts with many actin-binding proteins and calcium-dependent kinases that are known to mediate plasticity in the hippocampus. These interactions would almost certainly not have been discovered without using an unbiased, proteomic approach to understanding the interactions by which RGS14 mediates its function in the hippocampus and other regions of the brain. This interactome also uncovered the interaction between RGS14 and 14-3-3, which regulates not only RGS14's interaction with active

Gαi/o but also its transport into the nucleus through two unique, differentially-regulated 14-3-3 binding sites. Furthermore, by obtaining a comprehensive area CA2 proteome, we now better understand the cellular environement in which RGS14 is working to control LTP. The CA2 proteome also has implications far beyond the function of RGS14, as it has identified many proteins of interest that may help to explain the physiological differences between area CA2 and CA1, advancing the field of hippocampal research as a whole. Going forward, future experiments will focus on understanding exactly how RGS14 is interacting with its many binding partners to regulate LTP. Additional work will examine RGS14's contributions to cellular signaling outside the spine to determine its roles in the nucleus and axon terminal so that we may better understand the context in which 14-3-3 and other binding partners are regulating RGS14 localization and function outside the spine and in neurons of different brain regions.

References

Abramow-Newerly, M., H. Ming, and P. Chidiac. 2006. 'Modulation of subfamily B/R4 RGS protein function by 14-3-3 proteins', *Cell Signal*, 18: 2209-22.

Abramow-Newerly, M., A. A. Roy, C. Nunn, and P. Chidiac. 2006. 'RGS proteins have a signalling complex: interactions between RGS proteins and GPCRs, effectors, and auxiliary proteins', *Cell Signal*, 18: 579-91.

Aitken, A. 1995. '14-3-3 proteins on the MAP', *Trends Biochem Sci*, 20: 95-7.

Alam, R., N. Hachiya, M. Sakaguchi, S. Kawabata, S. Iwanaga, M. Kitajima, K. Mihara, and T. Omura. 1994. 'cDNA cloning and characterization of mitochondrial import stimulation factor (MSF) purified from rat liver cytosol', *J Biochem*, 116: 416-25.

Albin, R. L., A. B. Young, and J. B. Penney. 1989. 'The functional anatomy of basal ganglia disorders', *Trends Neurosci*, 12: 366-75.

Amstadter, A. B., K. C. Koenen, K. J. Ruggiero, R. Acierno, S. Galea, D. G. Kilpatrick, and J. Gelernter. 2009. 'Variant in RGS2 moderates posttraumatic stress symptoms following potentially traumatic event exposure', *J Anxiety Disord*, 23: 369-73.

Anderson, G. R., Y. Cao, S. Davidson, H. V. Truong, M. Pravetoni, M. J. Thomas, K. Wickman, G. J. Giesler, Jr., and K. A. Martemyanov. 2010. 'R7BP complexes with RGS9-2 and RGS7 in the striatum differentially control motor learning and locomotor responses to cocaine', *Neuropsychopharmacology*, 35: 1040-50.

Anderson, G. R., R. Lujan, and K. A. Martemyanov. 2009. 'Changes in striatal signaling induce remodeling of RGS complexes containing Gbeta5 and R7BP subunits', *Mol Cell Biol*, 29: 3033-44.

Anderson, G. R., R. Lujan, A. Semenov, M. Pravetoni, E. N. Posokhova, J. H. Song, V. Uversky, C. K. Chen, K. Wickman, and K. A. Martemyanov. 2007. 'Expression and localization of RGS9-2/G 5/R7BP complex in vivo is set by dynamic control of its constitutive degradation by cellular cysteine proteases', *J Neurosci*, 27: 14117-27.

Astuti, P., and B. Gabrielli. 2011. 'Phosphorylation of Cdc25B3 Ser169 regulates 14-3-3 binding to Ser151 and Cdc25B activity', *Cell Cycle*, 10: 1960-7.

Atkins, C. M., J. C. Selcher, J. J. Petraitis, J. M. Trzaskos, and J. D. Sweatt. 1998. 'The MAPK cascade is required for mammalian associative learning', *Nat Neurosci*, 1: 602-9.

Baughman, J. M., F. Perocchi, H. S. Girgis, M. Plovanich, C. A. Belcher-Timme, Y. Sancak, X. R. Bao, L. Strittmatter, O. Goldberger, R. L. Bogorad, V. Koteliansky, and V. K. Mootha. 2011. 'Integrative genomics identifies MCU as an essential component of the mitochondrial calcium uniporter', *Nature*, 476: 341-5.

Baxter, H. C., W. G. Liu, J. L. Forster, A. Aitken, and J. R. Fraser. 2002. 'Immunolocalisation of 14-3-3 isoforms in normal and scrapie-infected murine brain', *Neuroscience*, 109: 5-14.

Benzing, T., R. Brandes, L. Sellin, B. Schermer, S. Lecker, G. Walz, and E. Kim. 1999. 'Upregulation of RGS7 may contribute to tumor necrosis factor-induced changes in central nervous function', *Nat Med*, 5: 913-8.

Benzing, T., M. Kottgen, M. Johnson, B. Schermer, H. Zentgraf, G. Walz, and E. Kim. 2002. 'Interaction of 14-3-3 protein with regulator of G protein signaling 7 is dynamically regulated by tumor necrosis factor-alpha', *J Biol Chem*, 277: 32954-62.

Benzing, T., M. B. Yaffe, T. Arnould, L. Sellin, B. Schermer, B. Schilling, R. Schreiber, K. Kunzelmann, G. G. Leparc, E. Kim, and G. Walz. 2000. '14-3-3 interacts with regulator of G protein signaling proteins and modulates their activity', *J Biol Chem*, 275: 28167-72.

Berman, D. M., T. M. Wilkie, and A. G. Gilman. 1996. 'GAIP and RGS4 are GTPase-activating proteins for the Gi subfamily of G protein alpha subunits', *Cell*, 86: 445-52.

Betke, K. M., C. A. Wells, and H. E. Hamm. 2012. 'GPCR mediated regulation of synaptic transmission', *Prog Neurobiol*, 96: 304-21.

Bocchio, M., S. B. McHugh, D. M. Bannerman, T. Sharp, and M. Capogna. 2016. 'Serotonin, Amygdala and Fear: Assembling the Puzzle', *Front Neural Circuits*, 10: 24.

Bodenstein, J., R. K. Sunahara, and R. R. Neubig. 2007. 'N-terminal residues control proteasomal degradation of RGS2, RGS4, and RGS5 in human embryonic kidney 293 cells', *Mol Pharmacol*, 71: 1040-50.

Bormann, J. 1988. 'Electrophysiology of GABAA and GABAB receptor subtypes', *Trends Neurosci*, 11: 112-6.

Boulanger, L. M., P. J. Lombroso, A. Raghunathan, M. J. During, P. Wahle, and J. R. Naegele. 1995. 'Cellular and molecular characterization of a brain-enriched protein tyrosine phosphatase', *J Neurosci*, 15: 1532-44.

Bourne, H. R., D. A. Sanders, and F. McCormick. 1990. 'The GTPase superfamily: a conserved switch for diverse cell functions', *Nature*, 348: 125-32.

Branch, M. R., and J. R. Hepler. 2017. 'Endogenous RGS14 is a cytoplasmic-nuclear shuttling protein that localizes to juxtanuclear membranes and chromatin-rich regions of the nucleus', *PLoS One*, 12: e0184497.

Brown, D. A., and T. S. Sihra. 2008. 'Presynaptic signaling by heterotrimeric G-proteins', *Handb Exp Pharmacol*: 207-60.

Brown, N. E., D. Goswami, M. R. Branch, S. Ramineni, E. A. Ortlund, P. R. Griffin, and J. R. Hepler. 2015. 'Integration of G Protein alpha (Galpha) Signaling by the Regulator of G Protein Signaling 14 (RGS14)', *J Biol Chem*, 290: 9037-49.

Brown, N. E., N. A. Lambert, and J. R. Hepler. 2016. 'RGS14 regulates the lifetime of Galpha-GTP signaling but does not prolong Gbetagamma signaling following receptor activation in live cells', *Pharmacol Res Perspect*, 4: e00249.

Bu, Y., N. Wang, S. Wang, T. Sheng, T. Tian, L. Chen, W. Pan, M. Zhu, J. Luo, and W. Lu. 2015. 'Myosin IIb-dependent Regulation of Actin Dynamics Is Required for N-Methyl-D-aspartate Receptor Trafficking during Synaptic Plasticity', *J Biol Chem*, 290: 25395-410.

Burchett, S. A. 2000. 'Regulators of G protein signaling: a bestiary of modular protein binding domains', *J Neurochem*, 75: 1335-51.

Burchett, S. A. 2003. 'In through the out door: nuclear localization of the regulators of G protein signaling', *J Neurochem*, 87: 551-9.

Burchett, S. A., M. L. Volk, M. J. Bannon, and J. G. Granneman. 1998. 'Regulators of G protein signaling: rapid changes in mRNA abundance in response to amphetamine', *J Neurochem*, 70: 2216-9.

Burgon, P. G., W. L. Lee, A. B. Nixon, E. G. Peralta, and P. J. Casey. 2001. 'Phosphorylation and nuclear translocation of a regulator of G protein signaling (RGS10)', *J Biol Chem*, 276: 32828-34.

Campbell, J. K., R. Gurung, S. Romero, C. J. Speed, R. K. Andrews, M. C. Berndt, and C. A. Mitchell. 1997. 'Activation of the 43 kDa inositol polyphosphate 5-phosphatase by 14-3-3zeta', *Biochemistry*, 36: 15363-70.

Canela, L., V. Fernandez-Duenas, C. Albergaria, M. Watanabe, C. Lluis, J. Mallol, E. I. Canela, R. Franco, R. Lujan, and F. Ciruela. 2009. 'The association of metabotropic glutamate

receptor type 5 with the neuronal Ca2+-binding protein 2 modulates receptor function', *J Neurochem*, 111: 555-67.

Canela, L., R. Lujan, C. Lluis, J. Burgueno, J. Mallol, E. I. Canela, R. Franco, and F. Ciruela. 2007. 'The neuronal Ca(2+) -binding protein 2 (NECAB2) interacts with the adenosine A(2A) receptor and modulates the cell surface expression and function of the receptor', *Mol Cell Neurosci*, 36: 1-12.

Carstens, K. E., M. L. Phillips, L. Pozzo-Miller, R. J. Weinberg, and S. M. Dudek. 2016. 'Perineuronal Nets Suppress Plasticity of Excitatory Synapses on CA2 Pyramidal Neurons', *J Neurosci*, 36: 6312-20.

Caruana, D. A., G. M. Alexander, and S. M. Dudek. 2012. 'New insights into the regulation of synaptic plasticity from an unexpected place: hippocampal area CA2', *Learn Mem*, 19: 391-400.

Celver, J., M. Sharma, and A. Kovoor. 2010. 'RGS9-2 mediates specific inhibition of agonist-induced internalization of D2-dopamine receptors', *J Neurochem*, 114: 739-49.

Chalifoux, J. R., and A. G. Carter. 2010. 'GABAB receptors modulate NMDA receptor calcium signals in dendritic spines', *Neuron*, 66: 101-13.

Chatterjee, T. K., and R. A. Fisher. 2000. 'Novel alternative splicing and nuclear localization of human RGS12 gene products', *J Biol Chem*, 275: 29660-71.

Chatterjee, T. K., and R. A. Fisher. 2002. 'RGS12TS-S localizes at nuclear matrix-associated subnuclear structures and represses transcription: structural requirements for subnuclear targeting and transcriptional repression', *Mol Cell Biol*, 22: 4334-45.

Chatterjee, T. K., and R. A. Fisher. 2003. 'Mild heat and proteotoxic stress promote unique subcellular trafficking and nucleolar accumulation of RGS6 and other RGS proteins. Role of the RGS domain in stress-induced trafficking of RGS proteins', *J Biol Chem*, 278: 30272-82.

Chen, C. K., P. Eversole-Cire, H. Zhang, V. Mancino, Y. J. Chen, W. He, T. G. Wensel, and M. I. Simon. 2003. 'Instability of GGL domain-containing RGS proteins in mice lacking the G protein beta-subunit Gbeta5', *Proc Natl Acad Sci U S A*, 100: 6604-9.

Chen, H., and N. A. Lambert. 2000. 'Endogenous regulators of G protein signaling proteins regulate presynaptic inhibition at rat hippocampal synapses', *Proc Natl Acad Sci U S A*, 97: 12810-5.

Chen, J., C. T. Lee, S. L. Errico, K. G. Becker, and W. J. Freed. 2007. 'Increases in expression of 14-3-3 eta and 14-3-3 zeta transcripts during neuroprotection induced by delta9-tetrahydrocannabinol in AF5 cells', *J Neurosci Res*, 85: 1724-33.

Chevaleyre, V., and S. A. Siegelbaum. 2010. 'Strong CA2 pyramidal neuron synapses define a powerful disynaptic cortico-hippocampal loop', *Neuron*, 66: 560-72.

Cho, H., D. U. Kim, and J. H. Kehrl. 2005. 'RGS14 is a centrosomal and nuclear cytoplasmic shuttling protein that traffics to promyelocytic leukemia nuclear bodies following heat shock', *J Biol Chem*, 280: 805-14.

Cho, H., T. Kozasa, K. Takekoshi, J. De Gunzburg, and J. H. Kehrl. 2000. 'RGS14, a GTPase-activating protein for Gialpha, attenuates Gialpha- and G13alpha-mediated signaling pathways', *Mol Pharmacol*, 58: 569-76.

Clark, G. J., J. K. Drugan, K. L. Rossman, J. W. Carpenter, K. Rogers-Graham, H. Fu, C. J. Der, and S. L. Campbell. 1997. '14-3-3 zeta negatively regulates raf-1 activity by interactions with the Raf-1 cysteine-rich domain', *J Biol Chem*, 272: 20990-3.

Cohan, C. H., H. M. Stradecki-Cohan, K. C. Morris-Blanco, N. Khoury, K. B. Koronowski, M. Youbi, C. B. Wright, and M. A. Perez-Pinzon. 2017. 'Protein kinase C epsilon delays latency until anoxic depolarization through arc expression and GluR2 internalization', *J Cereb Blood Flow Metab*, 37: 3774-88.

Correia, S. S., S. Bassani, T. C. Brown, M. F. Lise, D. S. Backos, A. El-Husseini, M. Passafaro, and J. A. Esteban. 2008. 'Motor protein-dependent transport of AMPA receptors into spines during long-term potentiation', *Nat Neurosci*, 11: 457-66.

Cowan, C. W., R. N. Fariss, I. Sokal, K. Palczewski, and T. G. Wensel. 1998. 'High expression levels in cones of RGS9, the predominant GTPase accelerating protein of rods', *Proc Natl Acad Sci U S A*, 95: 5351-6.

Cox, J., M. Y. Hein, C. A. Luber, I. Paron, N. Nagaraj, and M. Mann. 2014a. 'Accurate proteome-wide label-free quantification by delayed normalization and maximal peptide ratio extraction, termed MaxLFQ', *Mol Cell Proteomics*, 13: 2513-26.

Cox, Jürgen, Marco Y. Hein, Christian A. Luber, Igor Paron, Nagarjuna Nagaraj, and Matthias Mann. 2014b. 'Accurate Proteome-wide Label-free Quantification by Delayed Normalization and Maximal Peptide Ratio Extraction, Termed MaxLFQ', *Molecular & Cellular Proteomics*, 13: 2513-26.

Cox, Jürgen, Nadin Neuhauser, Annette Michalski, Richard A. Scheltema, Jesper V. Olsen, and Matthias Mann. 2011. 'Andromeda: A Peptide Search Engine Integrated into the MaxQuant Environment', *J Proteome Res*, 10: 1794-805.

Cui, H., N. Nishiguchi, E. Ivleva, M. Yanagi, M. Fukutake, H. Nushida, Y. Ueno, N. Kitamura, K. Maeda, and O. Shirakawa. 2008. 'Association of RGS2 gene polymorphisms with suicide and increased RGS2 immunoreactivity in the postmortem brain of suicide victims', *Neuropsychopharmacology*, 33: 1537-44.

Dascal, N. 1997. 'Signalling via the G protein-activated K+ channels', *Cell Signal*, 9: 551-73.

Davydov, I. V., and A. Varshavsky. 2000. 'RGS4 is arginylated and degraded by the N-end rule pathway in vitro', *J Biol Chem*, 275: 22931-41.

De Vries, L., B. Zheng, T. Fischer, E. Elenko, and M. G. Farquhar. 2000. 'The regulator of G protein signaling family', *Annu Rev Pharmacol Toxicol*, 40: 235-71.

Demirkan, G., K. Yu, J. M. Boylan, A. R. Salomon, and P. A. Gruppuso. 2011. 'Phosphoproteomic profiling of in vivo signaling in liver by the mammalian target of rapamycin complex 1 (mTORC1)', *PLoS One*, 6: e21729.

DiBello, P. R., T. R. Garrison, D. M. Apanovitch, G. Hoffman, D. J. Shuey, K. Mason, M. I. Cockett, and H. G. Dohlman. 1998. 'Selective uncoupling of RGS action by a single point mutation in the G protein alpha-subunit', *J Biol Chem*, 273: 5780-4.

Ding, J., J. N. Guzman, T. Tkatch, S. Chen, J. A. Goldberg, P. J. Ebert, P. Levitt, C. J. Wilson, H. E. Hamm, and D. J. Surmeier. 2006. 'RGS4-dependent attenuation of M4 autoreceptor function in striatal cholinergic interneurons following dopamine depletion', *Nat Neurosci*, 9: 832-42.

Ding, L., and A. N. Hegde. 2009. 'Expression of RGS4 splice variants in dorsolateral prefrontal cortex of schizophrenic and bipolar disorder patients', *Biol Psychiatry*, 65: 541-5.

Doupnik, C. A., N. Davidson, H. A. Lester, and P. Kofuji. 1997. 'RGS proteins reconstitute the rapid gating kinetics of gbetagamma-activated inwardly rectifying K+ channels', *Proc Natl Acad Sci U S A*, 94: 10461-6.

Drago, I., D. De Stefani, R. Rizzuto, and T. Pozzan. 2012. 'Mitochondrial Ca2+ uptake contributes to buffering cytoplasmic Ca2+ peaks in cardiomyocytes', *Proc Natl Acad Sci U S A*, 109: 12986-91.

Drenan, R. M., C. A. Doupnik, M. P. Boyle, L. J. Muglia, J. E. Huettner, M. E. Linder, and K. J. Blumer. 2005. 'Palmitoylation regulates plasma membrane-nuclear shuttling of R7BP, a novel membrane anchor for the RGS7 family', *J Cell Biol*, 169: 623-33.

Drenan, R. M., C. A. Doupnik, M. Jayaraman, A. L. Buchwalter, K. M. Kaltenbronn, J. E. Huettner, M. E. Linder, and K. J. Blumer. 2006. 'R7BP augments the function of RGS7*Gbeta5 complexes by a plasma membrane-targeting mechanism', *J Biol Chem*, 281: 28222-31.

Dudek, S. M., G. M. Alexander, and S. Farris. 2016. 'Rediscovering area CA2: unique properties and functions', *Nat Rev Neurosci*, 17: 89-102.

Dulin, N. O., P. Pratt, C. Tiruppathi, J. Niu, T. Voyno-Yasenetskaya, and M. J. Dunn. 2000. 'Regulator of G protein signaling RGS3T is localized to the nucleus and induces apoptosis', *J Biol Chem*, 275: 21317-23.

English, J. D., and J. D. Sweatt. 1997. 'A requirement for the mitogen-activated protein kinase cascade in hippocampal long term potentiation', *J Biol Chem*, 272: 19103-6.

Erondu, N. E., and M. B. Kennedy. 1985. 'Regional distribution of type II Ca2+/calmodulin-dependent protein kinase in rat brain', *J Neurosci*, 5: 3270-7.

Evans, P. R., S. M. Dudek, and J. R. Hepler. 2015. 'Regulator of G Protein Signaling 14: A Molecular Brake on Synaptic Plasticity Linked to Learning and Memory', *Prog Mol Biol Transl Sci*, 133: 169-206.

Evans, P. R., K. J. Gerber, E. B. Dammer, D. M. Duong, D. Goswami, D. J. Lustberg, J. Zou, J. J. Yang, S. M. Dudek, P. R. Griffin, N. T. Seyfried, and J. R. Hepler. 2018. 'Interactome Analysis Reveals Regulator of G Protein Signaling 14 (RGS14) is a Novel Calcium/Calmodulin (Ca(2+)/CaM) and CaM Kinase II (CaMKII) Binding Partner', *J Proteome Res*.

Evans, P. R., S. E. Lee, Y. Smith, and J. R. Hepler. 2014. 'Postnatal developmental expression of regulator of G protein signaling 14 (RGS14) in the mouse brain', *J Comp Neurol*, 522: 186-203.

Evans, P. R., P. Parra-Bueno, M. S. Smirnov, D. J. Lustberg, S. M. Dudek, J. R. Hepler, and R. Yasuda. 2018. 'RGS14 Restricts Plasticity in Hippocampal CA2 by Limiting Postsynaptic Calcium Signaling', *eNeuro*, 5.

Evans, PR, and JR Hepler. 2012. 'Regulator of G protein signaling 14 (RGS14) interacts with calmodulin (CaM) in a calcium-dependent manner', *Society for Neuroscience*.

Fadok, V. A., D. L. Bratton, D. M. Rose, A. Pearson, R. A. Ezekewitz, and P. M. Henson. 2000. 'A receptor for phosphatidylserine-specific clearance of apoptotic cells', *Nature*, 405: 85-90.

Fajardo-Serrano, A., N. Wydeven, D. Young, M. Watanabe, R. Shigemoto, K. A. Martemyanov, K. Wickman, and R. Lujan. 2013. 'Association of Rgs7/Gbeta5 complexes with Girk channels and GABAB receptors in hippocampal CA1 pyramidal neurons', *Hippocampus*, 23: 1231-45.

Fiermonte, G., L. Palmieri, S. Todisco, G. Agrimi, F. Palmieri, and J. E. Walker. 2002. 'Identification of the mitochondrial glutamate transporter. Bacterial expression, reconstitution, functional characterization, and tissue distribution of two human isoforms', *J Biol Chem*, 277: 19289-94.

Fischer, A., A. Baljuls, J. Reinders, E. Nekhoroshkova, C. Sibilski, R. Metz, S. Albert, K. Rajalingam, M. Hekman, and U. R. Rapp. 2009. 'Regulation of RAF activity by 14-3-3 proteins: RAF kinases associate functionally with both homo- and heterodimeric forms of 14-3-3 proteins', *J Biol Chem*, 284: 3183-94.

Fredriksson, R., M. C. Lagerstrom, L. G. Lundin, and H. B. Schioth. 2003. 'The G-protein-coupled receptors in the human genome form five main families. Phylogenetic analysis, paralogon groups, and fingerprints', *Mol Pharmacol*, 63: 1256-72.

Fu, H., J. Coburn, and R. J. Collier. 1993. 'The eukaryotic host factor that activates exoenzyme S of Pseudomonas aeruginosa is a member of the 14-3-3 protein family', *Proc Natl Acad Sci U S A*, 90: 2320-4.

Fu, H., R. R. Subramanian, and S. C. Masters. 2000. '14-3-3 proteins: structure, function, and regulation', *Annu Rev Pharmacol Toxicol*, 40: 617-47.

Fu, Y., H. Zhong, M. Nanamori, R. M. Mortensen, X. Huang, K. Lan, and R. R. Neubig. 2004. 'RGS-insensitive G-protein mutations to study the role of endogenous RGS proteins', *Methods Enzymol*, 389: 229-43.

Garzon, J., A. Lopez-Fando, and P. Sanchez-Blazquez. 2003. 'The R7 subfamily of RGS proteins assists tachyphylaxis and acute tolerance at mu-opioid receptors', *Neuropsychopharmacology*, 28: 1983-90.

Gavin, C. F., M. D. Rubio, E. Young, C. Miller, and G. Rumbaugh. 2012. 'Myosin II motor activity in the lateral amygdala is required for fear memory consolidation', *Learn Mem*, 19: 9-14.

Gerber, K. J., K. E. Squires, and J. R. Hepler. 2018. '14-3-3gamma binds regulator of G protein signaling 14 (RGS14) at distinct sites to inhibit the RGS14:Galphai-AlF4(-) signaling complex and RGS14 nuclear localization', *J Biol Chem*, 293: 14616-31.

Gerfen, C. R., T. M. Engber, L. C. Mahan, Z. Susel, T. N. Chase, F. J. Monsma, Jr., and D. R. Sibley. 1990. 'D1 and D2 dopamine receptor-regulated gene expression of striatonigral and striatopallidal neurons', *Science*, 250: 1429-32.

Geurts, M., J. M. Maloteaux, and E. Hermans. 2003. 'Altered expression of regulators of G-protein signaling (RGS) mRNAs in the striatum of rats undergoing dopamine depletion', *Biochem Pharmacol*, 66: 1163-70.

Gold, S. J., Y. G. Ni, H. G. Dohlman, and E. J. Nestler. 1997. 'Regulators of G-protein signaling (RGS) proteins: region-specific expression of nine subtypes in rat brain', *J Neurosci*, 17: 8024-37.

Goldenstein, B. L., B. W. Nelson, K. Xu, E. J. Luger, J. A. Pribula, J. M. Wald, L. A. O'Shea, D. Weinshenker, R. A. Charbeneau, X. Huang, R. R. Neubig, and V. A. Doze. 2009. 'Regulator of G protein signaling protein suppression of Galphao protein-mediated alpha2A adrenergic receptor inhibition of mouse hippocampal CA3 epileptiform activity', *Mol Pharmacol*, 75: 1222-30.

Gozal, E., D. Gozal, W. M. Pierce, V. Thongboonkerd, J. A. Scherzer, L. R. Sachleben, Jr., K. R. Brittian, S. Z. Guo, J. Cai, and J. B. Klein. 2002. 'Proteomic analysis of CA1 and CA3 regions of rat hippocampus and differential susceptibility to intermittent hypoxia', *J Neurochem*, 83: 331-45.

Grabowska, D., M. Jayaraman, K. M. Kaltenbronn, S. L. Sandiford, Q. Wang, S. Jenkins, V. Z. Slepak, Y. Smith, and K. J. Blumer. 2008. 'Postnatal induction and localization of R7BP, a membrane-anchoring protein for regulator of G protein signaling 7 family-Gbeta5 complexes in brain', *Neuroscience*, 151: 969-82.

Grafstein-Dunn, E., K. H. Young, M. I. Cockett, and X. Z. Khawaja. 2001. 'Regional distribution of regulators of G-protein signaling (RGS) 1, 2, 13, 14, 16, and GAIP messenger ribonucleic acids by in situ hybridization in rat brain', *Brain Res Mol Brain Res*, 88: 113-23.

Gu, J., B. L. Firestein, and J. Q. Zheng. 2008. 'Microtubules in dendritic spine development', *J Neurosci*, 28: 12120-4.

Gu, Z., Q. Jiang, and Z. Yan. 2007. 'RGS4 modulates serotonin signaling in prefrontal cortex and links to serotonin dysfunction in a rat model of schizophrenia', *Mol Pharmacol*, 71: 1030-9.

Hackos, D. H., and J. E. Hanson. 2017. 'Diverse modes of NMDA receptor positive allosteric modulation: Mechanisms and consequences', *Neuropharmacology*, 112: 34-45.

Hales, C. M., E. B. Dammer, Q. Deng, D. M. Duong, M. Gearing, J. C. Troncoso, M. Thambisetty, J. J. Lah, J. M. Shulman, A. I. Levey, and N. T. Seyfried. 2016. 'Changes in the detergent-insoluble brain proteome linked to amyloid and tau in Alzheimer's Disease progression', *Proteomics*, 16: 3042-53.

Hamm, H. E. 1998. 'The many faces of G protein signaling', *J Biol Chem*, 273: 669-72.

Han, J., M. D. Mark, X. Li, M. Xie, S. Waka, J. Rettig, and S. Herlitze. 2006. 'RGS2 determines short-term synaptic plasticity in hippocampal neurons by regulating Gi/o-mediated inhibition of presynaptic Ca2+ channels', *Neuron*, 51: 575-86.

Haussler, U., K. Rinas, A. Kilias, U. Egert, and C. A. Haas. 2016. 'Mossy fiber sprouting and pyramidal cell dispersion in the hippocampal CA2 region in a mouse model of temporal lobe epilepsy', *Hippocampus*, 26: 577-88.

He, W., C. W. Cowan, and T. G. Wensel. 1998. 'RGS9, a GTPase accelerator for phototransduction', *Neuron*, 20: 95-102.

Heo, K., S. H. Ha, Y. C. Chae, S. Lee, Y. S. Oh, Y. H. Kim, S. H. Kim, J. H. Kim, A. Mizoguchi, T. J. Itoh, H. M. Kwon, S. H. Ryu, and P. G. Suh. 2006. 'RGS2 promotes formation of neurites by stimulating microtubule polymerization', *Cell Signal*, 18: 2182-92.

Hepler, J. R., D. M. Berman, A. G. Gilman, and T. Kozasa. 1997. 'RGS4 and GAIP are GTPase-activating proteins for Gq alpha and block activation of phospholipase C beta by gamma-thio-GTP-Gq alpha', *Proc Natl Acad Sci U S A*, 94: 428-32.

Hepler, J. R., and A. G. Gilman. 1992. 'G proteins', *Trends Biochem Sci*, 17: 383-7.

Heraud-Farlow, J. E., T. Sharangdhar, X. Li, P. Pfeifer, S. Tauber, D. Orozco, A. Hormann, S. Thomas, A. Bakosova, A. R. Farlow, D. Edbauer, H. D. Lipshitz, Q. D. Morris, M. Bilban, M. Doyle, and M. A. Kiebler. 2013. 'Staufen2 regulates neuronal target RNAs', *Cell Rep*, 5: 1511-8.

Herlitze, S., J. P. Ruppersberg, and M. D. Mark. 1999. 'New roles for RGS2, 5 and 8 on the ratio-dependent modulation of recombinant GIRK channels expressed in Xenopus oocytes', *J Physiol*, 517 (Pt 2): 341-52.

Hewitt, S. A., J. I. Wamsteeker, E. U. Kurz, and J. S. Bains. 2009. 'Altered chloride homeostasis removes synaptic inhibitory constraint of the stress axis', *Nat Neurosci*, 12: 438-43.

Heximer, S. P., S. P. Srinivasa, L. S. Bernstein, J. L. Bernard, M. E. Linder, J. R. Hepler, and K. J. Blumer. 1999. 'G protein selectivity is a determinant of RGS2 function', *J Biol Chem*, 274: 34253-9.

Heximer, S. P., N. Watson, M. E. Linder, K. J. Blumer, and J. R. Hepler. 1997. 'RGS2/G0S8 is a selective inhibitor of Gqalpha function', *Proc Natl Acad Sci U S A*, 94: 14389-93.

Hitti, F. L., and S. A. Siegelbaum. 2014. 'The hippocampal CA2 region is essential for social memory', *Nature*, 508: 88-92.

Hodges, J. L., S. M. Vilchez, H. Asmussen, L. A. Whitmore, and A. R. Horwitz. 2014. 'alpha-Actinin-2 mediates spine morphology and assembly of the post-synaptic density in hippocampal neurons', *PLoS One*, 9: e101770.

Hohoff, C., A. Neumann, K. Domschke, C. Jacob, W. Maier, J. Fritze, B. Bandelow, P. Krakowitzky, M. Rothermundt, V. Arolt, and J. Deckert. 2009. 'Association analysis of Rgs7 variants with panic disorder', *J Neural Transm*, 116: 1523-8.

Hohoff, C., H. Weber, J. Richter, K. Domschke, P. M. Zwanzger, P. Ohrmann, J. Bauer, T. Suslow, H. Kugel, C. Baumann, B. Klauke, C. P. Jacob, J. Fritze, B. Bandelow, A. T. Gloster, A. L. Gerlach, T. Kircher, T. Lang, G. W. Alpers, A. Strohle, L. Fehm, H. U. Wittchen, V. Arolt, P. Pauli, A. Hamm, A. Reif, and J. Deckert. 2015. 'RGS2 ggenetic variation: Association analysis with panic disorder and dimensional as well as intermediate phenotypes of anxiety', *Am J Med Genet B Neuropsychiatr Genet*, 168: 211-22.

Hollinger, S., and J. R. Hepler. 2002. 'Cellular regulation of RGS proteins: modulators and integrators of G protein signaling', *Pharmacol Rev*, 54: 527-59.

Hollinger, S., S. Ramineni, and J. R. Hepler. 2003. 'Phosphorylation of RGS14 by protein kinase A potentiates its activity toward G alpha i', *Biochemistry*, 42: 811-9.

Hollinger, S., J. B. Taylor, E. H. Goldman, and J. R. Hepler. 2001. 'RGS14 is a bifunctional regulator of Galphai/o activity that exists in multiple populations in brain', *J Neurochem*, 79: 941-9.

Hooks, S. B., G. L. Waldo, J. Corbitt, E. T. Bodor, A. M. Krumins, and T. K. Harden. 2003. 'RGS6, RGS7, RGS9, and RGS11 stimulate GTPase activity of Gi family G-proteins with differential selectivity and maximal activity', *J Biol Chem*, 278: 10087-93.

Hornbeck, P. V., B. Zhang, B. Murray, J. M. Kornhauser, V. Latham, and E. Skrzypek. 2015. 'PhosphoSitePlus, 2014: mutations, PTMs and recalibrations', *Nucleic Acids Res*, 43: D512-20.

Huang, C., J. R. Hepler, A. G. Gilman, and S. M. Mumby. 1997. 'Attenuation of Gi- and Gq-mediated signaling by expression of RGS4 or GAIP in mammalian cells', *Proc Natl Acad Sci U S A*, 94: 6159-63.

Huang da, W., B. T. Sherman, and R. A. Lempicki. 2009a. 'Bioinformatics enrichment tools: paths toward the comprehensive functional analysis of large gene lists', *Nucleic Acids Res*, 37: 1-13.

Huang da, W., B. T. Sherman, and R. A. Lempicki. 2009b. 'Systematic and integrative analysis of large gene lists using DAVID bioinformatics resources', *Nat Protoc*, 4: 44-57.

Huang, J., H. Zhou, S. Mahavadi, W. Sriwai, and K. S. Murthy. 2007. 'Inhibition of Galphaq-dependent PLC-beta1 activity by PKG and PKA is mediated by phosphorylation of RGS4 and GRK2', *Am J Physiol Cell Physiol*, 292: C200-8.

Hutchison, R. M., P. Chidiac, and L. S. Leung. 2009. 'Hippocampal long-term potentiation is enhanced in urethane-anesthetized RGS2 knockout mice', *Hippocampus*, 19: 687-91.

Ikeda, S. R. 1996. 'Voltage-dependent modulation of N-type calcium channels by G-protein beta gamma subunits', *Nature*, 380: 255-8.

Ingi, T., and Y. Aoki. 2002. 'Expression of RGS2, RGS4 and RGS7 in the developing postnatal brain', *Eur J Neurosci*, 15: 929-36.

Ingi, T., A. M. Krumins, P. Chidiac, G. M. Brothers, S. Chung, B. E. Snow, C. A. Barnes, A. A. Lanahan, D. P. Siderovski, E. M. Ross, A. G. Gilman, and P. F. Worley. 1998. 'Dynamic regulation of RGS2 suggests a novel mechanism in G-protein signaling and neuronal plasticity', *J Neurosci*, 18: 7178-88.

Jacoby, E., R. Bouhelal, M. Gerspacher, and K. Seuwen. 2006. 'The 7 TM G-protein-coupled receptor target family', *ChemMedChem*, 1: 761-82.

Jayaraman, M., H. Zhou, L. Jia, M. D. Cain, and K. J. Blumer. 2009. 'R9AP and R7BP: traffic cops for the RGS7 family in phototransduction and neuronal GPCR signaling', *Trends Pharmacol Sci*, 30: 17-24.

Jeong, S. W., and S. R. Ikeda. 2000. 'Endogenous regulator of G-protein signaling proteins modify N-type calcium channel modulation in rat sympathetic neurons', *J Neurosci*, 20: 4489-96.

Jia, L., M. Chisari, M. H. Maktabi, C. Sobieski, H. Zhou, A. M. Konopko, B. R. Martin, S. J. Mennerick, and K. J. Blumer. 2014. 'A mechanism regulating G protein-coupled receptor signaling that requires cycles of protein palmitoylation and depalmitoylation', *J Biol Chem*, 289: 6249-57.

Jia, L., M. E. Linder, and K. J. Blumer. 2011. 'Gi/o signaling and the palmitoyltransferase DHHC2 regulate palmitate cycling and shuttling of RGS7 family-binding protein', *J Biol Chem*, 286: 13695-703.

Jin, Y., M. S. Dai, S. Z. Lu, Y. Xu, Z. Luo, Y. Zhao, and H. Lu. 2006. '14-3-3gamma binds to MDMX that is phosphorylated by UV-activated Chk1, resulting in p53 activation', *EMBO J*, 25: 1207-18.

Jockusch, W. J., D. Speidel, A. Sigler, J. B. Sorensen, F. Varoqueaux, J. S. Rhee, and N. Brose. 2007. 'CAPS-1 and CAPS-2 are essential synaptic vesicle priming proteins', *Cell*, 131: 796-808.

Johnson, C., S. Crowther, M. J. Stafford, D. G. Campbell, R. Toth, and C. MacKintosh. 2010. 'Bioinformatic and experimental survey of 14-3-3-binding sites', *Biochem J*, 427: 69-78.

Kaasinen, S. K., G. Goldsteins, L. Alhonen, J. Janne, and J. Koistinaho. 2002. 'Induction and activation of protein kinase C delta in hippocampus and cortex after kainic acid treatment', *Exp Neurol*, 176: 203-12.

Kajikawa, Y., N. Saitoh, and T. Takahashi. 2001. 'GTP-binding protein beta gamma subunits mediate presynaptic calcium current inhibition by GABA(B) receptor', *Proc Natl Acad Sci U S A*, 98: 8054-8.

Käll, Lukas, Jesse D Canterbury, Jason Weston, William Stafford Noble, and Michael J MacCoss. 2007. 'Semi-supervised learning for peptide identification from shotgun proteomics datasets', *Nature methods*, 4: 923.

Kammermeier, P. J., and S. R. Ikeda. 1999. 'Expression of RGS2 alters the coupling of metabotropic glutamate receptor 1a to M-type K+ and N-type Ca2+ channels', *Neuron*, 22: 819-29.

Katoh, Y., B. Ritter, T. Gaffry, F. Blondeau, S. Honing, and P. S. McPherson. 2009. 'The clavesin family, neuron-specific lipid- and clathrin-binding Sec14 proteins regulating lysosomal morphology', *J Biol Chem*, 284: 27646-54.

Kaur, K., J. M. Kehrl, R. A. Charbeneau, and R. R. Neubig. 2011. 'RGS-insensitive Galpha subunits: probes of Galpha subtype-selective signaling and physiological functions of RGS proteins', *Methods Mol Biol*, 756: 75-98.

Kaya, L., B. Meissner, M. C. Riedl, M. Muik, C. Schwarzer, F. Ferraguti, B. Sarg, H. Lindner, R. Schweigreiter, H. G. Knaus, C. Romanin, and C. E. Bandtlow. 2013. 'Direct association of the reticulon protein RTN1A with the ryanodine receptor 2 in neurons', *Biochim Biophys Acta*, 1833: 1421-33.

Khawaja, X. Z., J. J. Liang, J. A. Saugstad, P. G. Jones, S. Harnish, P. J. Conn, and M. I. Cockett. 1999. 'Immunohistochemical distribution of RGS7 protein and cellular selectivity in colocalizing with Galphaq proteins in the adult rat brain', *J Neurochem*, 72: 174-84.

Kiel, C., S. Wohlgemuth, F. Rousseau, J. Schymkowitz, J. Ferkinghoff-Borg, F. Wittinghofer, and L. Serrano. 2005. 'Recognizing and defining true Ras binding domains II: in silico prediction based on homology modelling and energy calculations', *J Mol Biol*, 348: 759-75.

Kim, G., S. Jung, H. Son, S. Kim, J. Choi, D. H. Lee, G. S. Roh, S. S. Kang, G. J. Cho, W. S. Choi, and H. J. Kim. 2014. 'The GABAB receptor associates with regulators of G-protein signaling 4 protein in the mouse prefrontal cortex and hypothalamus', *BMB Rep*, 47: 324-9.

Kimple, R. J., L. De Vries, H. Tronchere, C. I. Behe, R. A. Morris, M. Gist Farquhar, and D. P. Siderovski. 2001. 'RGS12 and RGS14 GoLoco motifs are G alpha(i) interaction sites with guanine nucleotide dissociation inhibitor Activity', *J Biol Chem*, 276: 29275-81.

Kirino, T. 1982. 'Delayed neuronal death in the gerbil hippocampus following ischemia', *Brain Res*, 239: 57-69.

Klug, J. R., B. N. Mathur, T. L. Kash, H. D. Wang, R. T. Matthews, A. J. Robison, M. E. Anderson, A. Y. Deutch, D. M. Lovinger, R. J. Colbran, and D. G. Winder. 2012. 'Genetic inhibition of CaMKII in dorsal striatal medium spiny neurons reduces functional excitatory synapses and enhances intrinsic excitability', *PLoS One*, 7: e45323.

Knox, D. 2016. 'The role of basal forebrain cholinergic neurons in fear and extinction memory', *Neurobiol Learn Mem*, 133: 39-52.

Koenen, K. C., A. B. Amstadter, K. J. Ruggiero, R. Acierno, S. Galea, D. G. Kilpatrick, and J. Gelernter. 2009. 'RGS2 and generalized anxiety disorder in an epidemiologic sample of hurricane-exposed adults', *Depress Anxiety*, 26: 309-15.

Koganezawa, N., K. Hanamura, Y. Sekino, and T. Shirao. 2017. 'The role of drebrin in dendritic spines', *Mol Cell Neurosci*, 84: 85-92.

Kohara, K., M. Pignatelli, A. J. Rivest, H. Y. Jung, T. Kitamura, J. Suh, D. Frank, K. Kajikawa, N. Mise, Y. Obata, I. R. Wickersham, and S. Tonegawa. 2014. 'Cell type-specific genetic and optogenetic tools reveal hippocampal CA2 circuits', *Nat Neurosci*, 17: 269-79.

Kotapka, M. J., D. I. Graham, J. H. Adams, and T. A. Gennarelli. 1992. 'Hippocampal pathology in fatal non-missile human head injury', *Acta Neuropathol*, 83: 530-4.

Kovoor, A., C. K. Chen, W. He, T. G. Wensel, M. I. Simon, and H. A. Lester. 2000. 'Co-expression of Gbeta5 enhances the function of two Ggamma subunit-like domain-containing regulators of G protein signaling proteins', *J Biol Chem*, 275: 3397-402.

Kovoor, A., P. Seyffarth, J. Ebert, S. Barghshoon, C. K. Chen, S. Schwarz, J. D. Axelrod, B. N. Cheyette, M. I. Simon, H. A. Lester, and J. Schwarz. 2005. 'D2 dopamine receptors colocalize regulator of G-protein signaling 9-2 (RGS9-2) via the RGS9 DEP domain, and RGS9 knock-out mice develop dyskinesias associated with dopamine pathways', *J Neurosci*, 25: 2157-65.

Kreitzer, A. C., and R. C. Malenka. 2005. 'Dopamine modulation of state-dependent endocannabinoid release and long-term depression in the striatum', *J Neurosci*, 25: 10537-45.

Kreitzer, A. C., and R. C. Malenka. 2008. 'Striatal plasticity and basal ganglia circuit function', *Neuron*, 60: 543-54.

Labouebe, G., M. Lomazzi, H. G. Cruz, C. Creton, R. Lujan, M. Li, Y. Yanagawa, K. Obata, M. Watanabe, K. Wickman, S. B. Boyer, P. A. Slesinger, and C. Luscher. 2007. 'RGS2 modulates coupling between GABAB receptors and GIRK channels in dopamine neurons of the ventral tegmental area', *Nat Neurosci*, 10: 1559-68.

Lagerstrom, M. C., and H. B. Schioth. 2008. 'Structural diversity of G protein-coupled receptors and significance for drug discovery', *Nat Rev Drug Discov*, 7: 339-57.

Lamprecht, R. 2016. 'The Role of Actin Cytoskeleton in Memory Formation in Amygdala', *Front Mol Neurosci*, 9: 23.

Lan, K. L., N. A. Sarvazyan, R. Taussig, R. G. Mackenzie, P. R. DiBello, H. G. Dohlman, and R. R. Neubig. 1998. 'A point mutation in Galphao and Galphai1 blocks interaction with regulator of G protein signaling proteins', *J Biol Chem*, 273: 12794-7.

Larminie, C., P. Murdock, J. P. Walhin, M. Duckworth, K. J. Blumer, M. A. Scheideler, and M. Garnier. 2004. 'Selective expression of regulators of G-protein signaling (RGS) in the human central nervous system', *Brain Res Mol Brain Res*, 122: 24-34.

Laurberg, S., and J. Zimmer. 1980. 'Aberrant hippocampal mossy fibers in cats', *Brain Res*, 188: 555-9.

Lee, J. H., S. Lee, and J. H. Kim. 2016. 'Amygdala Circuits for Fear Memory: A Key Role for Dopamine Regulation', *Neuroscientist*.

Lee, J. K., and M. G. Tansey. 2015. 'Physiology of RGS10 in Neurons and Immune Cells', *Prog Mol Biol Transl Sci*, 133: 153-67.

Lee, M. J., T. Tasaki, K. Moroi, J. Y. An, S. Kimura, I. V. Davydov, and Y. T. Kwon. 2005. 'RGS4 and RGS5 are in vivo substrates of the N-end rule pathway', *Proc Natl Acad Sci U S A*, 102: 15030-5.

Lee, S. E., S. B. Simons, S. A. Heldt, M. Zhao, J. P. Schroeder, C. P. Vellano, D. P. Cowan, S. Ramineni, C. K. Yates, Y. Feng, Y. Smith, J. D. Sweatt, D. Weinshenker, K. J. Ressler, S. M. Dudek, and J. R. Hepler. 2010. 'RGS14 is a natural suppressor of both synaptic plasticity in CA2 neurons and hippocampal-based learning and memory', *Proc Natl Acad Sci U S A*, 107: 16994-8.

Lein, E. S., M. J. Hawrylycz, N. Ao, M. Ayres, A. Bensinger, A. Bernard, A. F. Boe, M. S. Boguski, K. S. Brockway, E. J. Byrnes, L. Chen, L. Chen, T. M. Chen, M. C. Chin, J. Chong, B. E. Crook, A. Czaplinska, C. N. Dang, S. Datta, N. R. Dee, A. L. Desaki, T. Desta, E. Diep, T. A. Dolbeare, M. J. Donelan, H. W. Dong, J. G. Dougherty, B. J. Duncan, A. J. Ebbert, G. Eichele, L. K. Estin, C. Faber, B. A. Facer, R. Fields, S. R. Fischer, T. P. Fliss, C. Frensley, S. N. Gates, K. J. Glattfelder, K. R. Halverson, M. R. Hart, J. G. Hohmann, M. P. Howell, D. P. Jeung, R. A. Johnson, P. T. Karr, R. Kawal, J. M. Kidney, R. H. Knapik, C. L. Kuan, J. H. Lake, A. R. Laramee, K. D. Larsen, C. Lau, T. A. Lemon, A. J. Liang, Y. Liu, L. T. Luong, J. Michaels, J. J. Morgan, R. J. Morgan, M. T. Mortrud, N. F. Mosqueda, L. L. Ng, R. Ng, G. J. Orta, C. C. Overly, T. H. Pak, S. E. Parry, S. D. Pathak, O. C. Pearson, R. B. Puchalski, Z. L. Riley, H. R. Rockett, S. A. Rowland, J. J. Royall, M. J. Ruiz, N. R. Sarno, K. Schaffnit, N. V. Shapovalova, T. Sivisay, C. R. Slaughterbeck, S. C. Smith, K. A. Smith, B. I. Smith, A. J. Sodt, N. N.

Stewart, K. R. Stumpf, S. M. Sunkin, M. Sutram, A. Tam, C. D. Teemer, C. Thaller, C. L. Thompson, L. R. Varnam, A. Visel, R. M. Whitlock, P. E. Wohnoutka, C. K. Wolkey, V. Y. Wong, M. Wood, M. B. Yaylaoglu, R. C. Young, B. L. Youngstrom, X. F. Yuan, B. Zhang, T. A. Zwingman, and A. R. Jones. 2007. 'Genome-wide atlas of gene expression in the adult mouse brain', *Nature*, 445: 168-76.

Lerner, T. N., E. A. Horne, N. Stella, and A. C. Kreitzer. 2010. 'Endocannabinoid signaling mediates psychomotor activation by adenosine A2A antagonists', *J Neurosci*, 30: 2160-4.

Lerner, T. N., and A. C. Kreitzer. 2012. 'RGS4 is required for dopaminergic control of striatal LTD and susceptibility to parkinsonian motor deficits', *Neuron*, 73: 347-59.

Levano, K., V. Punia, M. Raghunath, P. R. Debata, G. M. Curcio, A. Mogha, S. Purkayastha, D. McCloskey, J. Fata, and P. Banerjee. 2012. 'Atp8a1 deficiency is associated with phosphatidylserine externalization in hippocampus and delayed hippocampus-dependent learning', *J Neurochem*, 120: 302-13.

Li, S., P. Janosch, M. Tanji, G. C. Rosenfeld, J. C. Waymire, H. Mischak, W. Kolch, and J. M. Sedivy. 1995. 'Regulation of Raf-1 kinase activity by the 14-3-3 family of proteins', *EMBO J*, 14: 685-96.

Lifschytz, T., E. C. Broner, P. Zozulinsky, A. Slonimsky, R. Eitan, L. Greenbaum, and B. Lerer. 2012. 'Relationship between Rgs2 gene expression level and anxiety and depression-like behaviour in a mutant mouse model: serotonergic involvement', *Int J Neuropsychopharmacol*, 15: 1307-18.

Light, Y., H. Paterson, and R. Marais. 2002. '14-3-3 antagonizes Ras-mediated Raf-1 recruitment to the plasma membrane to maintain signaling fidelity', *Mol Cell Biol*, 22: 4984-96.

Liu, W., E. Y. Yuen, P. B. Allen, J. Feng, P. Greengard, and Z. Yan. 2006. 'Adrenergic modulation of NMDA receptors in prefrontal cortex is differentially regulated by RGS proteins and spinophilin', *Proc Natl Acad Sci U S A*, 103: 18338-43.

Liu, X., M. J. Betzenhauser, S. Reiken, A. C. Meli, W. Xie, B. X. Chen, O. Arancio, and A. R. Marks. 2012. 'Role of leaky neuronal ryanodine receptors in stress-induced cognitive dysfunction', *Cell*, 150: 1055-67.

Lopez-Aranda, M. F., M. J. Acevedo, F. J. Carballo, A. Gutierrez, and Z. U. Khan. 2006. 'Localization of the GoLoco motif carrier regulator of G-protein signalling 12 and 14 proteins in monkey and rat brain', *Eur J Neurosci*, 23: 2971-82.

Lopez-Fando, A., M. Rodriguez-Munoz, P. Sanchez-Blazquez, and J. Garzon. 2005. 'Expression of neural RGS-R7 and Gbeta5 Proteins in Response to Acute and Chronic Morphine', *Neuropsychopharmacology*, 30: 99-110.

Lorente de No, Rafael. 1934. 'Studies on the structure of the cerebral cortex. II. Continuation of the study of the ammonic system', *J Psychol Neurol*: 113-77.

Luber, C. A., J. Cox, H. Lauterbach, B. Fancke, M. Selbach, J. Tschopp, S. Akira, M. Wiegand, H. Hochrein, M. O'Keeffe, and M. Mann. 2010. 'Quantitative proteomics reveals subset-specific viral recognition in dendritic cells', *Immunity*, 32: 279-89.

Lundby, A., A. Secher, K. Lage, N. B. Nordsborg, A. Dmytriyev, C. Lundby, and J. V. Olsen. 2012. 'Quantitative maps of protein phosphorylation sites across 14 different rat organs and tissues', *Nat Commun*, 3: 876.

Lur, G., and M. J. Higley. 2015. 'Glutamate Receptor Modulation Is Restricted to Synaptic Microdomains', *Cell Rep*, 12: 326-34.

Makino, E. R., J. W. Handy, T. Li, and V. Y. Arshavsky. 1999. 'The GTPase activating factor for transducin in rod photoreceptors is the complex between RGS9 and type 5 G protein beta subunit', *Proc Natl Acad Sci U S A*, 96: 1947-52.

Malenka, R. C., and M. F. Bear. 2004. 'LTP and LTD: an embarrassment of riches', *Neuron*, 44: 5-21.

Mancuso, J. J., Y. Qian, C. Long, G. Y. Wu, and T. G. Wensel. 2010. 'Distribution of RGS9-2 in neurons of the mouse striatum', *J Neurochem*, 112: 651-61.

Mandelli, L., and A. Serretti. 2013. 'Gene environment interaction studies in depression and suicidal behavior: An update', *Neurosci Biobehav Rev*, 37: 2375-97.

Mannaioni, G., M. J. Marino, O. Valenti, S. F. Traynelis, and P. J. Conn. 2001. 'Metabotropic glutamate receptors 1 and 5 differentially regulate CA1 pyramidal cell function', *J Neurosci*, 21: 5925-34.

Mark, M. D., S. Wittemann, and S. Herlitze. 2000. 'G protein modulation of recombinant P/Q-type calcium channels by regulators of G protein signalling proteins', *J Physiol*, 528 Pt 1: 65-77.

Martemyanov, K. A., P. J. Yoo, N. P. Skiba, and V. Y. Arshavsky. 2005. 'R7BP, a novel neuronal protein interacting with RGS proteins of the R7 family', *J Biol Chem*, 280: 5133-6.

Martin-Montanez, E., M. J. Acevedo, J. F. Lopez-Tellez, R. S. Duncan, A. G. Mateos, J. Pavia, P. Koulen, and Z. U. Khan. 2010. 'Regulator of G-protein signaling 14 protein modulates Ca(2)+ influx through Cav1 channels', *Neuroreport*, 21: 1034-9.

Mascagni, F., and A. J. McDonald. 2003. 'Immunohistochemical characterization of cholecystokinin containing neurons in the rat basolateral amygdala', *Brain Res*, 976: 171-84.

Masters, S. C., K. J. Pederson, L. Zhang, J. T. Barbieri, and H. Fu. 1999. 'Interaction of 14-3-3 with a nonphosphorylated protein ligand, exoenzyme S of Pseudomonas aeruginosa', *Biochemistry*, 38: 5216-21.

Matsuzaki, M., N. Honkura, G. C. Ellis-Davies, and H. Kasai. 2004. 'Structural basis of long-term potentiation in single dendritic spines', *Nature*, 429: 761-6.

Matt, L., K. Kim, A. C. Hergarden, T. Patriarchi, Z. A. Malik, D. K. Park, D. Chowdhury, O. R. Buonarati, P. B. Henderson, C. Gokcek Sarac, Y. Zhang, D. Mohapatra, M. C. Horne, J. B. Ames, and J. W. Hell. 2018. 'alpha-Actinin Anchors PSD-95 at Postsynaptic Sites', *Neuron*, 97: 1094-109 e9.

Maxwell, W. L., K. Dhillon, L. Harper, J. Espin, T. K. MacIntosh, D. H. Smith, and D. I. Graham. 2003. 'There is differential loss of pyramidal cells from the human hippocampus with survival after blunt head injury', *J Neuropathol Exp Neurol*, 62: 272-9.

Mayya, V., D. H. Lundgren, S. I. Hwang, K. Rezaul, L. Wu, J. K. Eng, V. Rodionov, and D. K. Han. 2009. 'Quantitative phosphoproteomic analysis of T cell receptor signaling reveals system-wide modulation of protein-protein interactions', *Sci Signal*, 2: ra46.

McDonald, A. J., and F. Mascagni. 2001. 'Colocalization of calcium-binding proteins and GABA in neurons of the rat basolateral amygdala', *Neuroscience*, 105: 681-93.

Mercer, A., H. L. Trigg, and A. M. Thomson. 2007. 'Characterization of neurons in the CA2 subfield of the adult rat hippocampus', *J Neurosci*, 27: 7329-38.

Minkova, L., R. Sladky, G. S. Kranz, M. Woletz, N. Geissberger, C. Kraus, R. Lanzenberger, and C. Windischberger. 2017. 'Task-dependent modulation of amygdala connectivity in social anxiety disorder', *Psychiatry Res*, 262: 39-46.

Mirnics, K., F. A. Middleton, G. D. Stanwood, D. A. Lewis, and P. Levitt. 2001. 'Disease-specific changes in regulator of G-protein signaling 4 (RGS4) expression in schizophrenia', *Mol Psychiatry*, 6: 293-301.

Mittal, V., and M. E. Linder. 2004. 'The RGS14 GoLoco domain discriminates among Galphai isoforms', *J Biol Chem*, 279: 46772-8.

Mittal, V., and M. E. Linder. 2006. 'Biochemical characterization of RGS14: RGS14 activity towards G-protein alpha subunits is independent of its binding to Rap2A', *Biochem J*, 394: 309-15.

Mizui, T., Y. Sekino, H. Yamazaki, Y. Ishizuka, H. Takahashi, N. Kojima, M. Kojima, and T. Shirao. 2014. 'Myosin II ATPase activity mediates the long-term potentiation-induced exodus of stable F-actin bound by drebrin A from dendritic spines', *PLoS One*, 9: e85367.

Molzan, M., and C. Ottmann. 2012. 'Synergistic binding of the phosphorylated S233- and S259-binding sites of C-RAF to one 14-3-3zeta dimer', *J Mol Biol*, 423: 486-95.

Moser, M. B. 1999. 'Making more synapses: a way to store information?', *Cell Mol Life Sci*, 55: 593-600.

Muller, J. F., F. Mascagni, and A. J. McDonald. 2006. 'Pyramidal cells of the rat basolateral amygdala: synaptology and innervation by parvalbumin-immunoreactive interneurons', *J Comp Neurol*, 494: 635-50.

Muslin, A. J., J. W. Tanner, P. M. Allen, and A. S. Shaw. 1996. 'Interaction of 14-3-3 with signaling proteins is mediated by the recognition of phosphoserine', *Cell*, 84: 889-97.

Ni, Y. G., S. J. Gold, P. A. Iredale, R. Z. Terwilliger, R. S. Duman, and E. J. Nestler. 1999. 'Region-specific regulation of RGS4 (Regulator of G-protein-signaling protein type 4) in brain by stress and glucocorticoids: in vivo and in vitro studies', *J Neurosci*, 19: 3674-80.

Nicoll, R. A. 2017. 'A Brief History of Long-Term Potentiation', *Neuron*, 93: 281-90.

Niu, J., A. Scheschonka, K. M. Druey, A. Davis, E. Reed, V. Kolenko, R. Bodnar, T. Voyno-Yasenetskaya, X. Du, J. Kehrl, and N. O. Dulin. 2002. 'RGS3 interacts with 14-3-3 via the N-terminal region distinct from the RGS (regulator of G-protein signalling) domain', *Biochem J*, 365: 677-84.

Nufer, O., and H. P. Hauri. 2003. 'ER export: call 14-3-3', *Curr Biol*, 13: R391-3.

O'Kelly, I., M. H. Butler, N. Zilberberg, and S. A. Goldstein. 2002. 'Forward transport. 14-3-3 binding overcomes retention in endoplasmic reticulum by dibasic signals', *Cell*, 111: 577-88.

Obenauer, J. C., L. C. Cantley, and M. B. Yaffe. 2003. 'Scansite 2.0: Proteome-wide prediction of cell signaling interactions using short sequence motifs', *Nucleic Acids Res*, 31: 3635-41.

Obsil, T., R. Ghirlando, D. C. Klein, S. Ganguly, and F. Dyda. 2001. 'Crystal structure of the 14-3-3zeta:serotonin N-acetyltransferase complex. a role for scaffolding in enzyme regulation', *Cell*, 105: 257-67.

Okimoto, N., O. J. Bosch, D. A. Slattery, K. Pflaum, H. Matsushita, F. Y. Wei, M. Ohmori, T. Nishiki, I. Ohmori, Y. Hiramatsu, H. Matsui, I. D. Neumann, and K. Tomizawa. 2012. 'RGS2 mediates the anxiolytic effect of oxytocin', *Brain Res*, 1453: 26-33.

Okuwaki, M., K. Kato, and K. Nagata. 2010. 'Functional characterization of human nucleosome assembly protein 1-like proteins as histone chaperones', *Genes Cells*, 15: 13-27.

Oliveira-Dos-Santos, A. J., G. Matsumoto, B. E. Snow, D. Bai, F. P. Houston, I. Q. Whishaw, S. Mariathasan, T. Sasaki, A. Wakeham, P. S. Ohashi, J. C. Roder, C. A. Barnes, D. P.

Siderovski, and J. M. Penninger. 2000. 'Regulation of T cell activation, anxiety, and male aggression by RGS2', *Proc Natl Acad Sci U S A*, 97: 12272-7.

Orlandi, C., E. Posokhova, I. Masuho, T. A. Ray, N. Hasan, R. G. Gregg, and K. A. Martemyanov. 2012. 'GPR158/179 regulate G protein signaling by controlling localization and activity of the RGS7 complexes', *J Cell Biol*, 197: 711-9.

Orlandi, C., K. Xie, I. Masuho, A. Fajardo-Serrano, R. Lujan, and K. A. Martemyanov. 2015. 'Orphan Receptor GPR158 is an Allosteric Modulator of Regulator of G Protein Signaling 7 (RGS7) Catalytic Activity with Essential Role in Dictating its Expression and Localization in the Brain', *J Biol Chem*.

Osterweil, E., D. G. Wells, and M. S. Mooseker. 2005. 'A role for myosin VI in postsynaptic structure and glutamate receptor endocytosis', *J Cell Biol*, 168: 329-38.

Ostrovskaya, O., K. Xie, I. Masuho, A. Fajardo-Serrano, R. Lujan, K. Wickman, and K. A. Martemyanov. 2014. 'RGS7/Gbeta5/R7BP complex regulates synaptic plasticity and memory by modulating hippocampal GABABR-GIRK signaling', *Elife*, 3: e02053.

Otowa, T., T. Shimada, Y. Kawamura, N. Sugaya, E. Yoshida, K. Inoue, S. Yasuda, X. Liu, T. Minato, M. Tochigi, T. Umekage, K. Kasai, H. Tanii, Y. Okazaki, H. Kaiya, and T. Sasaki. 2011. 'Association of RGS2 variants with panic disorder in a Japanese population', *Am J Med Genet B Neuropsychiatr Genet*, 156B: 430-4.

Ottersen, O. P., and A. S. Landsend. 1997. 'Organization of glutamate receptors at the synapse', *Eur J Neurosci*, 9: 2219-24.

Pacey, L. K., L. Doss, C. Cifelli, D. van der Kooy, S. P. Heximer, and D. R. Hampson. 2011. 'Genetic deletion of regulator of G-protein signaling 4 (RGS4) rescues a subset of fragile X related phenotypes in the FMR1 knockout mouse', *Mol Cell Neurosci*, 46: 563-72.

Pagani, J. H., M. Zhao, Z. Cui, S. K. Williams Avram, D. A. Caruana, S. M. Dudek, and W. S. Young. 2014. 'Role of the vasopressin 1b receptor in rodent aggressive behavior and synaptic plasticity in hippocampal area CA2', *Mol Psychiatry*.

Parker, C. C., G. Sokoloff, R. Cheng, and A. A. Palmer. 2012. 'Genome-wide association for fear conditioning in an advanced intercross mouse line', *Behav Genet*, 42: 437-48.

Parker, M. W., H. F. Guo, X. Li, A. D. Linkugel, and C. W. Vander Kooi. 2012. 'Function of members of the neuropilin family as essential pleiotropic cell surface receptors', *Biochemistry*, 51: 9437-46.

Paspalas, C. D., L. D. Selemon, and A. F. Arnsten. 2009. 'Mapping the regulator of G protein signaling 4 (RGS4): presynaptic and postsynaptic substrates for neuroregulation in prefrontal cortex', *Cereb Cortex*, 19: 2145-55.

Pegg, A. E. 2014. 'The function of spermine', *IUBMB Life*, 66: 8-18.

Perez, Y., F. Morin, and J. C. Lacaille. 2001. 'A hebbian form of long-term potentiation dependent on mGluR1a in hippocampal inhibitory interneurons', *Proc Natl Acad Sci U S A*, 98: 9401-6.

Petosa, C., S. C. Masters, L. A. Bankston, J. Pohl, B. Wang, H. Fu, and R. C. Liddington. 1998. '14-3-3zeta binds a phosphorylated Raf peptide and an unphosphorylated peptide via its conserved amphipathic groove', *J Biol Chem*, 273: 16305-10.

Pichler, Peter, Thomas Köcher, Johann Holzmann, Michael Mazanek, Thomas Taus, Gustav Ammerer, and Karl Mechtler. 2010. 'Peptide Labeling with Isobaric Tags Yields Higher Identification Rates Using iTRAQ 4-Plex Compared to TMT 6-Plex and iTRAQ 8-Plex on LTQ Orbitrap', *Analytical Chemistry*, 82: 6549-58.

Pinto, S. M., R. S. Nirujogi, P. L. Rojas, A. H. Patil, S. S. Manda, Y. Subbannayya, J. C. Roa, A. Chatterjee, T. S. Prasad, and A. Pandey. 2015. 'Quantitative phosphoproteomic analysis of IL-33-mediated signaling', *Proteomics*, 15: 532-44.

Posner, B. A., A. G. Gilman, and B. A. Harris. 1999. 'Regulators of G protein signaling 6 and 7. Purification of complexes with gbeta5 and assessment of their effects on g protein-mediated signaling pathways', *J Biol Chem*, 274: 31087-93.

Prasad, K. M., L. Almasy, R. C. Gur, R. E. Gur, M. Pogue-Geile, K. V. Chowdari, M. E. Talkowski, and V. L. Nimgaonkar. 2010. 'RGS4 polymorphisms associated with variability of cognitive performance in a family-based schizophrenia sample', *Schizophr Bull*, 36: 983-90.

Prasad, K. M., K. V. Chowdari, V. L. Nimgaonkar, M. E. Talkowski, D. A. Lewis, and M. S. Keshavan. 2005. 'Genetic polymorphisms of the RGS4 and dorsolateral prefrontal cortex morphometry among first episode schizophrenia patients', *Mol Psychiatry*, 10: 213-9.

Psifogeorgou, K., P. Papakosta, S. J. Russo, R. L. Neve, D. Kardassis, S. J. Gold, and V. Zachariou. 2007. 'RGS9-2 is a negative modulator of mu-opioid receptor function', *J Neurochem*, 103: 617-25.

Qiao, H., M. Foote, K. Graham, Y. Wu, and Y. Zhou. 2014. '14-3-3 proteins are required for hippocampal long-term potentiation and associative learning and memory', *J Neurosci*, 34: 4801-8.

Qiao, H., Y. Li, C. Feng, S. Duo, F. Ji, and J. Jiao. 2018. 'Nap1l1 Controls Embryonic Neural Progenitor Cell Proliferation and Differentiation in the Developing Brain', *Cell Rep*, 22: 2279-93.

Rahman, Z., S. J. Gold, M. N. Potenza, C. W. Cowan, Y. G. Ni, W. He, T. G. Wensel, and E. J. Nestler. 1999. 'Cloning and characterization of RGS9-2: a striatal-enriched alternatively spliced product of the RGS9 gene', *J Neurosci*, 19: 2016-26.

Rahman, Z., J. Schwarz, S. J. Gold, V. Zachariou, M. N. Wein, K. H. Choi, A. Kovoor, C. K. Chen, R. J. DiLeone, S. C. Schwarz, D. E. Selley, L. J. Sim-Selley, M. Barrot, R. R. Luedtke, D. Self, R. L. Neve, H. A. Lester, M. I. Simon, and E. J. Nestler. 2003. 'RGS9 modulates dopamine signaling in the basal ganglia', *Neuron*, 38: 941-52.

Rajalingam, K., R. Schreck, U. R. Rapp, and S. Albert. 2007. 'Ras oncogenes and their downstream targets', *Biochim Biophys Acta*, 1773: 1177-95.

Ratzliff, A. D., and I. Soltesz. 2001. 'Differential immunoreactivity for alpha-actinin-2, an N-methyl-D-aspartate-receptor/actin binding protein, in hippocampal interneurons', *Neuroscience*, 103: 337-49.

Rezabkova, L., E. Boura, P. Herman, J. Vecer, L. Bourova, M. Sulc, P. Svoboda, V. Obsilova, and T. Obsil. 2010. '14-3-3 protein interacts with and affects the structure of RGS domain of regulator of G protein signaling 3 (RGS3)', *J Struct Biol*, 170: 451-61.

Rezabkova, L., P. Man, P. Novak, P. Herman, J. Vecer, V. Obsilova, and T. Obsil. 2011. 'Structural basis for the 14-3-3 protein-dependent inhibition of the regulator of G protein signaling 3 (RGS3) function', *J Biol Chem*, 286: 43527-36.

Rojas, A., and R. Dingledine. 2013. 'Ionotropic glutamate receptors: regulation by G-protein-coupled receptors', *Mol Pharmacol*, 83: 746-52.

Rose, J. J., J. B. Taylor, J. Shi, M. I. Cockett, P. G. Jones, and J. R. Hepler. 2000. 'RGS7 is palmitoylated and exists as biochemically distinct forms', *J Neurochem*, 75: 2103-12.

Ross, E. M., and T. M. Wilkie. 2000. 'GTPase-activating proteins for heterotrimeric G proteins: regulators of G protein signaling (RGS) and RGS-like proteins', *Annu Rev Biochem*, 69: 795-827.

Roy, S., R. A. McPherson, A. Apolloni, J. Yan, A. Lane, J. Clyde-Smith, and J. F. Hancock. 1998. '14-3-3 facilitates Ras-dependent Raf-1 activation in vitro and in vivo', *Mol Cell Biol*, 18: 3947-55.

Ryu, J., L. Liu, T. P. Wong, D. C. Wu, A. Burette, R. Weinberg, Y. T. Wang, and M. Sheng. 2006. 'A critical role for myosin IIb in dendritic spine morphology and synaptic function', *Neuron*, 49: 175-82.

Sadowski, M., H. M. Wisniewski, K. Jakubowska-Sadowska, M. Tarnawski, J. W. Lazarewicz, and M. J. Mossakowski. 1999. 'Pattern of neuronal loss in the rat hippocampus following experimental cardiac arrest-induced ischemia', *J Neurol Sci*, 168: 13-20.

Sahoo, P. K., D. S. Smith, N. Perrone-Bizzozero, and J. L. Twiss. 2018. 'Axonal mRNA transport and translation at a glance', *J Cell Sci*, 131.

Saitoh, O., Y. Kubo, Y. Miyatani, T. Asano, and H. Nakata. 1997. 'RGS8 accelerates G-protein-mediated modulation of K+ currents', *Nature*, 390: 525-9.

Saitoh, O., Y. Kubo, M. Odagiri, M. Ichikawa, K. Yamagata, and T. Sekine. 1999. 'RGS7 and RGS8 differentially accelerate G protein-mediated modulation of K+ currents', *J Biol Chem*, 274: 9899-904.

Saitoh, O., I. Masuho, I. Terakawa, S. Nomoto, T. Asano, and Y. Kubo. 2001. 'Regulator of G protein signaling 8 (RGS8) requires its NH2 terminus for subcellular localization and acute desensitization of G protein-gated K+ channels', *J Biol Chem*, 276: 5052-8.

San Antonio, A., K. Liban, T. Ikrar, E. Tsyganovskiy, and X. Xu. 2014. 'Distinct physiological and developmental properties of hippocampal CA2 subfield revealed by using anti-Purkinje cell protein 4 (PCP4) immunostaining', *J Comp Neurol*, 522: 1333-54.

Sanchez-Blazquez, P., M. Rodriguez-Diaz, A. Lopez-Fando, M. Rodriguez-Munoz, and J. Garzon. 2003. 'The GBeta5 subunit that associates with the R7 subfamily of RGS proteins regulates mu-opioid effects', *Neuropharmacology*, 45: 82-95.

Saugstad, J. A., M. J. Marino, J. A. Folk, J. R. Hepler, and P. J. Conn. 1998. 'RGS4 inhibits signaling by group I metabotropic glutamate receptors', *J Neurosci*, 18: 905-13.

Schwendt, M., and J. F. McGinty. 2007. 'Regulator of G-protein signaling 4 interacts with metabotropic glutamate receptor subtype 5 in rat striatum: relevance to amphetamine behavioral sensitization', *J Pharmacol Exp Ther*, 323: 650-7.

Seeman, P., F. Ko, E. Jack, R. Greenstein, and B. Dean. 2007. 'Consistent with dopamine supersensitivity, RGS9 expression is diminished in the amphetamine-treated animal model of schizophrenia and in postmortem schizophrenia brain', *Synapse*, 61: 303-9.

Sethakorn, N., D. M. Yau, and N. O. Dulin. 2010. 'Non-canonical functions of RGS proteins', *Cell Signal*, 22: 1274-81.

Seyfried, Nicholas T, Eric B Dammer, Vivek Swarup, Divya Nandakumar, Duc M Duong, Luming Yin, Qiudong Deng, Tram Nguyen, Chadwick M Hales, and Thomas Wingo. 2017. 'A multi-network approach identifies protein-specific co-expression in asymptomatic and symptomatic Alzheimer's disease', *Cell systems*, 4: 60-72. e4.

Shelat, P. B., A. P. Coulibaly, Q. Wang, A. Y. Sun, G. Y. Sun, and A. Simonyi. 2006. 'Ischemia-induced increase in RGS7 mRNA expression in gerbil hippocampus', *Neurosci Lett*, 403: 157-61.

Sheynin, J., and I. Liberzon. 2016. 'Circuit dysregulation and circuit-based treatments in posttraumatic stress disorder', *Neurosci Lett*.

Shibata, H., T. Kanadome, H. Sugiura, T. Yokoyama, M. Yamamuro, S. E. Moss, and M. Maki. 2015. 'A new role for annexin A11 in the early secretory pathway via stabilizing Sec31A protein at the endoplasmic reticulum exit sites (ERES)', *J Biol Chem*, 290: 4981-93.

Shimizu, H., M. Fukaya, M. Yamasaki, M. Watanabe, T. Manabe, and H. Kamiya. 2008. 'Use-dependent amplification of presynaptic Ca2+ signaling by axonal ryanodine receptors at the hippocampal mossy fiber synapse', *Proc Natl Acad Sci U S A*, 105: 11998-2003.

Shu, F. J., S. Ramineni, W. Amyot, and J. R. Hepler. 2007. 'Selective interactions between Gi alpha1 and Gi alpha3 and the GoLoco/GPR domain of RGS14 influence its dynamic subcellular localization', *Cell Signal*, 19: 163-76.

Shu, F. J., S. Ramineni, and J. R. Hepler. 2010. 'RGS14 is a multifunctional scaffold that integrates G protein and Ras/Raf MAPkinase signalling pathways', *Cell Signal*, 22: 366-76.

Shuey, D. J., M. Betty, P. G. Jones, X. Z. Khawaja, and M. I. Cockett. 1998. 'RGS7 attenuates signal transduction through the G(alpha q) family of heterotrimeric G proteins in mammalian cells', *J Neurochem*, 70: 1964-72.

Siderovski, D. P., A. Hessel, S. Chung, T. W. Mak, and M. Tyers. 1996. 'A new family of regulators of G-protein-coupled receptors?', *Curr Biol*, 6: 211-2.

Simon, M. I., M. P. Strathmann, and N. Gautam. 1991. 'Diversity of G proteins in signal transduction', *Science*, 252: 802-8.

Simons, S. B., D. A. Caruana, M. Zhao, and S. M. Dudek. 2012. 'Caffeine-induced synaptic potentiation in hippocampal CA2 neurons', *Nat Neurosci*, 15: 23-5.

Simons, S. B., Y. Escobedo, R. Yasuda, and S. M. Dudek. 2009. 'Regional differences in hippocampal calcium handling provide a cellular mechanism for limiting plasticity', *Proc Natl Acad Sci U S A*, 106: 14080-4.

Sinnarajah, S., C. W. Dessauer, D. Srikumar, J. Chen, J. Yuen, S. Yilma, J. C. Dennis, E. E. Morrison, V. Vodyanoy, and J. H. Kehrl. 2001. 'RGS2 regulates signal transduction in olfactory neurons by attenuating activation of adenylyl cyclase III', *Nature*, 409: 1051-5.

Sloviter, R. S. 1991. 'Permanently altered hippocampal structure, excitability, and inhibition after experimental status epilepticus in the rat: the "dormant basket cell" hypothesis and its possible relevance to temporal lobe epilepsy', *Hippocampus*, 1: 41-66.

Smoller, J. W., M. P. Paulus, J. A. Fagerness, S. Purcell, L. H. Yamaki, D. Hirshfeld-Becker, J. Biederman, J. F. Rosenbaum, J. Gelernter, and M. B. Stein. 2008. 'Influence of RGS2 on anxiety-related temperament, personality, and brain function', *Arch Gen Psychiatry*, 65: 298-308.

Snow, B. E., L. Antonio, S. Suggs, H. B. Gutstein, and D. P. Siderovski. 1997. 'Molecular cloning and expression analysis of rat Rgs12 and Rgs14', *Biochem Biophys Res Commun*, 233: 770-7.

Snow, B. E., L. Betts, J. Mangion, J. Sondek, and D. P. Siderovski. 1999. 'Fidelity of G protein beta-subunit association by the G protein gamma-subunit-like domains of RGS6, RGS7, and RGS11', *Proc Natl Acad Sci U S A*, 96: 6489-94.

Spangler, S. A., D. Jaarsma, E. De Graaff, P. S. Wulf, A. Akhmanova, and C. C. Hoogenraad. 2011. 'Differential expression of liprin-alpha family proteins in the brain suggests functional diversification', *J Comp Neurol*, 519: 3040-60.

Spangler, S. A., S. K. Schmitz, J. T. Kevenaar, E. de Graaff, H. de Wit, J. Demmers, R. F. Toonen, and C. C. Hoogenraad. 2013. 'Liprin-alpha2 promotes the presynaptic recruitment and turnover of RIM1/CASK to facilitate synaptic transmission', *J Cell Biol*, 201: 915-28.

Squires, K. E., K. J. Gerber, J. F. Pare, M. R. Branch, Y. Smith, and J. R. Hepler. 2018. 'Regulator of G protein signaling 14 (RGS14) is expressed pre- and postsynaptically in neurons of hippocampus, basal ganglia, and amygdala of monkey and human brain', *Brain Struct Funct*, 223: 233-53.

Srinivas, K. V., E. W. Buss, Q. Sun, B. Santoro, H. Takahashi, D. A. Nicholson, and S. A. Siegelbaum. 2017. 'The Dendrites of CA2 and CA1 Pyramidal Neurons Differentially Regulate Information Flow in the Cortico-Hippocampal Circuit', *J Neurosci*, 37: 3276-93.

Takahashi, H., T. Mizui, and T. Shirao. 2006. 'Down-regulation of drebrin A expression suppresses synaptic targeting of NMDA receptors in developing hippocampal neurones', *J Neurochem*, 97 Suppl 1: 110-5.

Takahashi, H., Y. Sekino, S. Tanaka, T. Mizui, S. Kishi, and T. Shirao. 2003. 'Drebrin-dependent actin clustering in dendritic filopodia governs synaptic targeting of postsynaptic density-95 and dendritic spine morphogenesis', *J Neurosci*, 23: 6586-95.

Takahashi, N., Y. Hozumi, T. Tanaka, M. Okada, K. Iseki, K. Hayasaka, and K. Goto. 2014. 'Cellular expression and localization of DGKzeta-interacting NAP1-like proteins in the brain and functional implications under hypoxic stress', *Histochem Cell Biol*, 142: 461-71.

Talbot, J. N., E. M. Jutkiewicz, S. M. Graves, C. F. Clemans, M. R. Nicol, R. M. Mortensen, X. Huang, R. R. Neubig, and J. R. Traynor. 2010. 'RGS inhibition at G(alpha)i2 selectively potentiates 5-HT1A-mediated antidepressant effects', *Proc Natl Acad Sci U S A*, 107: 11086-91.

Taymans, J. M., C. Wintmolders, P. Te Riele, M. Jurzak, H. J. Groenewegen, J. E. Leysen, and X. Langlois. 2002. 'Detailed localization of regulator of G protein signaling 2 messenger ribonucleic acid and protein in the rat brain', *Neuroscience*, 114: 39-53.

Tedford, H. W., and G. W. Zamponi. 2006. 'Direct G protein modulation of Cav2 calcium channels', *Pharmacol Rev*, 58: 837-62.

Traver, S., C. Bidot, N. Spassky, T. Baltauss, M. F. De Tand, J. L. Thomas, B. Zalc, I. Janoueix-Lerosey, and J. D. Gunzburg. 2000. 'RGS14 is a novel Rap effector that preferentially regulates the GTPase activity of galphao', *Biochem J*, 350 Pt 1: 19-29.

Tullio, A. N., D. Accili, V. J. Ferrans, Z. X. Yu, K. Takeda, A. Grinberg, H. Westphal, Y. A. Preston, and R. S. Adelstein. 1997. 'Nonmuscle myosin II-B is required for normal development of the mouse heart', *Proc Natl Acad Sci U S A*, 94: 12407-12.

Tully, K., and S. N. Treistman. 2004. 'Distinct intracellular calcium profiles following influx through N- versus L-type calcium channels: role of Ca2+-induced Ca2+ release', *J Neurophysiol*, 92: 135-43.

Tyanova, S., T. Temu, P. Sinitcyn, A. Carlson, M. Y. Hein, T. Geiger, M. Mann, and J. Cox. 2016. 'The Perseus computational platform for comprehensive analysis of (prote)omics data', *Nat Methods*, 13: 731-40.

Tzivion, G., Z. Luo, and J. Avruch. 1998. 'A dimeric 14-3-3 protein is an essential cofactor for Raf kinase activity', *Nature*, 394: 88-92.

Tzivion, G., Y. H. Shen, and J. Zhu. 2001. '14-3-3 proteins; bringing new definitions to scaffolding', *Oncogene*, 20: 6331-8.

Ulens, C., P. Daenens, and J. Tytgat. 2000. 'Changes in GIRK1/GIRK2 deactivation kinetics and basal activity in the presence and absence of RGS4', *Life Sci*, 67: 2305-17.

Umoh, M. E., E. B. Dammer, J. Dai, D. M. Duong, J. J. Lah, A. I. Levey, M. Gearing, J. D. Glass, and N. T. Seyfried. 2018a. 'A proteomic network approach across the ALS-FTD disease spectrum resolves clinical phenotypes and genetic vulnerability in human brain', *EMBO Mol Med*, 10: 48-62.

Umoh, Mfon E, Eric B Dammer, Jingting Dai, Duc M Duong, James J Lah, Allan I Levey, Marla Gearing, Jonathan D Glass, and Nicholas T Seyfried. 2018b. 'A proteomic network approach across the ALS-FTD disease spectrum resolves clinical phenotypes and genetic vulnerability in human brain', *EMBO Molecular Medicine*, 10: 48-62.

Vellano, C. P., N. E. Brown, J. B. Blumer, and J. R. Hepler. 2013. 'Assembly and function of the regulator of G protein signaling 14 (RGS14).H-Ras signaling complex in live cells are regulated by Galphai1 and Galphai-linked G protein-coupled receptors', *J Biol Chem*, 288: 3620-31.

Vellano, C. P., S. E. Lee, S. M. Dudek, and J. R. Hepler. 2011. 'RGS14 at the interface of hippocampal signaling and synaptic plasticity', *Trends Pharmacol Sci*, 32: 666-74.

Vellano, C. P., E. M. Maher, J. R. Hepler, and J. B. Blumer. 2011. 'G protein-coupled receptors and resistance to inhibitors of cholinesterase-8A (Ric-8A) both regulate the regulator of g protein signaling 14 RGS14.Galphai1 complex in live cells', *J Biol Chem*, 286: 38659-69.

Vermeren, M., R. Lyraki, S. Wani, R. Airik, O. Albagha, R. Mort, F. Hildebrandt, and T. Hurd. 2017. 'Osteoclast stimulation factor 1 (Ostf1) KNOCKOUT increases trabecular bone mass in mice', *Mamm Genome*, 28: 498-514.

Vicente-Manzanares, M., X. Ma, R. S. Adelstein, and A. R. Horwitz. 2009. 'Non-muscle myosin II takes centre stage in cell adhesion and migration', *Nat Rev Mol Cell Biol*, 10: 778-90.

Vizcaino, J. A., A. Csordas, N. Del-Toro, J. A. Dianes, J. Griss, I. Lavidas, G. Mayer, Y. Perez-Riverol, F. Reisinger, T. Ternent, Q. W. Xu, R. Wang, and H. Hermjakob. 2016. '2016 update of the PRIDE database and its related tools', *Nucleic Acids Res*, 44: 11033.

von Ziegler, L. M., N. Selevsek, R. Y. Tweedie-Cullen, E. Kremer, and I. M. Mansuy. 2018. 'Subregion-Specific Proteomic Signature in the Hippocampus for Recognition Processes in Adult Mice', *Cell Rep*, 22: 3362-74.

Vrajova, M., S. Pekova, J. Horacek, and C. Hoschl. 2011. 'The effects of siRNA-mediated RGS4 gene silencing on the whole genome transcription profile: implications for schizophrenia', *Neuro Endocrinol Lett*, 32: 246-52.

Wamsteeker Cusulin, J. I., T. Fuzesi, W. Inoue, and J. S. Bains. 2013. 'Glucocorticoid feedback uncovers retrograde opioid signaling at hypothalamic synapses', *Nat Neurosci*, 16: 596-604.

Wamsteeker, J. I., and J. S. Bains. 2010. 'A synaptocentric view of the neuroendocrine response to stress', *Eur J Neurosci*, 32: 2011-21.

Willard, F. S., M. D. Willard, A. J. Kimple, M. Soundararajan, E. A. Oestreich, X. Li, N. A. Sowa, R. J. Kimple, D. A. Doyle, C. J. Der, M. J. Zylka, W. D. Snider, and D. P. Siderovski. 2009. 'Regulator of G-protein signaling 14 (RGS14) is a selective H-Ras effector', *PLoS One*, 4: e4884.

Willars, G. B. 2006. 'Mammalian RGS proteins: multifunctional regulators of cellular signalling', *Semin Cell Dev Biol*, 17: 363-76.

Wingo, Thomas S, Duc M Duong, Maotian Zhou, Eric B Dammer, Hao Wu, David J Cutler, James J Lah, Allan I Levey, and Nicholas T Seyfried. 2017. 'Integrating next-generation

genomic sequencing and mass spectrometry to estimate allele-specific protein abundance in human brain', *Journal of proteome research*, 16: 3336-47.

Witherow, D. S., Q. Wang, K. Levay, J. L. Cabrera, J. Chen, G. B. Willars, and V. Z. Slepak. 2000. 'Complexes of the G protein subunit gbeta 5 with the regulators of G protein signaling RGS7 and RGS9. Characterization in native tissues and in transfected cells', *J Biol Chem*, 275: 24872-80.

Wyszynski, M., V. Kharazia, R. Shanghvi, A. Rao, A. H. Beggs, A. M. Craig, R. Weinberg, and M. Sheng. 1998. 'Differential regional expression and ultrastructural localization of alpha-actinin-2, a putative NMDA receptor-anchoring protein, in rat brain', *J Neurosci*, 18: 1383-92.

Xie, K., K. L. Allen, S. Kourrich, J. Colon-Saez, M. J. Thomas, K. Wickman, and K. A. Martemyanov. 2010. 'Gbeta5 recruits R7 RGS proteins to GIRK channels to regulate the timing of neuronal inhibitory signaling', *Nat Neurosci*, 13: 661-3.

Yaffe, M. B. 2002. 'How do 14-3-3 proteins work?-- Gatekeeper phosphorylation and the molecular anvil hypothesis', *FEBS Lett*, 513: 53-7.

Yaffe, M. B., K. Rittinger, S. Volinia, P. R. Caron, A. Aitken, H. Leffers, S. J. Gamblin, S. J. Smerdon, and L. C. Cantley. 1997. 'The structural basis for 14-3-3:phosphopeptide binding specificity', *Cell*, 91: 961-71.

Yalcin, B., S. A. Willis-Owen, J. Fullerton, A. Meesaq, R. M. Deacon, J. N. Rawlins, R. R. Copley, A. P. Morris, J. Flint, and R. Mott. 2004. 'Genetic dissection of a behavioral quantitative trait locus shows that Rgs2 modulates anxiety in mice', *Nat Genet*, 36: 1197-202.

Yang, G., K. Kitagawa, T. Ohtsuki, K. Kuwabara, T. Mabuchi, Y. Yagita, K. Takazawa, S. Tanaka, T. Yanagihara, M. Hori, and M. Matsumoto. 2000. 'Regional difference of neuronal vulnerability in the murine hippocampus after transient forebrain ischemia', *Brain Res*, 870: 195-8.

Yuan, H., K. Michelsen, and B. Schwappach. 2003. '14-3-3 dimers probe the assembly status of multimeric membrane proteins', *Curr Biol*, 13: 638-46.

Zachariou, V., D. Georgescu, N. Sanchez, Z. Rahman, R. DiLeone, O. Berton, R. L. Neve, L. J. Sim-Selley, D. E. Selley, S. J. Gold, and E. J. Nestler. 2003. 'Essential role for RGS9 in opiate action', *Proc Natl Acad Sci U S A*, 100: 13656-61.

Zambon, A. C., S. Gaj, I. Ho, K. Hanspers, K. Vranizan, C. T. Evelo, B. R. Conklin, A. R. Pico, and N. Salomonis. 2012. 'GO-Elite: a flexible solution for pathway and ontology over-representation', *Bioinformatics*, 28: 2209-10.

Zamponi, G. W., and K. P. Currie. 2013. 'Regulation of Ca(V)2 calcium channels by G protein coupled receptors', *Biochim Biophys Acta*, 1828: 1629-43.

Zhang, L., H. Wang, D. Liu, R. Liddington, and H. Fu. 1997. 'Raf-1 kinase and exoenzyme S interact with 14-3-3zeta through a common site involving lysine 49', *J Biol Chem*, 272: 13717-24.

Zhao, M., Y. S. Choi, K. Obrietan, and S. M. Dudek. 2007. 'Synaptic plasticity (and the lack thereof) in hippocampal CA2 neurons', *J Neurosci*, 27: 12025-32.

Zhao, P., C. Nunn, S. Ramineni, J. R. Hepler, and P. Chidiac. 2013. 'The Ras-binding domain region of RGS14 regulates its functional interactions with heterotrimeric G proteins', *J Cell Biochem*, 114: 1414-23.

Zimmermann, B., F. Girard, Z. Meszar, and M. R. Celio. 2013. 'Expression of the calcium binding proteins Necab-1,-2 and -3 in the adult mouse hippocampus and dentate gyrus', *Brain Res*, 1528: 1-7.

Zurner, M., T. Mittelstaedt, S. tom Dieck, A. Becker, and S. Schoch. 2011. 'Analyses of the spatiotemporal expression and subcellular localization of liprin-alpha proteins', *J Comp Neurol*, 519: 3019-39.